

DISCLAIMER

This report was prepared as an account of work sponsored by an agency of the United States Government. Neither the United States Government nor any agency thereof, nor any of their employees, makes any warranty, express or implied, or assumes any legal liability or responsibility for the accuracy, completeness, or usefulness of any information, apparatus, product, or process disclosed, or represents that its use would not infringe privately owned rights. Reference herein to any specific commercial product, process, or service by trade name, trademark, manufacturer, or otherwise does not necessarily constitute or imply its endorsement, recommendation, or favoring by the United States Government or any agency thereof. The views and opinions of authors expressed herein do not necessarily state or reflect those of the United States Government or any agency thereof.

This report has been reproduced directly from the best available copy.

Available to DOE and DOE contractors from the Office of Scientific and Technical Information, P.O. Box 62, Oak Ridge, TN 37831; prices available from (615)576-8401, FTS 626-8401.

Available to the public from the National Technical Information Service, U. S. Department of Commerce, 5285 Port Royal Rd., Springfield, VA 22161.

ADVANCED SENSOR DEVELOPMENT PROGRAM FOR THE PULP AND
PAPER INDUSTRY

DOE/CE/40748--T1

DE91 007688

By:

J. D. Allen
S. R. Charagundla
A. Macek
H. G. Semerjian
J. R. Whetstone

OCTOBER 1990

Work Performed Under DOE Contract No. A101-76PR06010
Task A123-AI01-85CE40748

National Institute of Standards and Technology
Center For Chemical Engineering
Gaithersburg, Maryland 20899

Prepared For:

Stanley F. Sobczynski
Program Manager CE-231

Office of Industrial Processes
U. S. DEPARTMENT OF ENERGY
Conservation and Renewable Energy
Washington, D.C. 20585

Table of Contents

	Page
List of Figures.....	ii
List of Tables.....	v
Nomenclature.....	vi
Executive Summary.....	vii
1. Introduction.....	1
1.1 Background.....	3
1.2 Line Intensity Ratio Technique.....	4
1.3 Sensor Development Approach.....	5
2. Spectral Data from Initial Recovery Boiler Observations.....	5
3. Research Investigations.....	6
3.1 Laboratory Investigations.....	6
3.2 Tests at Union-Camp Mill, Franklin, VA.....	6
3.3 Laboratory Investigation of Atomic Emissions.....	11
3.4 Four Color Sensor System.....	18
3.5 Tests at Weyerhaeuser Mills, New Bern, NC.....	20
4. Optical Depth Effects in the Recovery Boiler.....	20
4.1 Investigation of Optical Depth Using a Traversing Probe in the Recovery Boiler.....	26
4.2 Selection of Recovery Boiler.....	26
4.3 Probe Design and Fabrication.....	27
4.4 Mill Tests with the Traversing Probe.....	29
4.5 Test Results.....	34
5. Mathematical Modeling and Laboratory Verification.....	46
5.1 The Effect of Optical Depth on Observed Emission Intensity Profiles.....	46
5.1.1 Emission Line Intensity from a Radiant Gas Column - Integral Adsorption Approach.....	48
5.1.2 Line Shape and Optical Depth.....	50
5.2 Calculation of Optical Depth Base on the Integral Adsorption Model.....	53
5.2.1 Calculation Procedure.....	54
5.2.2 Sample Calculations.....	56
5.2.3 A. D. Little Model.....	56
5.2.4 Measured Line Widths.....	57
5.2.5 SOLGASMIX Model.....	57
5.2.6 Model Results.....	60
6. Emission Profile and Optical Depth Models.....	62
6.1 Emission/Absorption Model.....	62
6.2 Model Calculation Results.....	65
6.3 Optically Thick Gas - Analytical Expressions.....	68
6.4 Laboratory Tests.....	73
7. Summary and Conclusions.....	76
8. Acknowledgements.....	78
9. References.....	79

List of Figures	Page
Figure 1. Black liquor recovery boiler (schematic).....	2
Figure 2. Experimental arrangement.....	7
Figure 3. OH emission spectra obtained from premixed methane/air flames at two different stoichiometries.....	8
Figure 4. CH emission spectra obtained from a premixed methane/air flame.....	9
Figure 5. C2 emission spectra obtained from premixed methane/air flames at different stoichiometries.....	10
Figure 6. Potassium emission lines at 404.4 nm and 404.7 nm observed in recovery boiler mill tests (Union-Camp Mills, Franklin, VA).....	12
Figure 7. Sodium emission lines at 589 nm observed in recovery boiler mill tests (Union-Camp Mills, Franklin, VA).....	13
Figure 8. Sodium emission line at 330.2 nm observed in recovery boiler tests (Union-Camp Mills, Franklin, VA).....	14
Figure 9. Potassium emission lines at 404.4 nm and 404.7 nm obtained from a pre-mixed methane/air flame injected with KCl solution.....	16
Figure 10. Potassium emission lines at 766.5 nm and 769.9 nm obtained from a pre-mixed methane/air flame injected with KCl solution.....	17
Figure 11. Four-color temperature sensing system.....	19
Figure 12. Potassium emission lines at 404.4 nm and 404.7 nm observed in recovery boiler tests (Weyerhaeuser Mills, New Bern, NC).....	21
Figure 13. Variation of continuum emission in the neighborhood of potassium emission lines as observed in recovery boiler tests (Weyerhaeuser Mills, New Bern, NC).....	22
Figure 14. Potassium emission lines at 766.5 nm and 769.9 nm observed in recovery boiler tests (Weyerhaeuser Mills, New Bern, NC).....	23
Figure 15. Sodium emission lines at 589 nm observed in recovery boiler tests (Weyerhaeuser Mills, New Bern, NC).....	24
Figure 16. Measured boiler temperature.....	25

Figure 17. Probe body.....	28
Figure 18. Probe head.....	30
Figure 19. Probe support system.....	31
Figure 20. Experimental Arrangement for traversing probe tests (Photograph).....	32
Figure 21. Probe Head with Optical Fiber Bundle (Photograph).....	33
Figure 22. Optical probe section showing damage to heat flux probe terminals.....	35
Figure 23. Sodium emission lines at 589 nm observed at liquor gun level (Weyerhaeuser Mills, Plymouth, NC).....	36
Figure 24. Potassium emission lines at 766.49 nm observed at liquor gun level (Weyerhaeuser Mills, Plymouth, NC)....	37
Figure 25. Sodium emission lines at 589 nm observed at primary air level (Weyerhaeuser Mills, Plymouth, NC).....	38
Figure 26. Potassium emission lines at 766.49 nm observed at primary air level (Weyerhaeuser Mills, Plymouth, NC)...	39
Figure 27. Effect of probe penetration on emission spectra (Weyerhaeuser Mills, Plymouth, NC).....	41
Figure 28. Comparison of emission spectra from 0 degree probe with 180 degree probe, probe depth 2 ft (Weyerhaeuser Mills, Plymouth, NC).....	42
Figure 29. Comparison of emission spectra from 0 degree probe with 180 degree probe, probe depth 4 ft (Weyerhaeuser Mills, Plymouth, NC).....	43
Figure 30. Comparison of emission spectra from 0 degree probe with 180 degree probe, probe depth 5 ft (Weyerhaeuser Mills, Plymouth, NC).....	44
Figure 31. Comparison of emission spectra from 0 degree probe with 180 degree probe, probe depth 6 ft (Weyerhaeuser Mills, Plymouth, NC).....	45
Figure 32. Local heat flux, probe depth 52 in. (Weyerhaeuser Mills, Plymouth, NC).....	49
Figure 33. Computation procedure (flow chart).....	55
Figure 34. Integral absorption for various path lengths at 1200K (based on K atom concentrations from A. D. Little Equilibrium Model).....	58

Figure 35. Integral absorption for various path lengths at 1600K (based on K atom concentrations from A. D. Little Equilibrium Model).....	59
Figure 36. Integral absorption at 404.4 nm for various path lengths (based on K atom concentrations from SOLGAS MIX MODEL, T=1200K).....	61
Figure 37. Optically thin line shapes of potassium emission intensity.....	66
Figure 38. Emission line intensity shapes - effect of a cool layer.....	67
Figure 39. Emission line intensity shapes - effect of a cool layer $N_p = 2.4 \times 10^{11}$ atoms/cm ³	69
Figure 40. Emission line intensity shapes - effect of a cool layer $N_p = 1.29 \times 10^{12}$ atoms/cm ³	70
Figure 41. Emission line intensity shapes - effect of a cool layer and various K atom concentration levels.....	71
Figure 42. Measured line profiles from laboratory flames injected with KOH - optically thin emission.....	74
Figure 43. Measured emission line profiles - KOH injection for optically thin and thick cases.....	75

List of Tables

Page

Table 1.	Pre-mixed methane/air flame temperatures measured by line intensity ratio technique.....	15
Table 2.	Temperatures measured with four-color sensor system....	18
Table 3.	Black liquor composition data (expressed as weight % of dry liquor solids).....	27
Table 4.	Ratio of peak intensities ($I_{404.41}/I_{404.47}$) measured in recovery boiler mill tests.....	46
Table 5.	Ratio of peak intensities ($I_{766.49}/I_{769.9}$) measured in Weyerhaeuser recovery boiler at New Bern, NC.....	47
Table 6.	Comparison of calculated optical depths with Ariessohn's calculations.....	57
Table 7.	Black liquor composition.....	60
Table 8.	Computed optical depths.....	60

NOMENCLATURE

A_t	integral absorption
B_λ	radiance of an emission line
B_λ^b	black body radiation
c	speed of light
f	oscillator strength
h	Planck's constant
I	intensity of emission
k_T	Boltzmann constant
K	absorption coefficient
$k_{a\max}$	atomic absorption at line center
K_{\max}	absorption at line center
k_a	atomic absorption
L	optical depth
l	optical path length
M	atomic weight
n	number density
P	pressure
Q	partition function
T	temperature
N_L	Loschmidt's number
λ	wavelength
ν	frequency
ω	wave number

SUBSCRIPTS

D	Doppler
eff	effective
gen	generated
in	entering
L	Lorentzian
out	exiting
o	at center wavelength
V	Voigt profile
λ	at wavelength, λ
ν	at frequency, ν
l,p	lower energy level
u,q	upper energy level
0	ground state
1	excited state

Advanced Sensor Development Program for
the Pulp and Paper Industry

S. R. Charagundla, J. Whetstone, J. D. Allen,
A. Macek H. G. Semerjian

Executive Summary

This report describes experimental and theoretical studies toward development of a remote sensing technique for non-intrusive temperature measurement based on optical spectroscopic analysis of recovery boiler. The overall objectives were (a) construction of a fiber-optic system for measurement of spectroscopic emission intensities at several wavelengths and (b) development of a computer program relating these intensities to temperatures of the emitting species.

The emitting species for temperature measurements in flames can be either naturally occurring free radicals (OH, CH, C₂) or atoms which, in turn, can be either naturally occurring or seeded into flames. Sodium atoms, the obvious emitters in recovery boilers, are not promising as thermometric species because of their high concentration. At high concentrations, strong self-absorption results cause optical depths to be much smaller than the sampling depths desired for recovery boilers. An experimental program was, therefore, undertaken with the objective of identification and spectroscopic detection and measurement of other naturally occurring thermometric species. The program consisted of several laboratory studies and four field trips to different recovery boilers.

During the first field trip, preliminary wavelength scans were made through a boiler window to record spectral intensities from 300 to 600 nanometers (nm). These test results showed that temporal intensity variations were short relative to spectrometer recording times, making spectral line differentiation from background noise impossible except for the sodium line. A second field trip was therefore made for the purpose of similar tests but using an optical multichannel analyzer (OMA) to record spectral information. This allowed essentially instantaneous recording of a number of spectral segments, each 30 nm wide, over the same wavelength range (300 to 600 nm). The results of this work were: (a) no molecular spectral features (OH, CH, C₂) were observed; (b) the potassium atom doublet at 404.4/404.7 nm appeared with measurable intensities; and (c) there was significant background noise at all wavelengths.

As a result of the second field trip, it was decided that the best possibility for an optical on-line sensor would be a four-color fiber optic instrument capable of recording, simultaneously, the 404.4/404.7 nm and 766.5/769.9 nm potassium doublets, as well as the background continua adjacent to these two doublets, for purposes of subtraction for quantitative intensity measurements. (For brevity, these two potassium doublets will henceforth be referred to as the "blue" and the "red" line respectively.) Consequently, a laboratory study was undertaken, wherein

such a system was designed, constructed, and demonstrated to be suitable for temperature measurements from the intensity ratios of the blue and red lines. The demonstration was made on gaseous products from a laboratory burner seeded with potassium.

A third field trip was then made to a boiler site with two objectives: (a) to record the red line with the OMA; and (b) to make simultaneous intensity measurements of the red and blue lines with the 4-color system. The first objective was accomplished, but the second one was not, because the blue line was too weak for any quantitative measurements. This means that either the boiler temperature or the concentration of potassium in the black liquor (or both) was too low. A fourth boiler firing potassium-rich liquor at temperatures exceeding 1900 °F was, therefore, targeted for the next series of tests.

Analysis of spectra obtained both in the laboratory and in the field up to that point indicated a potential for three concerns: (a) the recovery boiler combustion gas streams may not meet the requirement of negligible self-absorption occurring between the emitting atoms and the boiler wall, which is needed for quantitative temperature measurement by the intensity-ratio technique; (b) the optical depths at the two wavelengths may be different; and (c) there may be self-absorption due to temperature gradients in the recovery furnace gas environment. As a consequence, theoretical investigations were undertaken, and plans were made for a major increase in the experimental capability of optical probing inside the boiler in the last field test. For this purpose, a cooled traversing probe, 12 ft long, was designed and constructed for horizontal insertion into the boiler. Two optic fibers were housed inside the probe, one viewing straight ahead and the other back toward the wall. Several heat sensors were attached to the outside wall of the probe.

A fourth field trip was undertaken with all the experimental equipment assembled in this project, i.e., both the traversing probe connected to the spectrometer/OMA detector with accessories and the 4-color fiber-optic system. Despite the fact that testing was interrupted before completion by an unscheduled shut-down of the mill, a wealth of OMA spectra of the red potassium line was obtained across boiler gas layers of varying thickness, both near the wall and up to 8 ft into the boiler. Heat sensors on the probe also revealed the existence of temperature gradients. However, attempts to measure the blue potassium line were again unsuccessful. In this series of tests the cause of the failure is known: it was ascertained by independent thermocouple measurements that boiler temperatures were only about 1700 °F, i.e., much lower than anticipated.

To complement the experimental studies, a computer program was written for interpretation of the OMA spectra, allowing for calculation of line intensities and shapes observed at any point in the boiler, either at the wall or in the interior, under various conditions. For example, the emitting gas layers can be isothermal or contain temperature gradients, concentrations of potassium can be constant or vary with the temperature in specified ways, etc. Application of the model to OMA results obtained both in the laboratory and in the boilers shows that the

following spectroscopic conditions obtain in boiler environments:

- (a) Optical absorption depths at line centers of both potassium lines are smaller than the boiler widths.
- (b) Absorption is much stronger for the red line, i.e., its optical depth is only a very small fraction of the boiler dimension. This means that the line becomes optically thin (i.e., negligibly re-absorbed) only far from its center.
- (c) There are temperature gradients not only near the wall, but also in the interior of the boiler, as shown by self-absorption of line centers at all insertion depths of the traversing probe.

It is concluded that boiler temperatures cannot be determined by measurement of total intensities of the two potassium lines as envisioned in the concept of the 4-color instrument. On the other hand, since the computer model is versatile enough to address various realistic boiler scenarios, such measurement by means of simultaneous dispersive recording of the two lines -- wings as well as center -- remains a possibility. The required recording instrument would consist of a bifurcated fiber, with a dispersive element and a linear array covering spectral segments around 404 and 767 nm respectively, at each branch end. On-line control by real-time integration of experimental data with line-shape software is also a possibility.

Advanced Sensor Development Program for the Pulp and Paper Industry

1. Introduction

The black liquor recovery boiler is essential to the kraft process for the manufacture of pulp, i.e., conversion of wood to cellulose fibers by delignification of the wood. In the kraft process wood chips are immersed in caustic chemicals at a sequence of elevated temperatures and pressures to remove the lignin binding the cellulose fibers of the wood together. After separation from the pulp mass the spent liquor is concentrated via evaporation and becomes black liquor. It is composed of the inorganic salts used for digestion of the wood, lignin compounds, and water. In order to make the kraft pulping process economically realistic, these inorganic salts must be recovered, chemically reduced to the original chemical state, and recycled for use in successive pulping cycles. This recovery process requires high temperatures. A sufficient quantity of lignin compounds are available in the black liquor to sustain combustion, thereby providing the means to sustain the high temperatures needed to drive the chemical reduction process. The recovery boiler takes advantage of this with black liquor as its primary fuel.

Black liquor is introduced into the furnace of the boiler by spray nozzles that produce droplets of a large size and distribution. These burn, form char particles, and fall to the boiler floor forming a smelt bed. The inorganic compounds are largely transferred to the smelt bed via char and are chemically reduced and removed for further processing and reuse in digestion, thereby closing the chemical recovery cycle. Sufficient heat is produced to maintain the smelt bed at a sufficiently high temperature to drive the chemical reduction process and to generate sufficient quantities of steam to completely or substantially supply high pressure steam for electrical power generation and subsequently to the various unit processes comprising an integrated pulp and paper mill.

A typical recovery boiler is shown schematically in figure 1, and operates on the staged combustion principle; combustion air is introduced at two levels, or three depending on the manufacturer of the boiler, while the black liquor is sprayed through nozzles into the boiler at the secondary, or tertiary, levels forming droplets that fall into the highest temperature zone where they undergo pyrolysis and combust. The majority of the lignin compounds in the droplets are volatilized in flight. Some remain in the char mixed with the inorganic salts of the black liquor and falls to smelt bed on the floor of the furnace. Therefore, the environment within the recovery boiler is heavily laden with particulates of char as the black liquor combusts and is quite aggressive chemically. Conventional, contacting thermometry techniques have a very short lifetime in such conditions. As a result, it is not possible to implement real-time control techniques. Current operation is based on the subjective judgment of the operator.

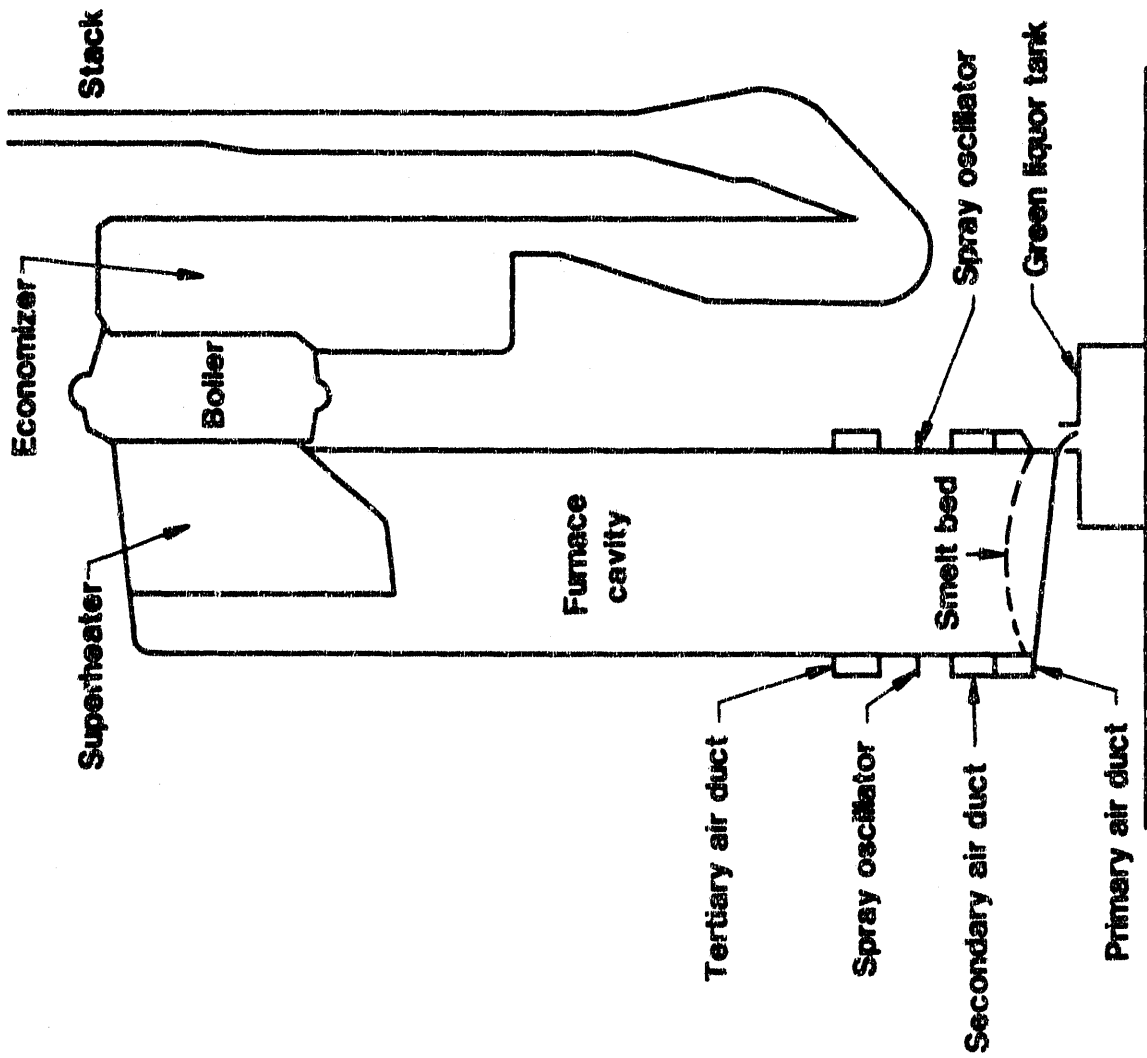


Figure 1. Black Liquor Recovery Boiler (Schematic)

A major obstacle to development of viable combustion control techniques is the lack of a reaction zone temperature sensing method. The objective of the research work reported here was to develop such a temperature measurement technique based on spectroscopic observation of the light coming from the combustion zone of the boiler. This technique is based on emission spectroscopy. Such a sensor is non-intrusive with potential for an on-line, line of sight measurement in a wide variety of applications [1]. This technique and details of early progress have been described in previous progress reports to DoE [2,3].

1.1 Background

The characteristics of optical emission spectra obtained from a generalized combustion zone depends upon the type and concentration of species present and on the temperature. Temperature distribution may also be an important parameter in some cases. Spectral features from three sources (1) continuum emissions, (2) molecular band emissions, and (3) atomic line emissions have potential to provide a means of temperature measurement in high temperature, particle-laden regions, such as recovery boiler environments.

Continuum, or blackbody, emissions are intense in the infrared region are much higher in the recovery boiler than in power boilers because they are black liquor fueled. As mentioned above black liquor combustion forms a char that exhibits wide size range. Char particle of several millimeter diameter are easily observed in the recovery boiler's combustion zone. Continuum emissions from these are significant. Additionally, char particles are a source of noise for any sensing method based on observation of continuum emissions because they are expected to have a surface temperature below that of the combustion gases themselves.

In hydrocarbon flames, molecular band emissions due to the hydrocarbon radicals OH, CH, and C_2 are usually observed. Since the individual line intensities depend on flame stoichiometry, Vaidya et al. [6] have used this dependency to measure hydrocarbon flame temperatures. Initial efforts in this work focused on the OH radical as a potential thermometric species and spectroscopic surveys were made to determine the intensity and structure of these molecular bands in recovery boilers.

During the first field trip to an operating recovery boiler, preliminary spectral surveys of a boiler's combustion zone were made from 300 to 600 nanometers (nm) through a boiler window. These test results showed that general intensity variations were short relative to spectrometer recording times, thereby making spectral line differentiation from background noise impossible except for the sodium emission line. To make effective observations of spectral line intensities from recovery boiler observations a recording method capable of recording regions spectral in a fraction of a second was needed. This recording method minimized the effects of overall intensity variations and was achieved by fitting the spectrometer with an optical multichannel analyzer (OMA).

A second field trip was made to survey spectral characteristics of observed in the recovery boiler using the OMA-equipped spectrometer. This allowed essentially instantaneous recording of a spectral segment, approximately 30 nm wide, over the same wavelength range (300 to 600 nm). The results of this work showed that:

- (a) no spectral features from molecular species (OH, CH, C₂) were observed;
- (b) the potassium atom doublet at 404.4/404.7 nm appeared with measurable intensities; and
- (c) there was significant background noise at all wavelengths.

It was originally proposed to use the intensity ratio of two selected lines in the molecular band emission spectrum of OH for temperature measurement. However, the spectral survey results of recovery boiler emissions established that no OH or other molecular band emissions could be observed. Analysis of the spectral survey data showed the presence of atomic potassium emission doublets at 404.5 and 766.5 nanometers (nm). Further investigation of these two spectral features were directed at determining their utility for temperature measurement using the line ratio technique.

1.2 Line Intensity Ratio Technique

In the past, the line intensity ratio technique has been used to determine the temperatures of hydrogen/oxygen flames, arc jets and plasmas; Boumans [7], and Alkemade et al. [8] have discussed this technique which is based on the assumption that the population of atoms, ions or molecules of any species emitting at different energy levels follow a Boltzmann distribution. The absolute intensity, I_{u1} of a spectral line involved in the transition from an upper energy level, u , to a lower one, l , can be written as,

$$I_{u1} = A_{u1} h \nu n_i g_{u1} \exp(-E_{u1}/k_B T) \quad (1)$$

where the spectral line constants, A_{u1} , ν , g_{u1} and E_{u1} are, respectively, the transition probability, frequency, statistical weight and energy level of the excited species at the energy level, u . n_i is the number density of the emitting species, i , and T is the temperature. Spectral line constants for a number of atomic emission lines are well documented [9,10]. Based on this relationship, the basic equation for temperature measurement using the line intensity ratio technique can be written as,

$$I_1/I_2 = (A_1 g_1 \lambda_2 / A_2 g_2 \lambda_1) \exp[-(E_1 - E_2)/k_B T] \quad (2)$$

where, I_1 and I_2 are the measured line intensities at two different wavelengths. In this equation, only I_1 , I_2 and T are unknown; consequently, once the line intensity ratio is measured, the temperature, T can be calculated. For this technique to be valid two conditions must be met: (1) both lines must belong to the emission

spectrum of the same neutral atom population, and (2) the combustion gas environment must be optically thin, i.e., the effect of re-absorption of emitted photons by like atoms in the combustion zone is negligible.

1.3 Sensor Development Approach

The approach originally proposed for the development of a spectroscopic temperature measurement technique consisted of four essential phases:

- 1) identification of spectra obtained from a black liquor recovery boiler,
- 2) development of the line intensity ratio technique for temperature measurement in the laboratory,
- 3) development of a prototype micro-computer based four color temperature sensing system, and
- 4) demonstration of the prototype in a mill environment.

The tasks associated with the first three phases were conducted as originally proposed. However, as the investigation of the characteristics of the emission spectra from the recovery proceeded it became clear that an evaluation of the optical thickness of the recovery boiler was needed and, the fourth phase, as originally proposed was not undertaken. Instead it was replaced with an experimental and modelling activity of emission and reabsorption of potassium in the recovery boiler. These additional tasks became necessary to assess the validity of the four color sensing technique as originally proposed for recovery boiler application, and involved the development of mathematical models and laboratory tests to assess optical emission characteristics of recovery boilers.

2. Spectral Data from Initial Recovery Boiler Observations

The early work performed prior to April 1983 and summarized in an earlier report [11], had the objective of characterizing the emission spectra from laboratory flames and from one recovery boiler. In these early investigations, an experimental arrangement consisting of a conventional scanning spectrometer equipped with a photo-multiplier was used to obtain spectra from laboratory flames. These data clearly showed the structure of the spectra due to molecular band emissions from the radical species, OH, CH and C₂. However, the results obtained in initial mill tests were inconclusive and demonstrated that a scanning type spectrometer system was not adequate to characterize emission spectra from the highly dynamic emission of recovery boilers. As a consequence, an optical multi-channel analyzer was substituted for the photomultiplier tube sensor of the spectrometer. It was used in all subsequent investigations.

3. Research Investigations

3.1 Laboratory Investigations

Laboratory investigations were used initially to establish the relationship between spectral line intensities and stoichiometry in a controlled environment and later to confirm the emitting species of the spectral profiles observed in black liquor recovery boilers. The experimental arrangement (fig. 2) used in these investigations [1] consists of a source (a premixed methane/air burner equipped with a mist injector or a particle feeder), a fiber optics probe, a spectrometer, and a linear detector array system.

The burner is of 3-inch nominal diameter and was designed to generate and stabilize a premixed methane/air flame; fuel and air are thoroughly mixed in the two chambers packed with spherical beads. The flame is stabilized on a distributor plate consisting of several equi-diameter holes arranged in an equi-distant pattern; the distributor plate generates several equi-distantly located turbulent flamelets to produce a steady flame approaching the characteristics of a "flat flame". The injector tube, coaxially located in the burner body, carries either particles from a solids feeder or mist from a nebulizer. The solids feeder was specially designed, based on fluidization principles, to yield a steady flow of dry uniform stream of particles while the nebulizer was designed to operate on the "venturi" effect.

The spectrometer used was a 0.5 meter scanning spectrometer equipped with a 1180 line/mm grating; the spectrometer's detector was a linear detector array system, an optical multi-channel analyzer (OMA) system, using a specially fabricated telescoping flange. The linear detector array consists of 1024 elements, a detector controller and a console with a monitor, two disc drives and a keyboard. The fiber optics probe, designed for the initial experimental studies, consists of a 3 mm diameter, quartz fiber bundle with collection optics at one end and focusing optics at the other.

Exploratory tests were conducted [1] to obtain the emission spectra from methane/air flames of known stoichiometry. Typically the emission spectra, obtained in the wavelength range of 300 nm to 600 nm, include the spectra due to OH, CH and C₂. The emission spectra due to OH, CH and C₂ are shown in figures 3 to 5 respectively. The spectral line intensities have been found to vary with flame temperature (stoichiometry) as evident from the observed spectra due to OH and C₂ shown in figures 3, 4 and 5.

3.2 Tests at Union-Camp Mill, Franklin, VA

The first series of mill tests [1] with the OMA/spectrometer system was performed at the recovery boiler of the Union-Camp Mill, Franklin, Virginia. These tests were conducted essentially to characterize emission spectra in the 300 to 600 nm region, specifically molecular band emissions due to OH, CH and C₂, from the recovery boiler. The

IN-SITU SPECTROSCOPIC TEMPERATURE MEASUREMENT

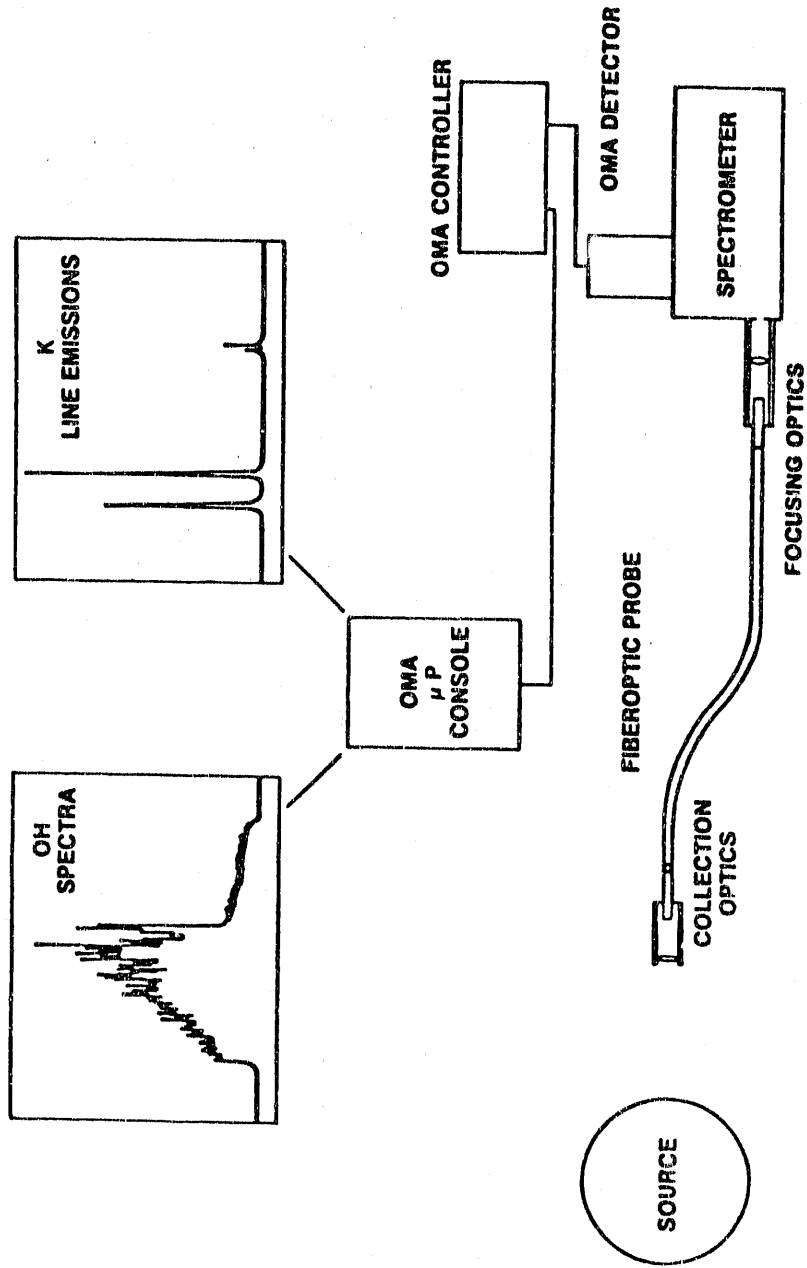


Figure 2. Experimental Arrangement

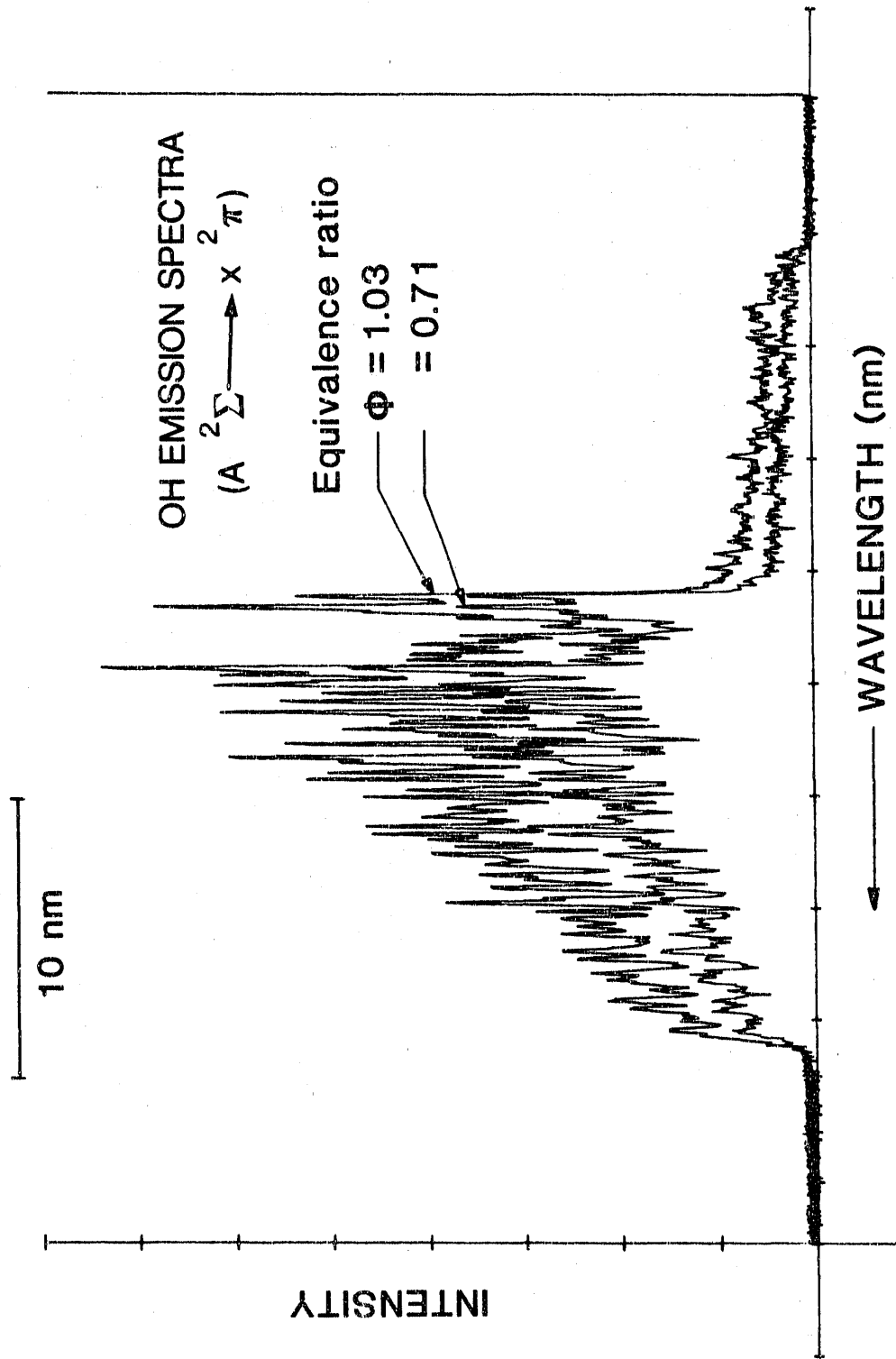


Figure 3. OH Emission Spectra Obtained from Premixed Methane/Air Flames at Two Different Stoichiometries

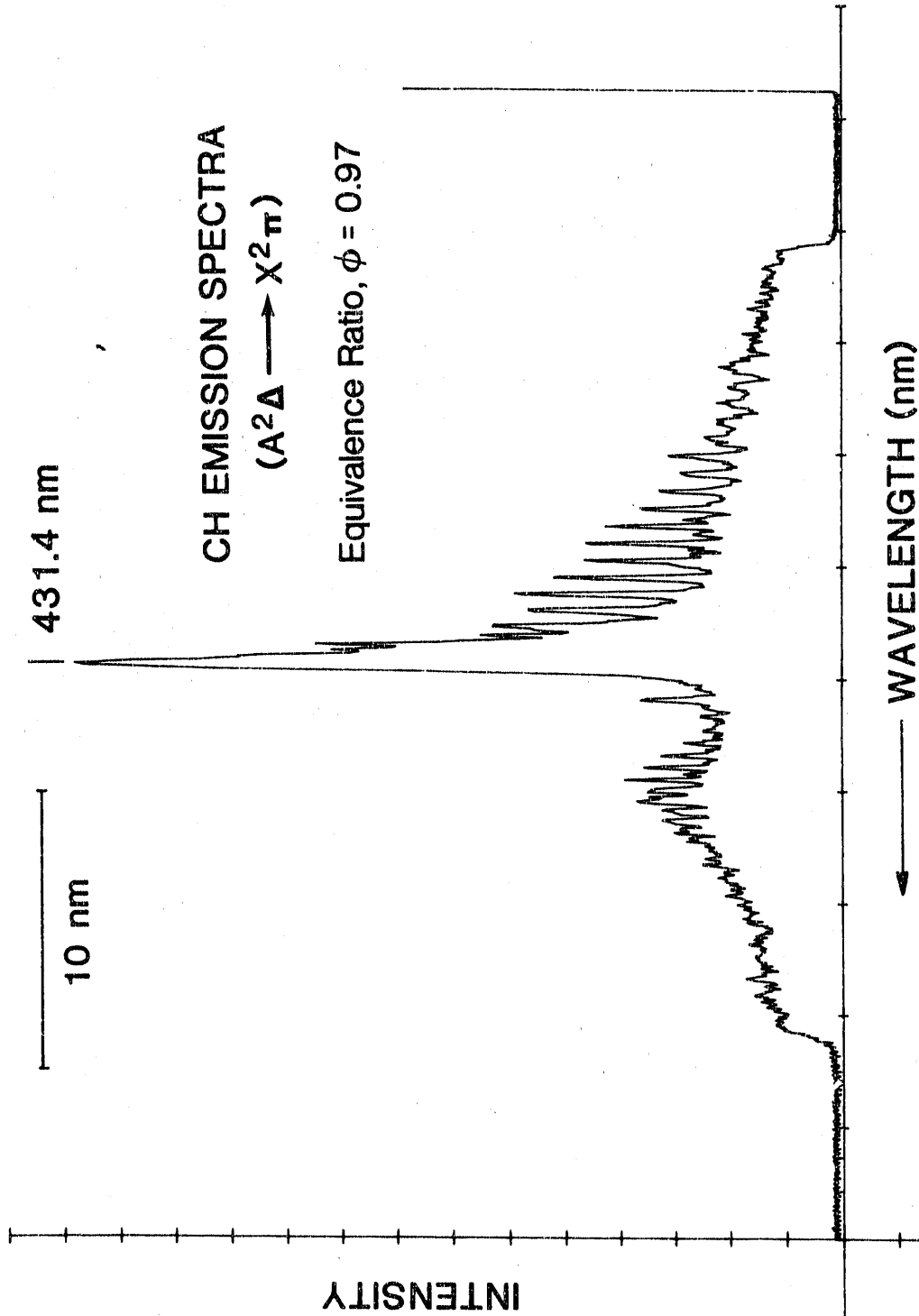


Figure 4. CH Emission Spectra Obtained from a Premixed Methane/Air Flame

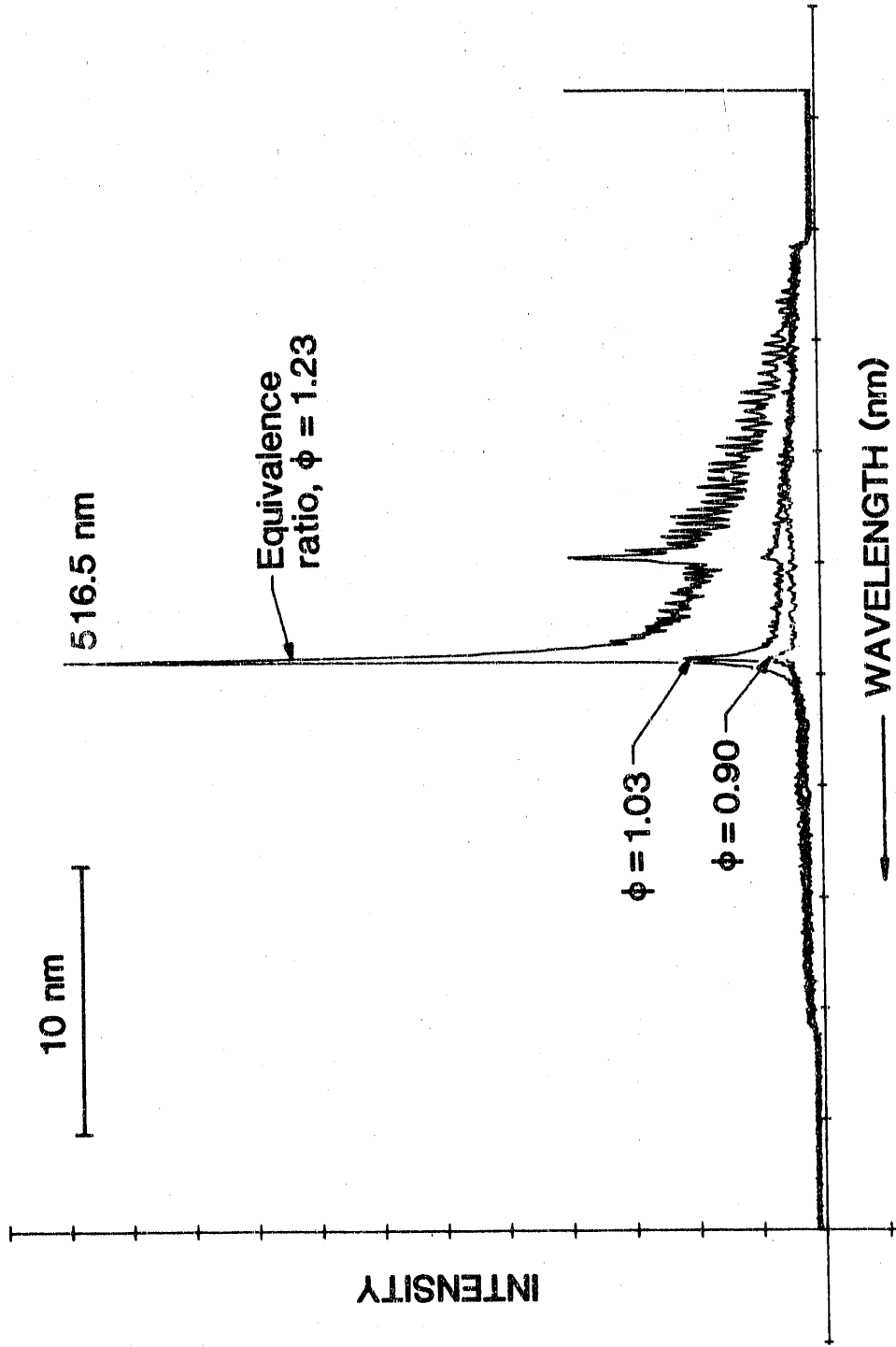


Figure 5. C₂ Emission Spectra Obtained from Premixed Methane/Air Flames at Different Stoichiometries

recovery boiler was of Babcock & Wilcox [12] design and was firing black liquor containing 3.1% inorganic potassium salts. During these tests, a fiber optic based viewing system for the spectrometer was used, as shown in figure 2, to obtain and record the emission spectra from observation ports located at the primary, secondary and tertiary air injection levels and at the liquor gun level. In these tests, because firing conditions varied substantially in the combustion zone, the emission intensity was found to vary extensively. As a consequence, the detector output was found to vary from a negligibly small value to the detector saturation point. These large changes required a compromise and spectra were selectively obtained only when the intensity level did not saturate the detector array.

Observations taken at all boiler levels were devoid of molecular band emissions due to the radicals, OH, CH, and C₂. However, a pair of emission lines were observed near 404.5 nm. Two records of spectra, obtained sequentially within a short time interval, are shown in figure 6: these records indicated two emission lines later confirmed by laboratory experiments to be the emission lines due to potassium at 404.4 nm and 404.7 nm. The intensity of these emission lines and of the background continuum emissions were found to vary considerably with time. Also observed were the strongly emitting sodium doublet at 589 nm, mostly in self-absorption, as shown in figure 7. These were obtained at the same port within short time intervals. Again, the variation in the intensity of these sodium spectra is indicative of the large general emission fluctuations in the combustion zone. In addition, observation of an emission line due to sodium at 330.2 nm was obtained (fig. 8); this weak sodium line was observed only once when viewing the bed surface directly through a port at the primary air injection level. In general, the intensity of emissions varied from port to port and with time. However, the emission intensity and the degree of fluctuations were found to diminish with boiler height. A review of all these spectral records clearly indicated significant levels of continuum emissions due to the presence of large amounts of particulate matter and hot radiating furnace walls.

3.3 Laboratory Investigation of Atomic Emissions

In the laboratory tests, black liquor solids were injected into a methane/air flame to obtain emission spectra from the resulting yellow flame in the wavelength range of 300 nm to 600 nm. In addition to the molecular band spectra due to radicals produced by the hydrocarbon flames, a total of four emission lines (two doublets) were observed: one doublet at about 404.5 nm, and the other at 589.0 nm and 590.6 nm. The source for doublet at 589 nm (emission lines at 589.0 nm and 590.6 nm) was readily identified as sodium; however, several species were candidates for the two emission lines at about 404.5 nm. Black liquor contains a number of substances including abundant quantities of inorganic sodium salts and carbonaceous matter, SO₂ and C₃ with emission lines at the wavelengths of 404.56 nm, 404.83 nm, and 404.98 nm respectively. In addition potassium (with emission lines at 404.4 nm, and 404.7 nm) and mercury with an emission line at 404.656 nm were

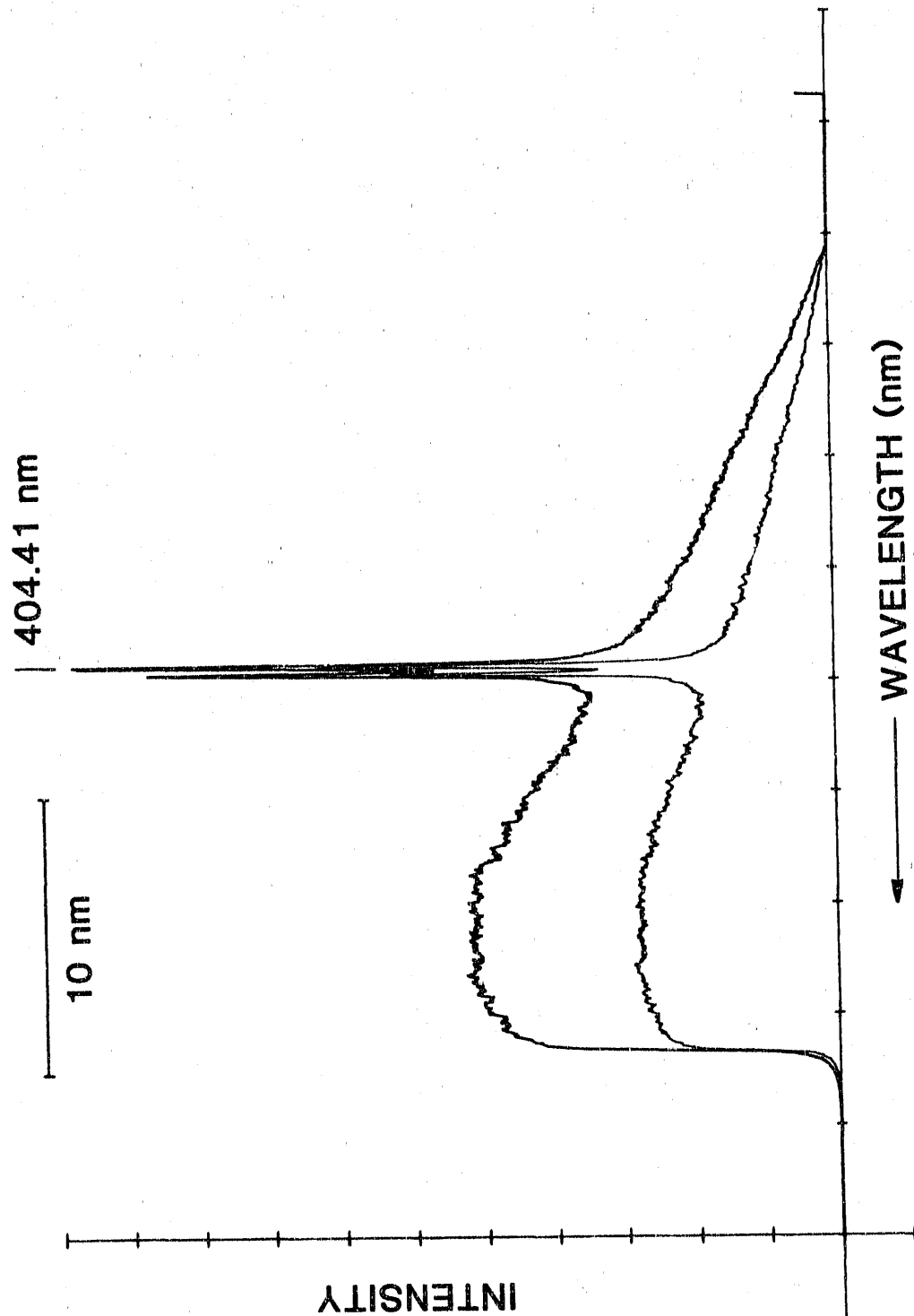


Figure 6. Potassium Emission Lines at 404.4 nm and 404.7 nm Observed in Recovery Boiler Mill Tests (Union-Camp Mills, Franklin, VA)

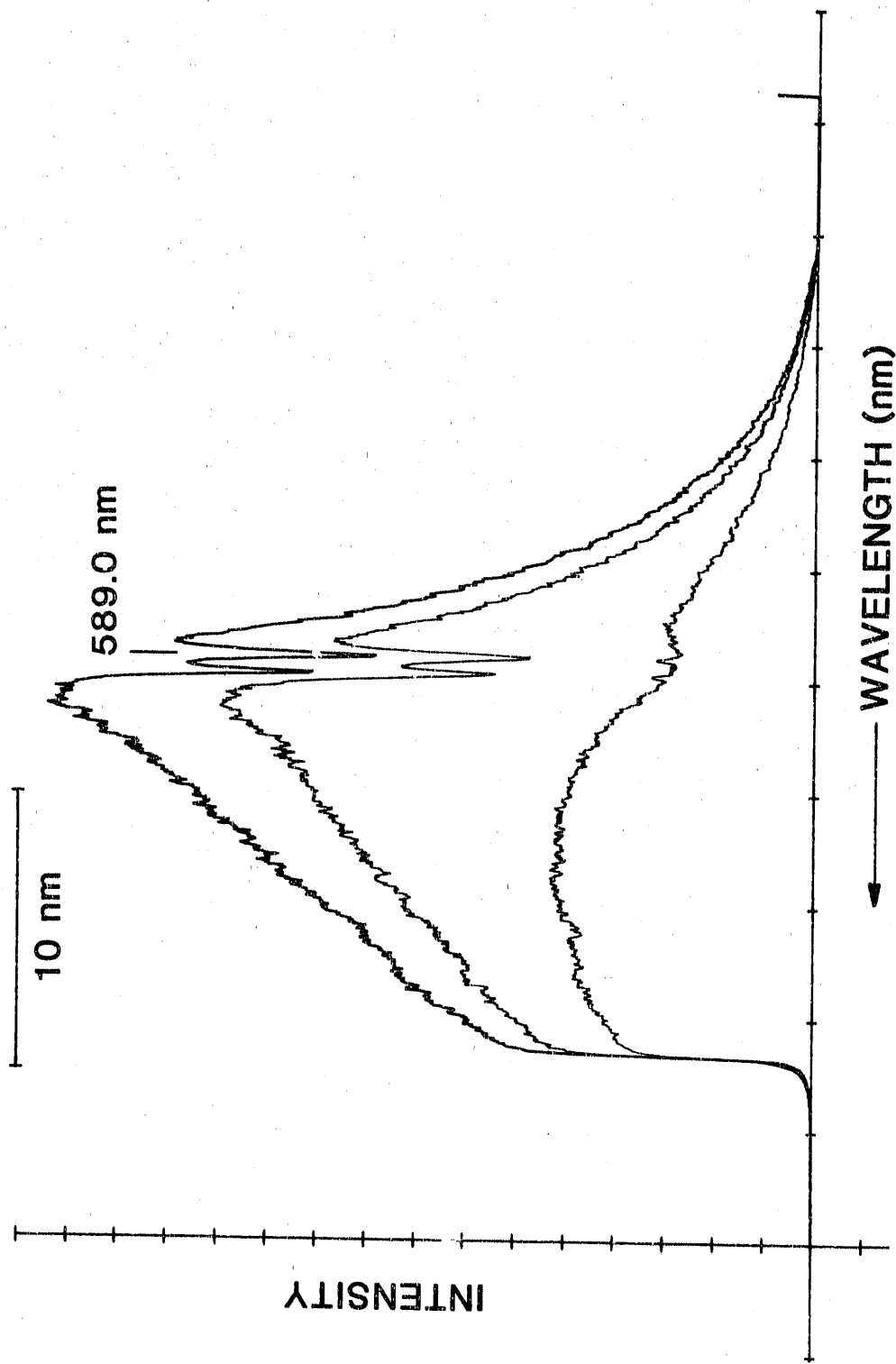


Figure 7. Sodium Emission Lines at 589 nm Observed in Recovery Boiler Mill Tests (Union-Camp Mills, Franklin, VA)

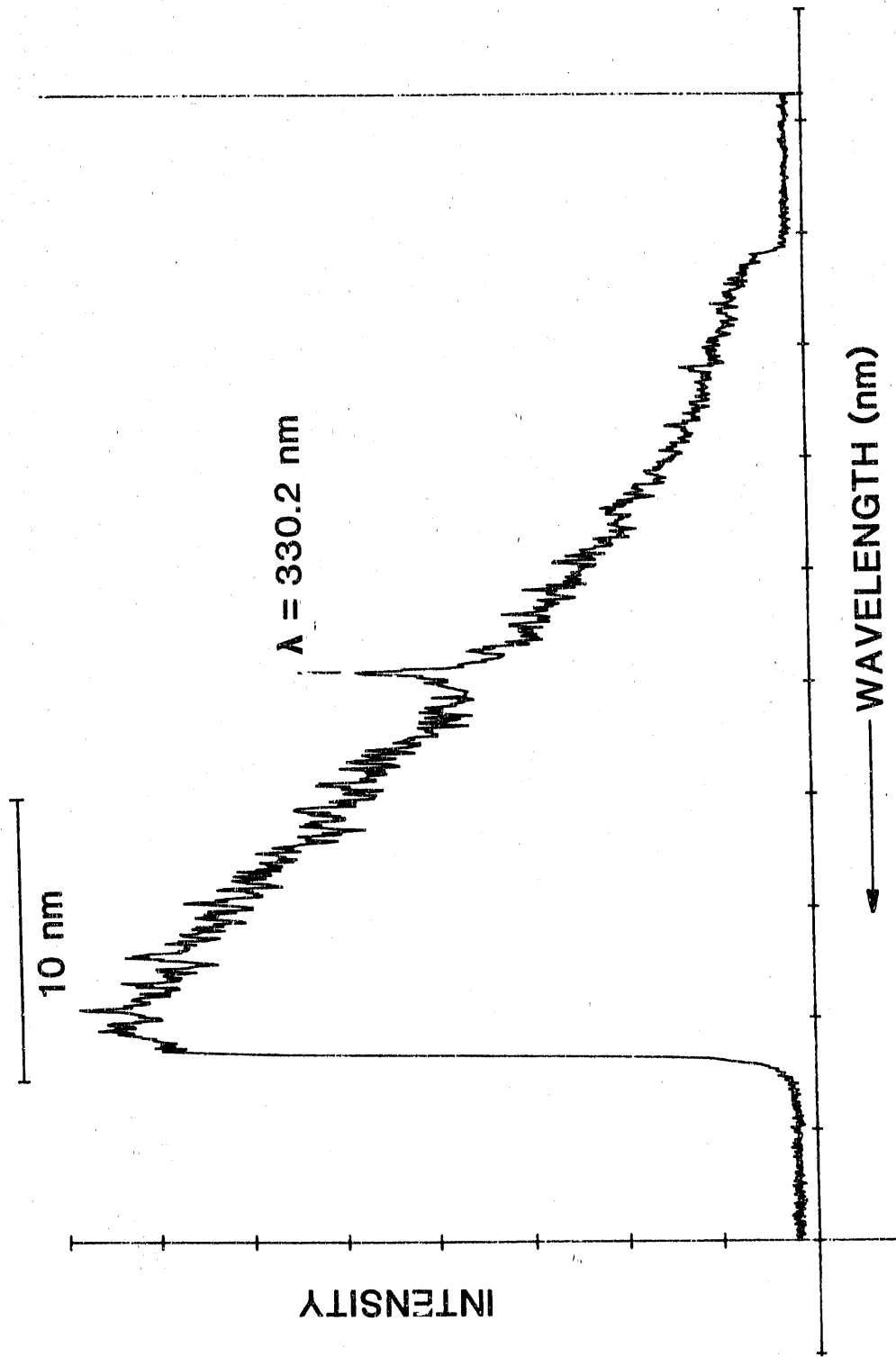


Figure 8. Sodium Emission Line at 330.2 nm Observed in Recovery Boiler Tests (Union-Camp Mills, Franklin, VA)

likely candidate emitters. In order to identify the emitter, different substances were selected so that each substance would contain only one candidate emitter. For example KCl and KOH were selected for potassium and sulfur and sulfur compounds for S and SO₂ emissions. Each of these compounds were then introduced individually into the flame and emission spectra around 405 nm were obtained. Initial observations indicated potassium to be the best candidate as the emitting species since the laboratory spectral profiles at 405 nm matched those from the recovery boiler best.

Further exploration in the laboratory with KCl injection into methane/air flames yielded not only emissions due to potassium at 404.4 nm and 404.7 nm, but also at 766.5 nm and 769.9 nm. Based on these results, the line intensity ratio technique was developed using the potassium emission doublets at 404.4 nm and 766.5 nm. Since these two lines are widely separated, simultaneous recording of intensity levels at these two wavelengths was not possible with a high resolution spectrometer. Consequently, these intensity levels were recorded by changing the spectrometer setting (figures 9 and 10) which introduced a time delay between measurements during which the flame characteristics could conceivably change. To minimize such changes, a nebulizer was used to introduce potassium solution and stabilize flame characteristics.

Several tests, using a methane/air flame with KCl solution mist injection, were conducted to obtain the line intensity ratio, I_1/I_2 . The gas temperature, T, was determined using eq 2 and spectral line constants [9,10]. These computations yielded reasonable but over estimated values of temperatures, as shown in table 1. For example, the line intensity ratio technique yielded a temperature of 2123 °C as compared to 1952 °C obtained from theoretical computations for a near stoichiometric methane/air flame. Likewise this technique over-estimated the flame temperatures for fuel-rich and fuel-lean flames. These discrepancies were attributed to calibration errors and to uncertainties in the spectroscopic constants. The results, despite the associated uncertainties, did indicate the potential for application of this technique to the black liquor recovery boiler.

Table 1. Pre-mixed methane/air flame temperatures measured by line intensity ratio technique

Equivalence Ratio	Measured Temperature T (K)	Calculated Temperature T _a (K)	T _a /T
1.0	2396	2225	1.08
1.1	2366	2210	1.07
0.84	2196	2053	1.07

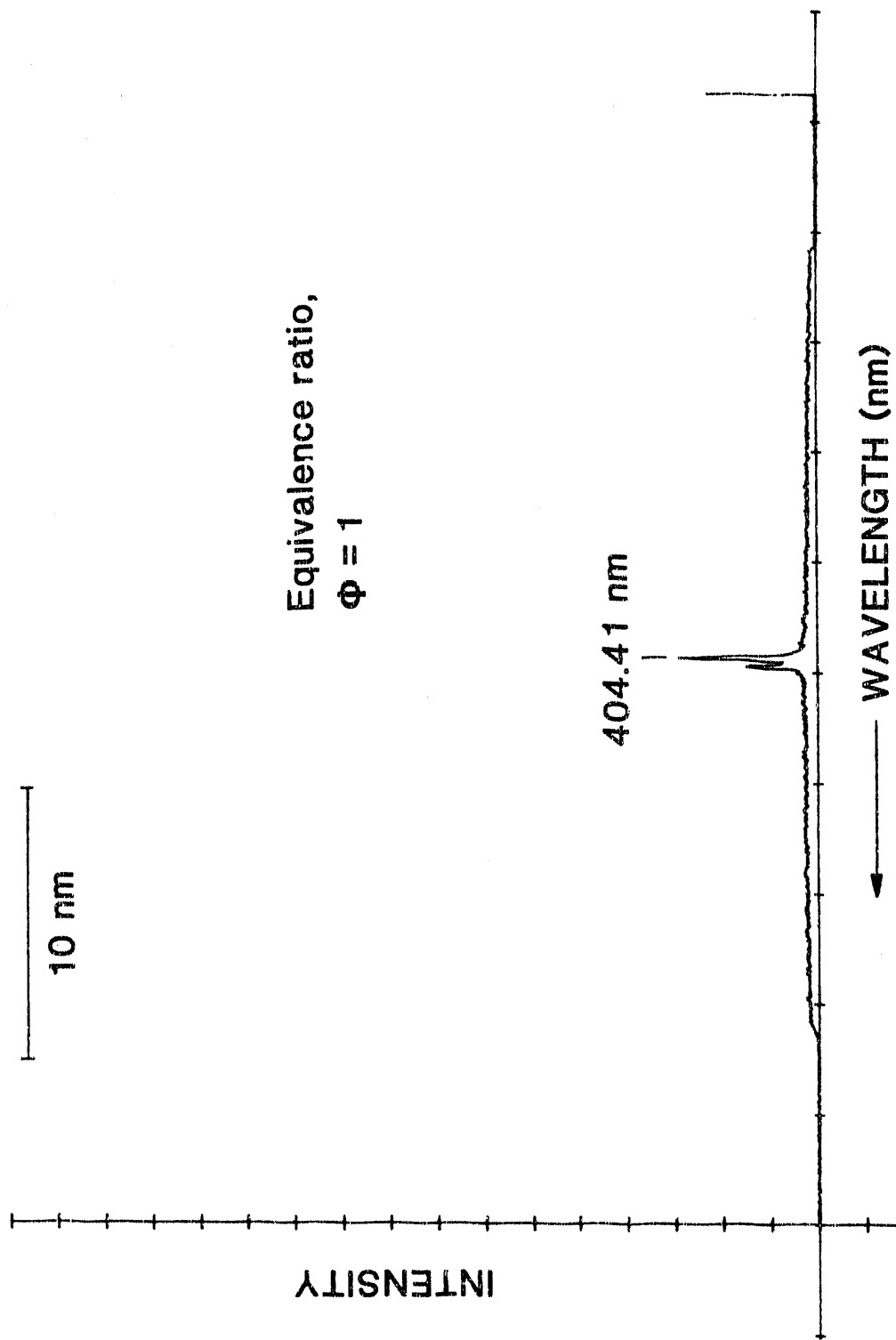


Figure 9. Potassium Emission Lines at 404.4 nm and 404.7 nm Obtained from a Premixed Methane/Air Flame Injected with KCl Solution

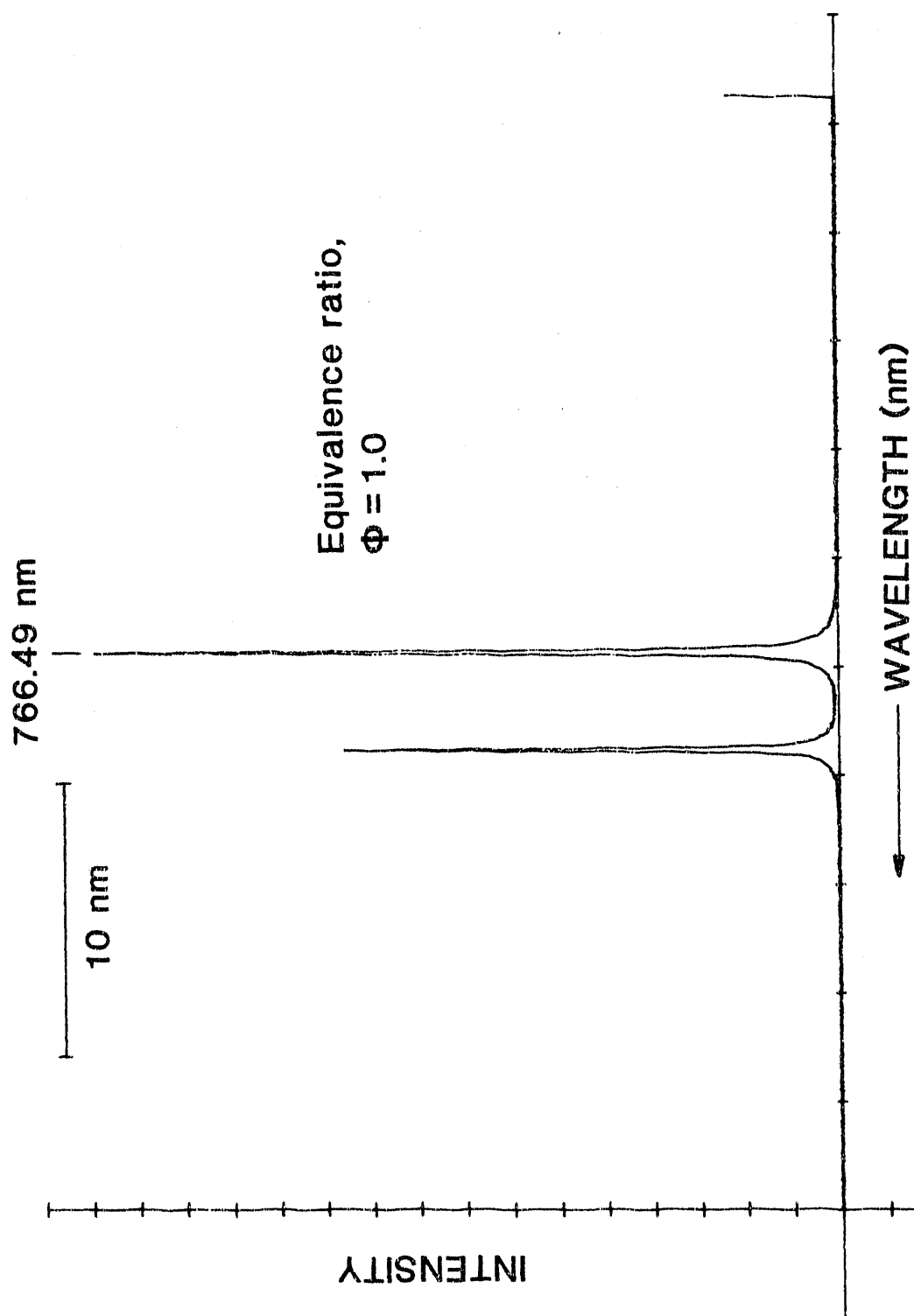


Figure 10. Potassium Emission Lines at 766.5 nm and 769.9 nm Obtained from a Premixed Methane/Air Flame Injected with KCl Solution

3.4 Four Color Sensor System

Due to the strong background emission in the recovery boiler, background subtraction was used in the prototype sensor system resulting in intensity measurement capability at four wavelengths; at the two potassium doublet locations and at two wavelengths slightly removed from each doublet to provide background intensity subtraction. A fiber optic system has been designed and developed to satisfy these requirements. This system, shown in figure 11, consists of a four-branched optical fiber bundle with the common end viewing the source (a calibration lamp, a laboratory flame, or the combustion zone in a black liquor recovery boiler). The common end collects the light from a source while the four branches split the light into four near-equal parts; each end of the four branches is equipped with a specific narrow band-pass filter, a silicon photodiode and an amplifier. The narrow band-pass filters were chosen so that the line intensities at the two emission wavelengths (λ_1 and λ_2) and the intensities of background continuum emission at wavelengths (λ_{1b} and λ_{2b}) could be obtained from the same source simultaneously. The outputs from the four detector/amplifiers were interfaced with an analog to digital convertor board with simultaneous sample and hold capability; the A/D convertor board is an integral part of a personal computer system. Observation data could be analyzed for temperatures based on conventional radiation (ratio) pyrometry using the continuum emission radiation measured at the wavelengths λ_{1b} and λ_{2b} (see for example references 4 and 5) in addition to temperatures based on the line intensity ratio technique.

Tests were conducted with the four color system utilizing ultra narrow bandpass interference filters; use of these filters reduced the signal level at 404.41 nm thereby reducing the signal to noise ratio. As a consequence, it was determined that further improvements would be required. The results obtained with this system are shown in table 2. These results were found to be encouraging and have indicated the potential of the four color sensing technique.

Table 2. Temperatures measured with four-color sensor system

Equivalence Ratio	Measured Temperature T (K)	Calculated Temperature T_a (K)	T/T_a
0.99	1933	2222	0.87
1.18	2027	2155	0.94
0.8	1828	2000	0.91

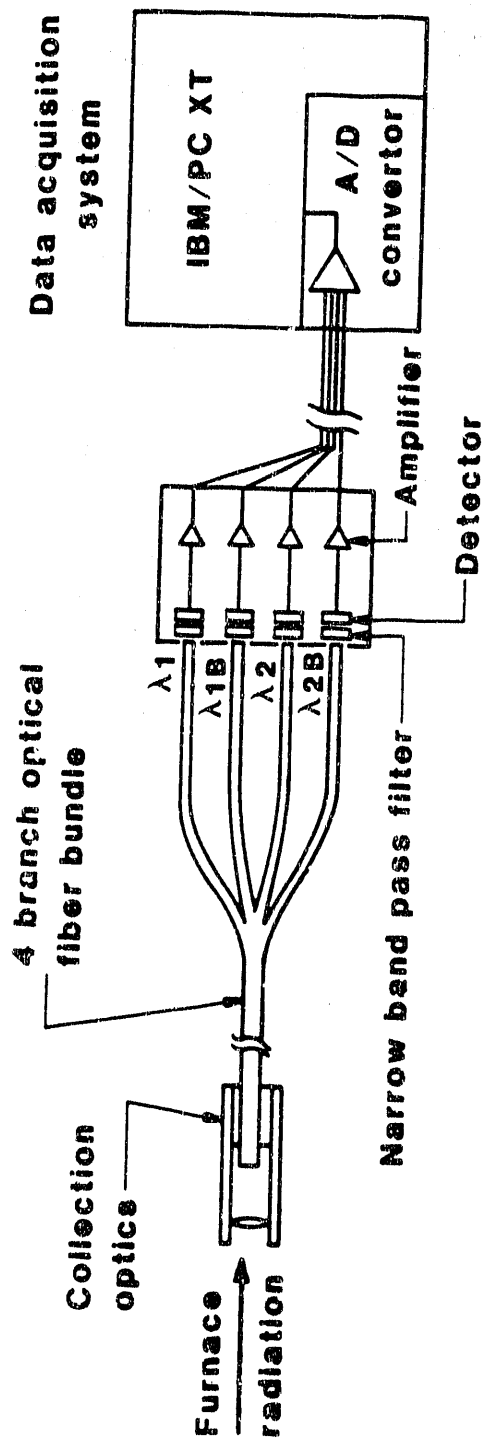


Figure 11. Four-Color Temperature Sensing System

3.5 Tests at Weyerhaeuser Mills, New Bern, NC

Mill tests performed at another recovery boiler of Combustion Engineering [12] design, i.e., without tertiary air injection, that was firing black liquor containing a low concentration (0.5 to 0.8 %) of potassium. During these tests, both spectral data in the wavelength range of 300 nm to 800 nm and four-color probe data were obtained; the spectra obtained confirmed the earlier recovery boiler data, i.e., both the 404.5 nm and the 766.5 nm were observed. However, potassium emission at 404.4 nm (fig. 12) obtained sequentially, clearly indicate that the emission lines at 404.4 nm and 404.7 nm were very weak. This can be attributed to the low concentrations of potassium in the black liquor fired. Typical intensity variations in recovery boiler emission spectra are shown in figure 13. Both the line intensities and the background continuum emission levels were observed to vary substantially. These mill tests confirmed for the first time the existence of potassium emission lines at 766.5 nm and 769.9 nm, as shown in figure 14. In addition, these spectra indicated rubidium emission line at 780 nm in the near infrared. As for emissions due to sodium, emission lines at 589.0 nm were readily observed as shown in figure 15; again, three records of spectra, obtained at the same port sequentially show the extent of changes in the recovery boilers. However, the weak sodium line at 330.2 nm observation in the previous boiler test was not observed.

In addition to obtaining the emission spectra with the OMA system, the four color temperature sensing system was used to obtain the line intensities and background emission levels. As the temperatures were low, the potassium emission intensities at 404.41 nm were weak and thereby the line intensity at 404.41 nm, which is essential for utilizing the line intensity ratio technique, could not be obtained. Consequently, the line intensity ratio technique could not be used for the measurement of gas temperature. However, the analysis, based on Planck's law and using the measured intensities of continuum emissions, yielded reasonable temperatures, shown as a function of time in figure 16. These temperature variations, which are indicative of the temperature of particulate matter, obviously point out that the changes in the reaction zone are relatively quick and significant.

4. Optical Depth Effects in the Recovery Boiler

Spectral profiles from mill tests have clearly shown two distinctive characteristics: 1) the emission line at the wavelength of 766.49 nm appears almost always in self-absorption, (see figure 15) and 2) the emission spectra appears to be broadened mostly from collisional processes. The dip at the line center is indicative of self-absorption, resulting essentially from the existence of temperature gradients. The observed trend of line widths indicates line broadening, a potential concern regarding the limitation due to optical depth at this particular wavelength. Preliminary estimates have indicated that the optical depths at the two wavelengths, 404.41 nm and 766.49 nm are quite different; the combustion zone may be optically thin for emissions at 404.41 nm but optically thick for the emissions at 766.49 nm. A large

K EMISSIONS FROM RECOVERY BOILER

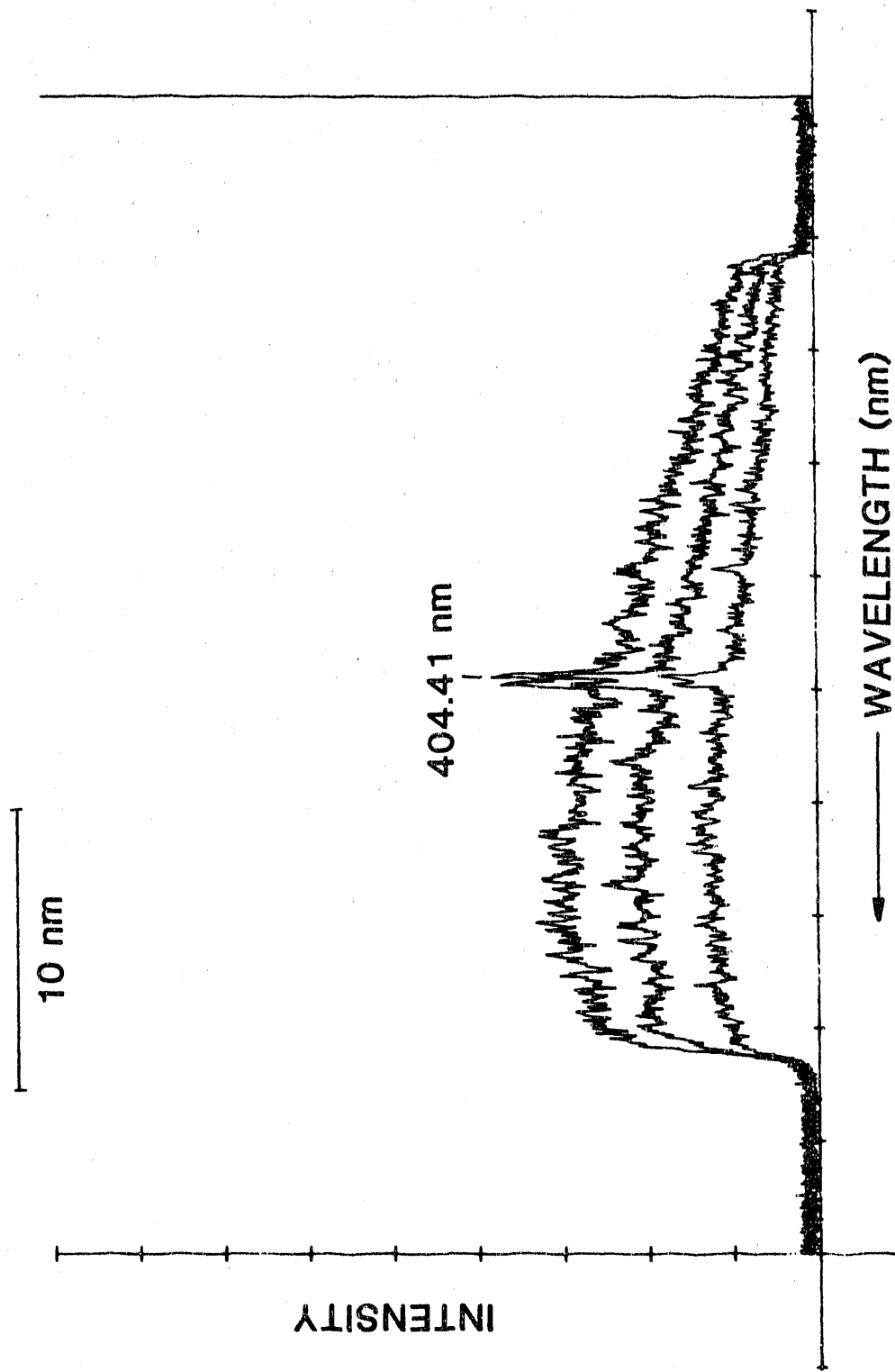


Figure 12. Potassium Emission Lines at 404.4 nm and 404.7 nm Observed in Recovery Boiler Tests (Weyerhaeuser Mills, New Bern, NC)

K EMISSIONS FROM RECOVERY BOILER

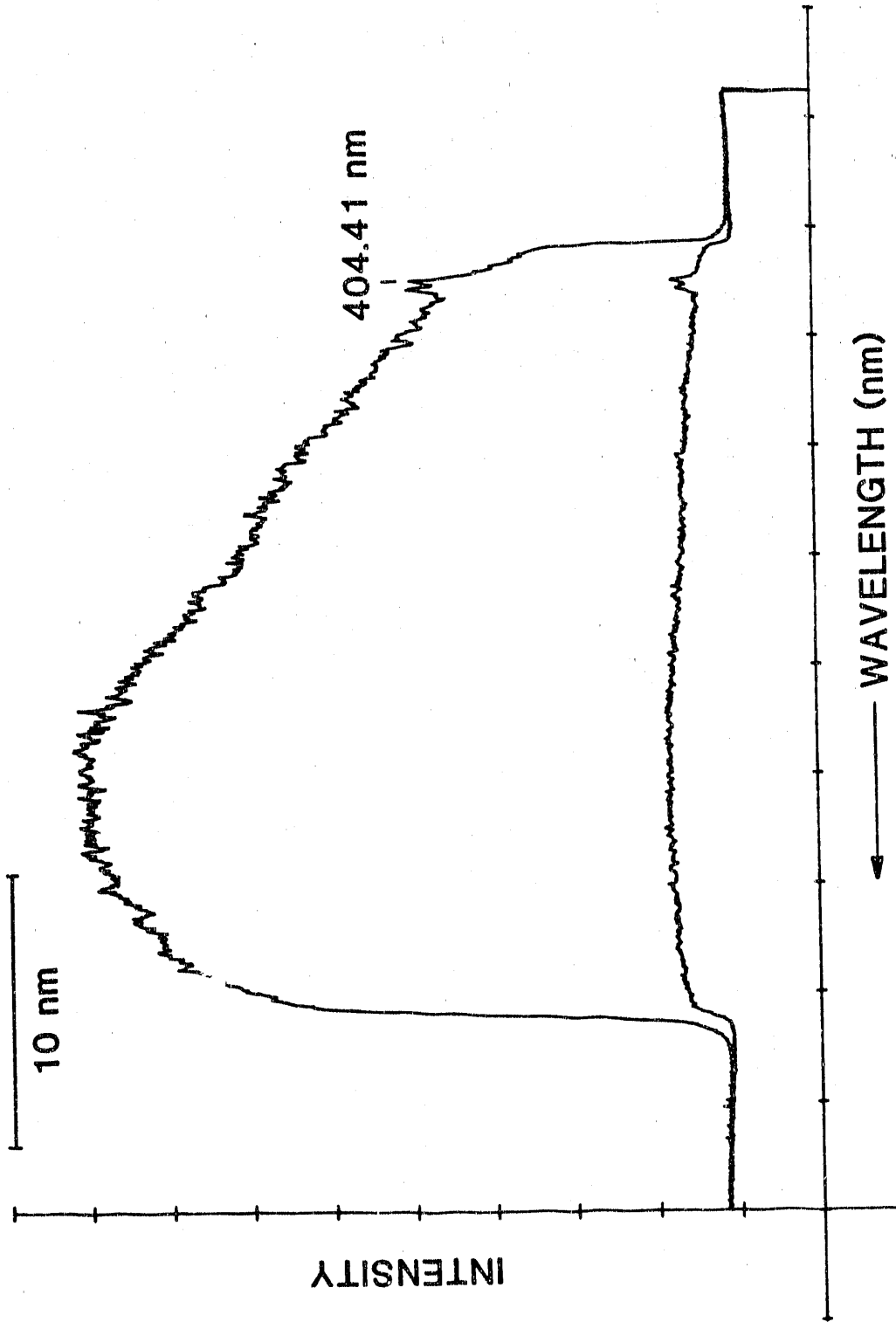


Figure 13. Variation of Continuum Emission in the Neighborhood of Potassium Emission Lines as Observed in Recovery Boiler Tests (Weyerhaeuser Mills, New Bern, NC)

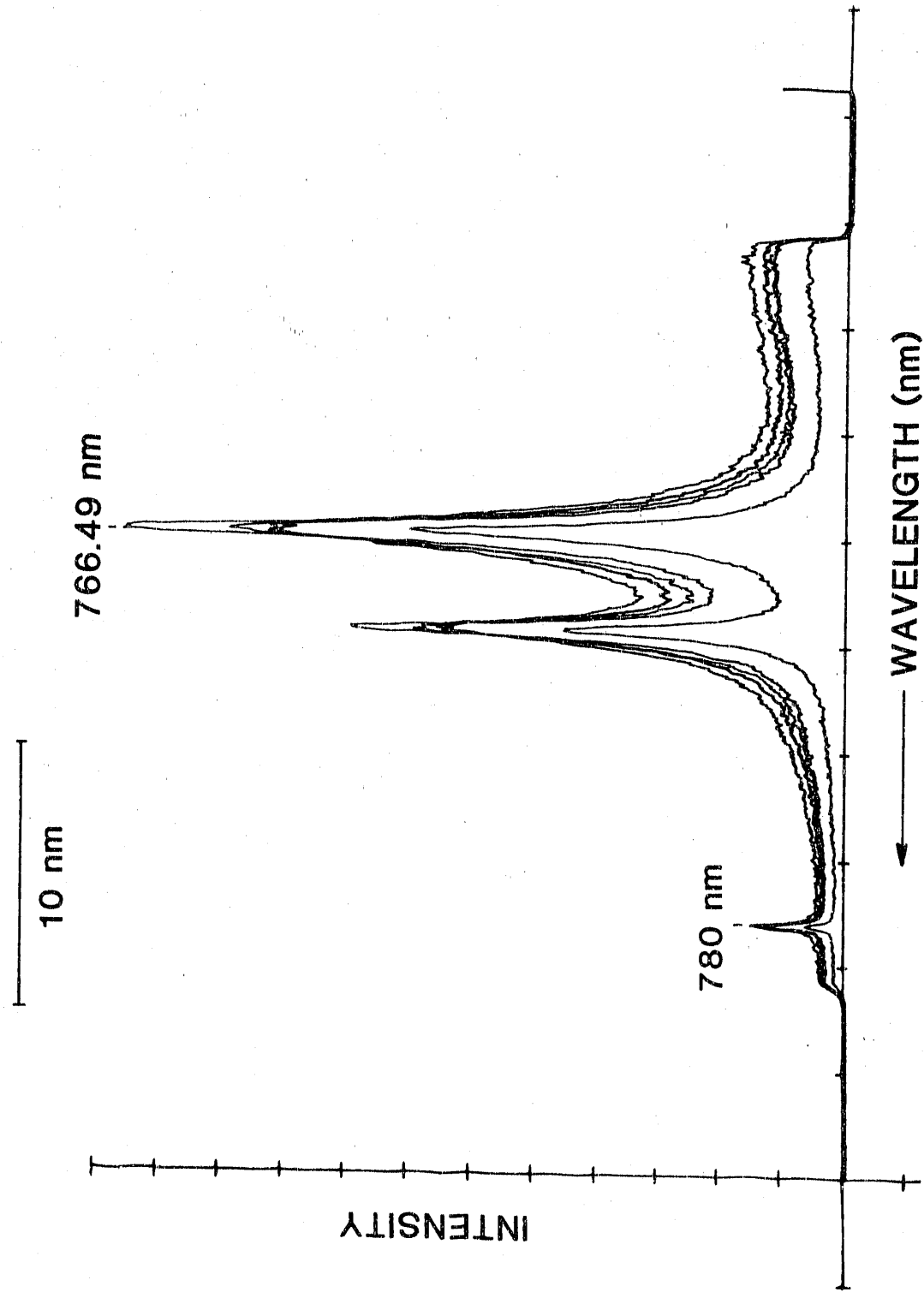


Figure 14. Potassium Emission Lines at 766.5 nm and 769.9 nm Observed in Recovery Boiler Tests (Weyerhaeuser Mills, New Bern, NC)

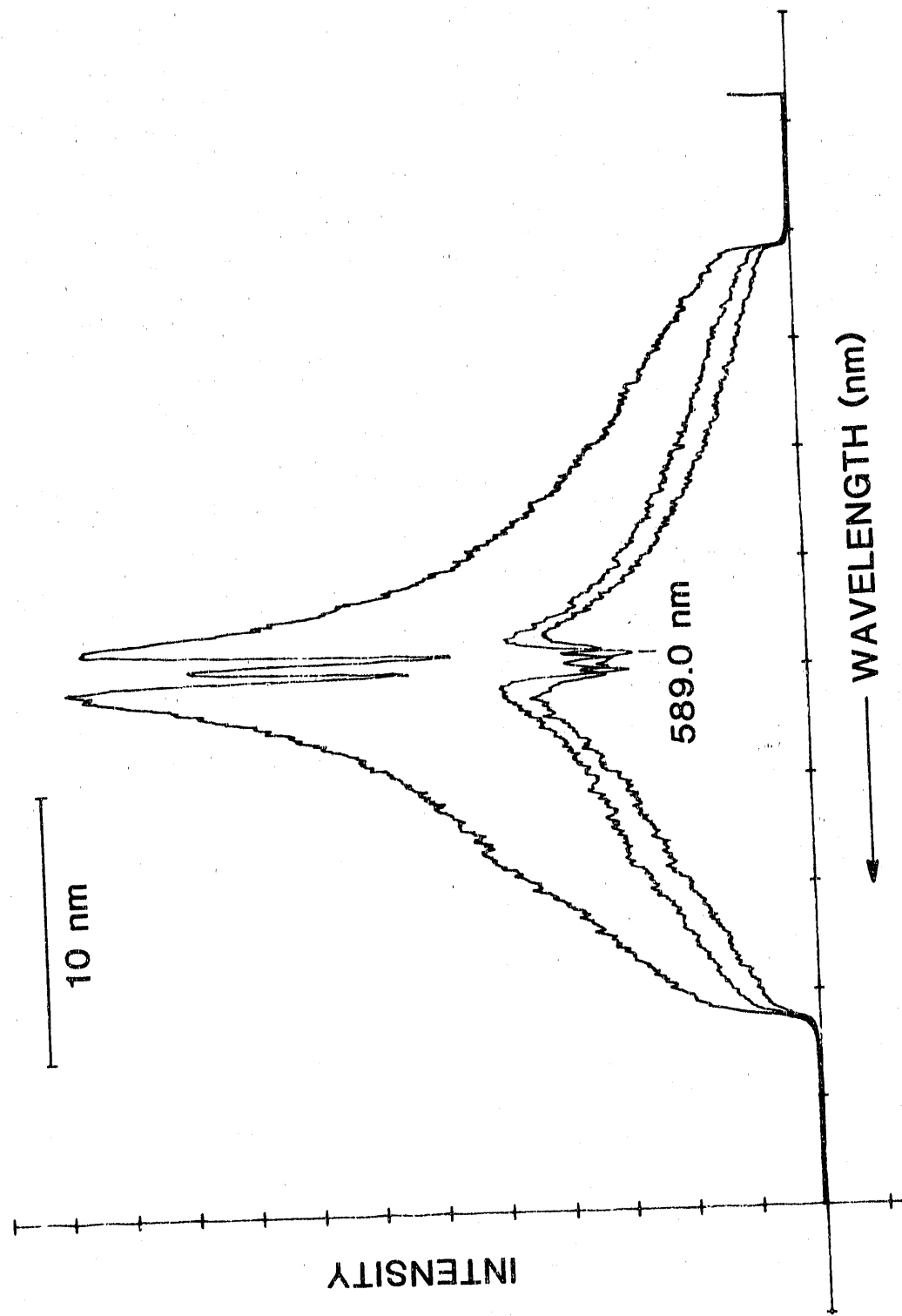


Figure 15. Sodium Emission Lines at 589 nm Observed in Recovery Boiler Tests
(Weyerhaeuser Mills, New Bern, NC)

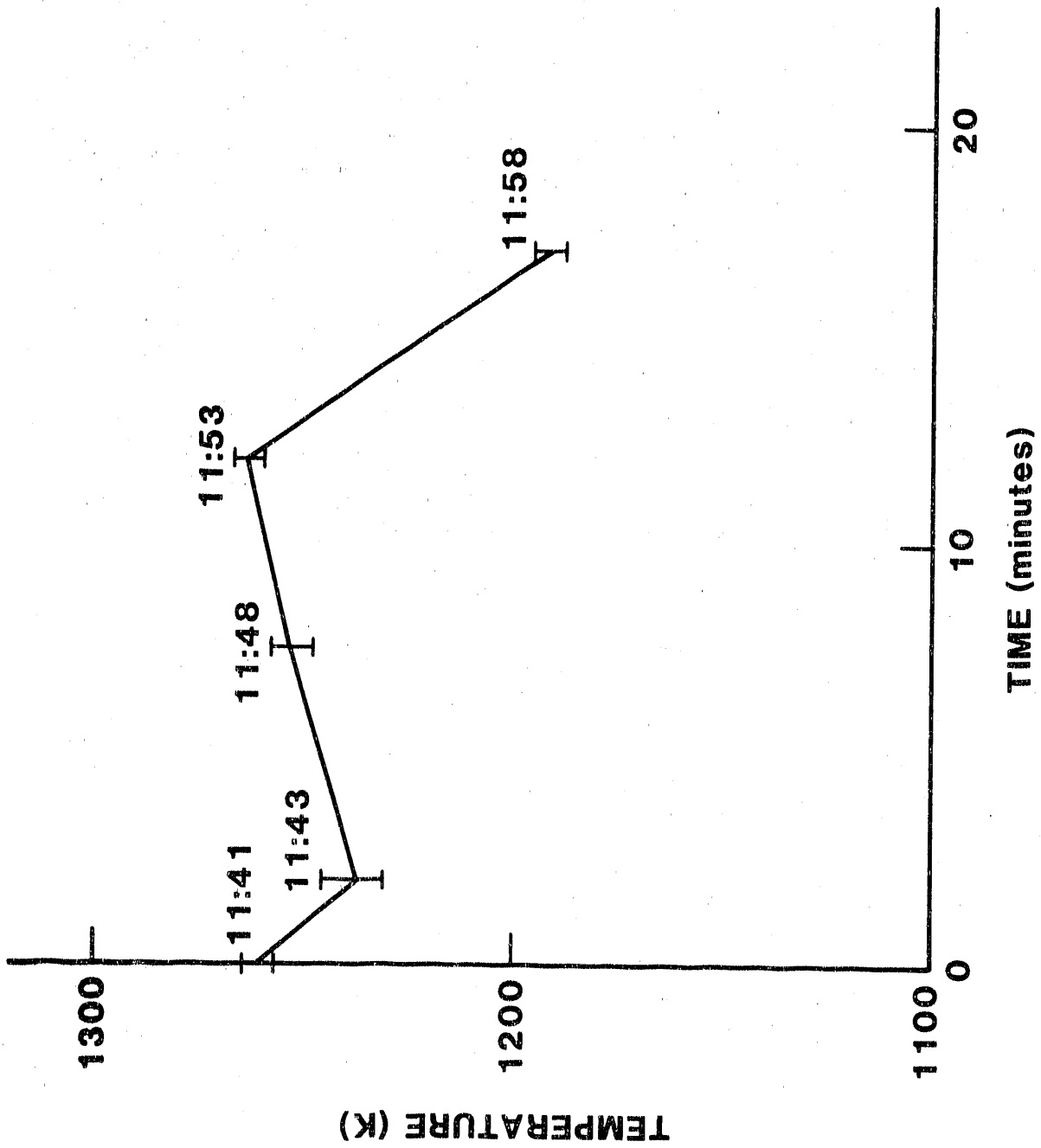


Figure 16. Measured Boiler Temperature

difference in the optical depth introduces significant inaccuracy in the temperatures calculated from, the line intensity ratio technique. A combined experimental and modelling effort was performed to study optical depth effects and to assess the impact of them on this temperature measurement technique.

4.1 Investigation of Optical Depth Using a Traversing Probe in the Recovery Boiler

Since it is impractical to simulate the recovery boiler environment in the laboratory, a sequence of traversing probe tests was planned and executed to estimate optical depths in the recovery boiler. The objective of these tests was to acquire spectroscopic data at various position in the boiler in two directions, i.e., toward opposite walls, to determine the magnitude of optical depth effects in the recovery boiler environment. The approach consisted of inserting an optical probe into the reaction zone to known depths and obtaining emission profiles at 404.41 nm and 766.49 nm looking straight into the reaction zone as well as looking directly backwards.

4.2 Selection of Recovery Boiler

The selection of a recovery boiler for these tests depended on both technical criteria and practical considerations. The two technical criteria were for recovery boiler operation: 1) operation temperatures above 1038 °C (1900 °F), and 2) high potassium concentration (in the range of 2 to 3%) in the black liquor. These criteria were essentially a statement of conditions required to manifest worst case optical depth differences in recovery boilers.

In addition to these technical criteria, there were three practical considerations used in the selection of the candidate boilers:

- 1) availability of optical probe access ports of sufficient size,
- 2) availability of ample room surrounding the boiler to accommodate a long traversing probe, and
- 3) boiler availability.

An industry survey of potassium concentrations in black liquors from various US mills (table 3) revealed that a number of recovery boilers are fired with black liquors containing about 1 to 2% potassium. It was also generally accepted that the operating temperatures in the recovery boiler combustion zone vary from a low 1038 °C (1900 °F) to a maximum of 1260 °C (2300 °F). Based on these criteria, a mill site was selected as the candidate for conducting the traversing probe tests.

Table 3. Black liquor composition data (expressed as weight % of dry liquor solids)

Mill No.	Na ₂ CO ₃	NA ₂ O ₄	Residual active alkali (as Na ₂ O)	Na	K	S	Msr'd sulfur ash	Calc. sulfur ash
1	8.3	1.5	4.8	17.2	2.4	2.56	60.3	58.4
2	10.5	1.0	6.35	19.6	0.88	0.35	63.3	62.5
3	10.7	4.3	5.45	19.4	1.0	3.96	63.4	62.1
4	9.1	2.6	6.5	18.6	0.93	3.49	62.3	99.5
5	6.8	2.6	5.9	17.2	2.7	4.28	60.4	94.1
6	10.3	4.1	4.25	18.9	0.8	3.05	59.8	60.1
7	8.3	4.3	6.3	18.9	1.0	4.58	62.4	60.2
8	7.5	3.8	6.0	18.0	0.92	3.68	59.4	57.4
9	9.9	5.8	5.8	19.6	2.5	4.61	66.9	66.1
10	9.9	2.9	5.0	18.7	1.0	3.89	60.4	68.0
11	12.3	3.2	7.75	20.5	1.4	4.29	69.2	66.4
12	9.4	2.2	6.0	18.7	1.8	3.92	63.2	61.7
13	7.1	2.3	5.3	17.3	1.2	3.35	59.0	56.1
14	6.9	8.3	6.0	19.8	1.1	6.24	63.9	63.6
15	8.4	4.6	6.8	18.4	1.2	3.95	62.6	59.5
16	9.0	1.6	6.25	17.9	1.5	3.30	60.3	58.6
17	9.6	4.6	4.9	19.3	1.5	4.82	62.9	62.9
18	7.0	2.5	5.55	17.4	0.97	3.38	57.3	55.9
19	10.9	3.2	4.05	18.1	0.88	3.77	60.1	57.8
20	8.7	3.9	7.4	19.4	2.2	3.49	65.1	64.8
21	8.1	4.5	3.9	18.2	1.8	3.79	60.6	60.2
22	7.8	3.2	6.05	18.6	2.1	3.51	63.3	62.1
23	6.7	3.3	6.3	18.6	1.1	4.45	61.1	59.9
24	7.8	0.9	7.3	19.2	1.6	4.02	63.2	62.8
25	9.1	2.6	5.55	18.0	0.44	3.69	59.0	56.5
26	8.9	2.8	5.6	18.3	1.2	3.95	61.3	59.2
27	6.6	2.7	6.85	18.5	1.2	5.57	61.9	59.8
28	7.3	1.5	8.6	20.5	0.86	3.28	65.3	65.2
average	8.7	3.2	5.95	18.7	1.36	3.83	62.1	60.7

4.3 Probe Design and Fabrication

Based on practical considerations, an experimental traversing probe system has been designed, developed and fabricated. A description of the probe's mechanical details are given elsewhere [13]. The probe design was specific to the test mill. The traversing probe (fig. 17) consisted of an inconel probe body (about 1.9 in OD, 1.12 in ID and 12 feet long). The inconel body was fabricated with three concentric inconel tubes providing a passage for the coolant (Dowtherm J [12]), circulated by a heavy duty pump. The probe body housed a probe head

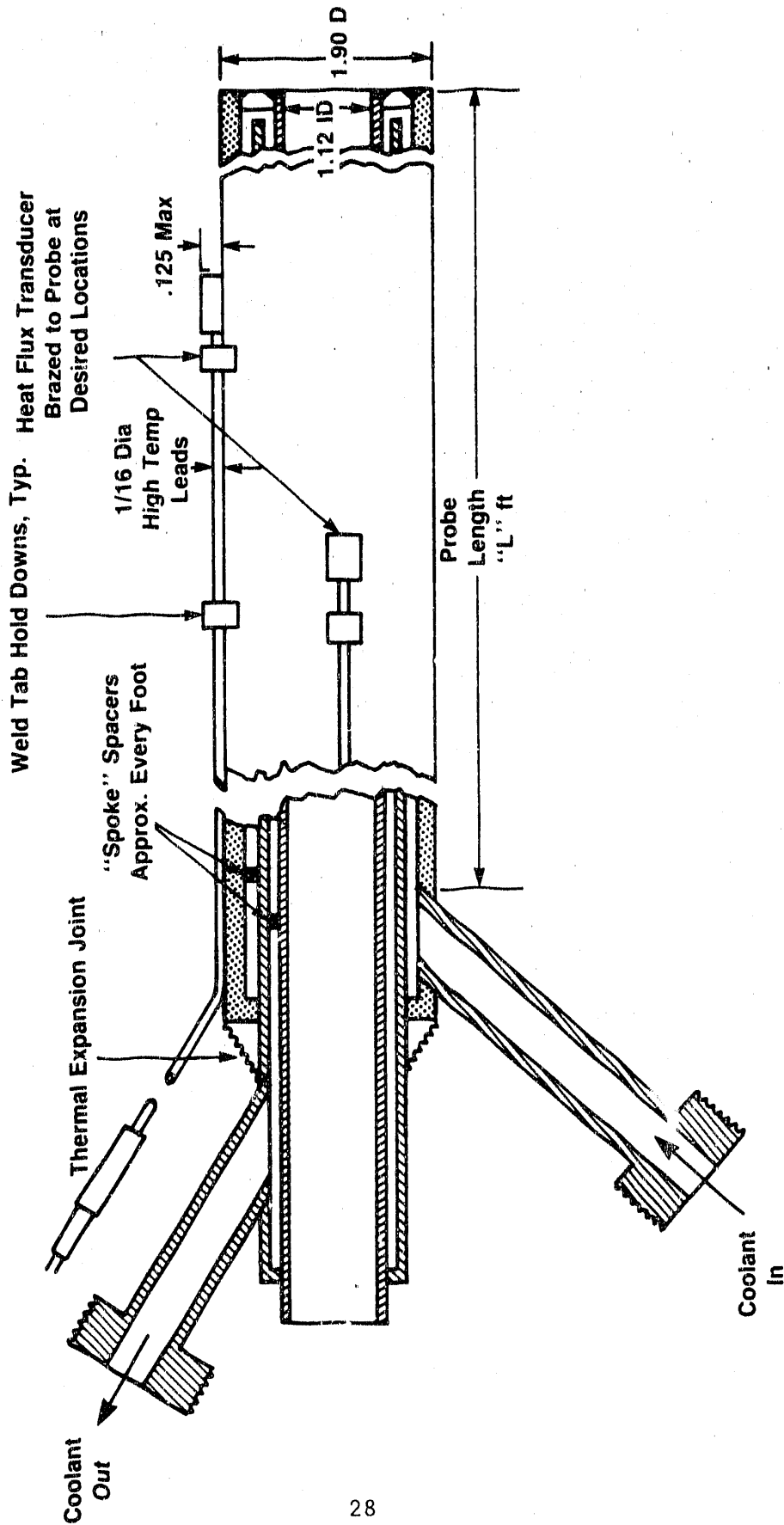


Figure 17. Probe Body

(fig. 18) consisting of two separate optical probes - one to view straight into the reaction zone and the other viewing backwards. The optical viewing ports were provided with inert gas purging to minimize deposits, and the probe head was cooled independently by circulating the coolant with another small pump. The outer surface of the probe body was provided with a total of ten heat flux transducers at selected intervals as shown in figure 17. The probe was provided with a support system (fig. 19) to facilitate extraction from the boiler.

4.4 Mill Tests with the Traversing Probe

A sequence of tests were planned to be carried out at the Weyerhaeuser Mills as documented in Appendix A. These tests required the positioning of the long traversing probe at one of the selected access ports for horizontal insertion to various depths. The experimental arrangement for obtaining emission spectra was in principle the same as the one used in the previous tests (fig. 2). The three major differences were:

- 1) there was no collection optics and the fiber optic bundles collected and transmitted the light incident on their ends,
- 2) the optical fiber bundle used in this arrangement was necessarily much longer than the one used in the earlier test arrangements, and
- 3) this arrangement had an additional (patch chord) bundle to interface the optical fiber bundles of the probe head with the spectrometer.

The general arrangement of the probe on its support system is shown in figure 20. The probe head and the optical fiber bundles associated with the probe are shown in figure 21. As the probe was designed for a maximum depth of penetration of about 8 feet, the penetration depth was changed at 2 foot intervals. At each probe location spectral scans were recorded of the emission spectra. The data obtained at each probe location consisted of the spectral profiles in the 404 nm and 766 nm regions, obtained with both fibers. In addition, these data were supplemented with the local heat flux data from the heat flux sensors.

These mill tests were originally planned to investigate the reaction zones at the first four floor levels, beginning the testing at the fourth floor level and concluding at the primary air level. Such a sequence was adopted to increase the survivability of the probe in the harsh environment especially at the primary air level. However, at the time of testing it was discovered that the recovery boiler was operating at temperatures of approximately 927 °C (1700 °F), substantially lower than the normal operating temperatures. As a consequence it became necessary to change the original sequence of the traversing probe tests and begin with the second floor level and later move to the primary air level; the tests were prematurely terminated at the primary air level because of an unplanned mill shut-down.

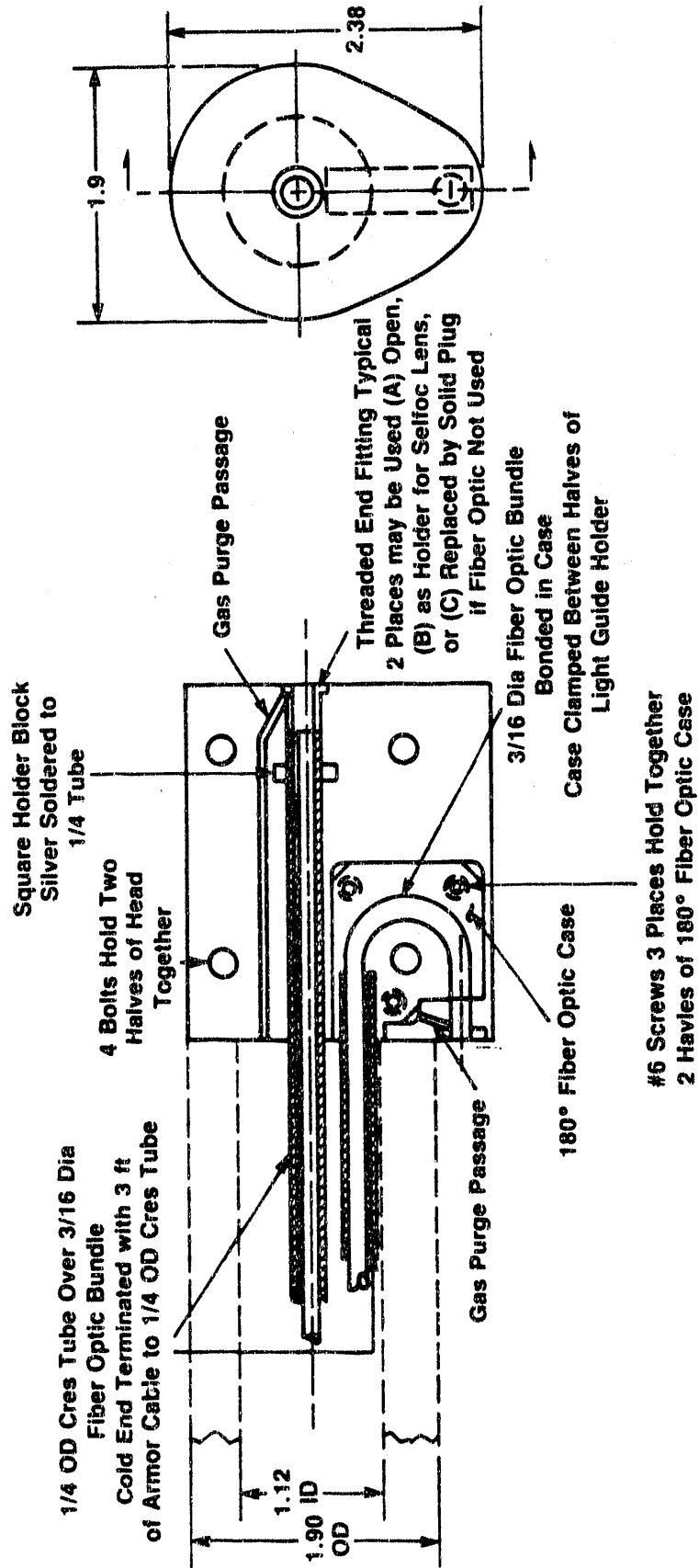


Figure 18. Probe Head

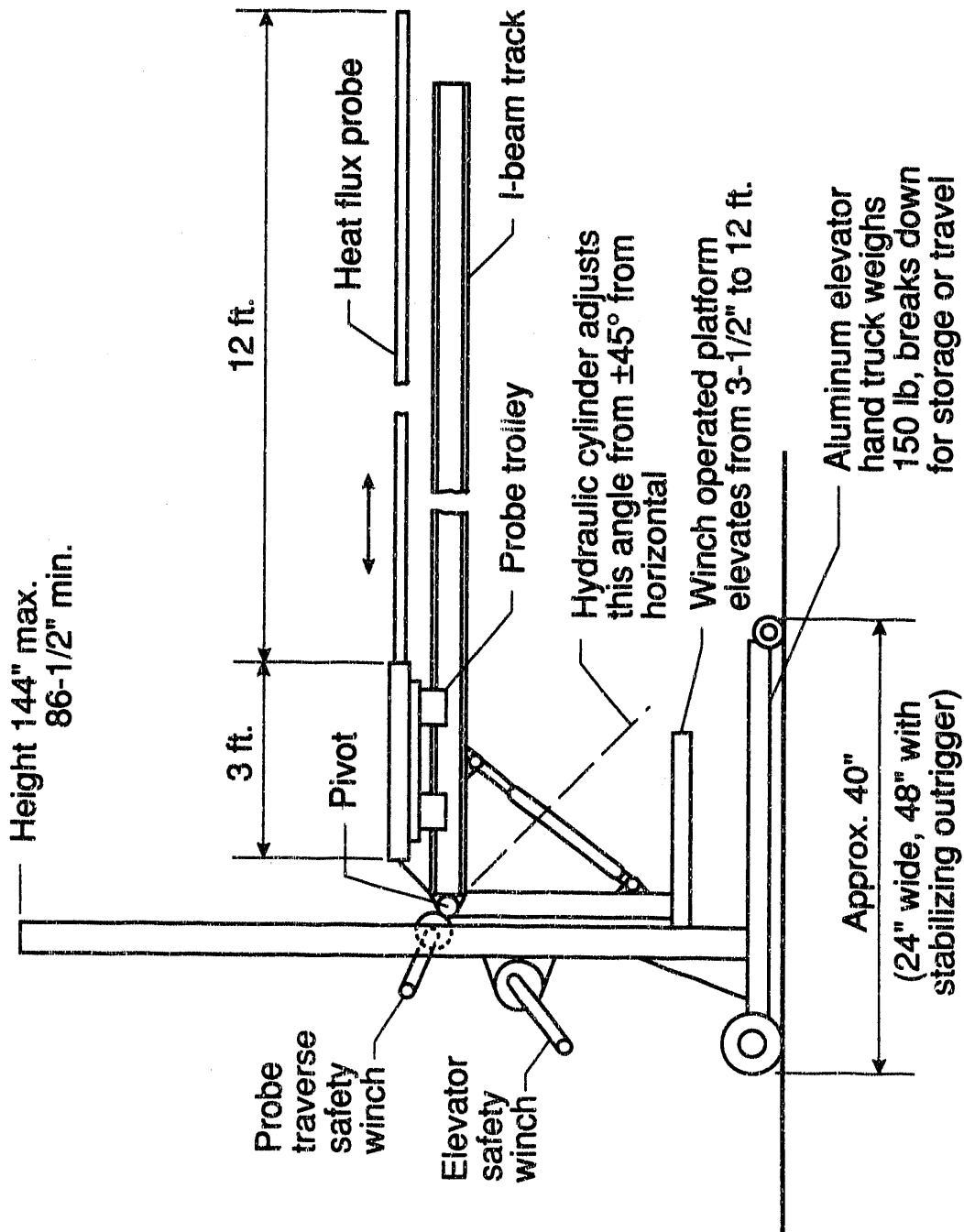


Figure 19. Probe Support System

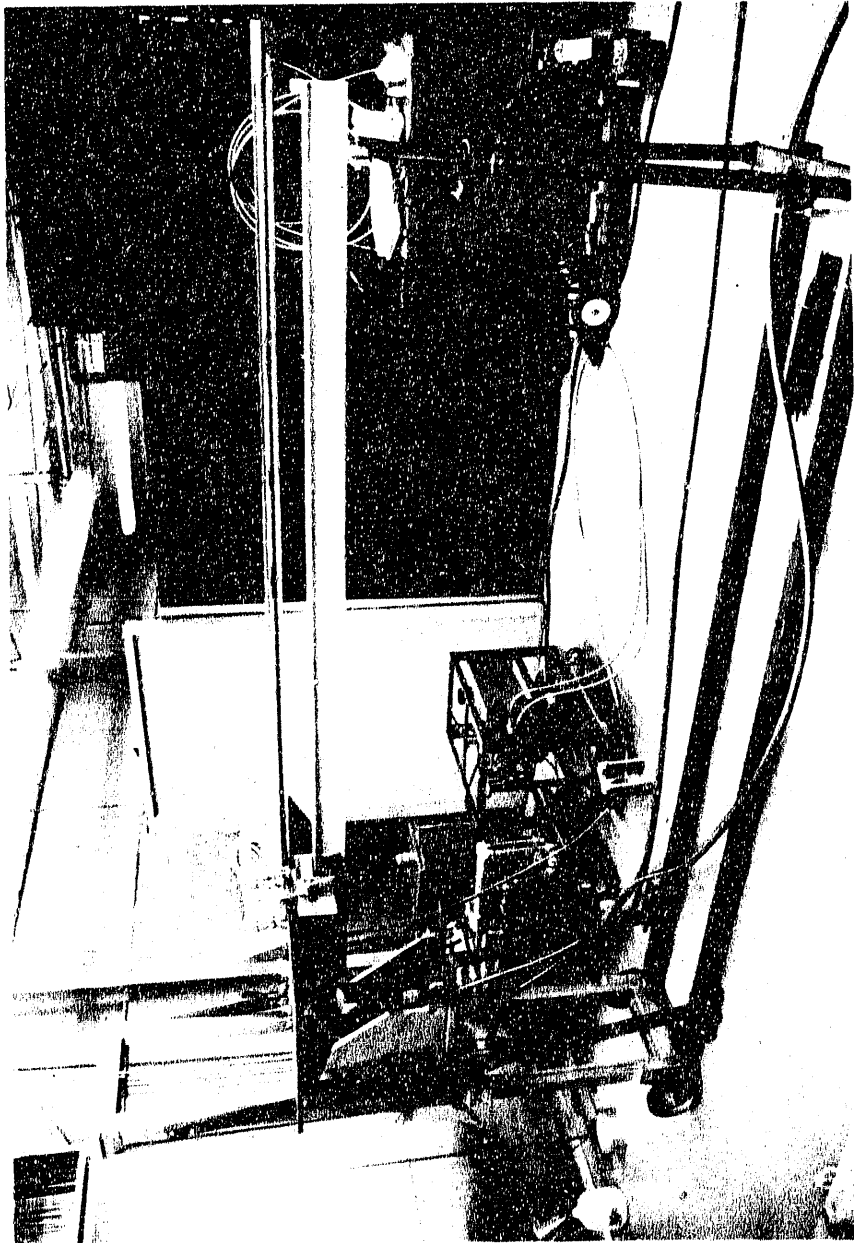


Figure 20. Experimental Arrangement for Traversing Probe Tests (Photograph)

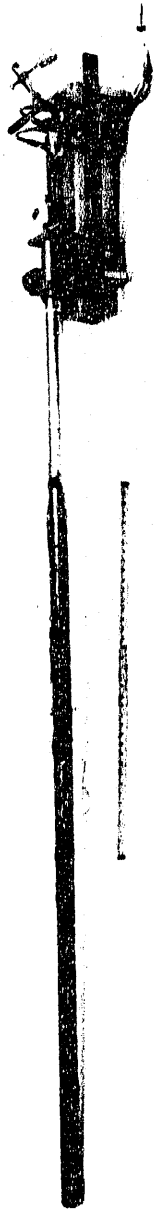


Figure 21. Probe Head with Optical Fiber Bundle (Photograph)

In these tests, the spectral records were obtained with the OMA/spectrometer system while the heat flux data were obtained with a micro-computer based data acquisition system, specially adapted for this purpose.

During each test, the probe was subjected to an extremely harsh environment; the top of the probe body was covered rapidly with black liquor and char. Within a brief period the heat flux sensors and the optical probe ports were found to be completely covered. As a consequence there was very limited time available for data acquisition; in between two successive insertions of the probe, an effort to clean-up the probe was required. As a result, there was some delay in the spectral data obtained at various probe locations. The black liquor was found to be very detrimental to the heat flux sensor leads. Black liquor would first seep under the sheath containing the sensor lead wires, expand and raise the sheath away from the probe tube. Once the sheath is separated from the cool surface of the probe body, the black liquor readily burns and damages the sheath and the lead wires as shown in figure 22. Therefore, data from some heat flux sensors could not be acquired because of this unexpected failure mode.

4.5 Test Results

Although these tests were terminated prematurely because of an unplanned mill shut-down, some useful data were obtained. These data include both the emission spectra and the local heat flux in the recovery boiler.

The initial tests were conducted without the use of the traversing probe. In these tests the OMA was used to obtain the emission spectra; the observed spectra were found to be weak. For example, figure 23 shows the emission spectra at 589 nm corresponding to sodium. In contrast to the extremely intense signal levels observed (mostly in self-absorption) in the other boilers, the emission spectra of sodium was weak and at times was found to vanish; also, the spectra did not indicate any dip at the line center. Likewise, the potassium emission lines at the wavelength of 766.49 nm, as shown in figure 24, were weak and didn't show any indication of self-absorption. Observation of the 404 nm region showed no signal above background. The only explanation for these weak signals was that the reaction zone temperature was low. This conclusion was confirmed independently by a thermocouple measurement which yielded a low temperature of 927 to 954 °C (1700 ° to 1750 °F).

Figure 25 shows the emission spectra of sodium obtained at the first floor level. These records, although only a few in number, clearly demonstrated the two important features - significant line broadening and the characteristic depression due to self-absorption - commonly found in all the mill tests. In addition, the emission intensities did fluctuate to some extent, but not as widely as in the previous mill tests.

The emission profiles of potassium at 766.49 nm viewing straight into the reaction zone clearly indicated self-absorption. Figure 26 shows two records of spectra obtained successively with the probe head



Figure 22. Optical Probe Section Showing Damage to Heat Flux Probe Terminals

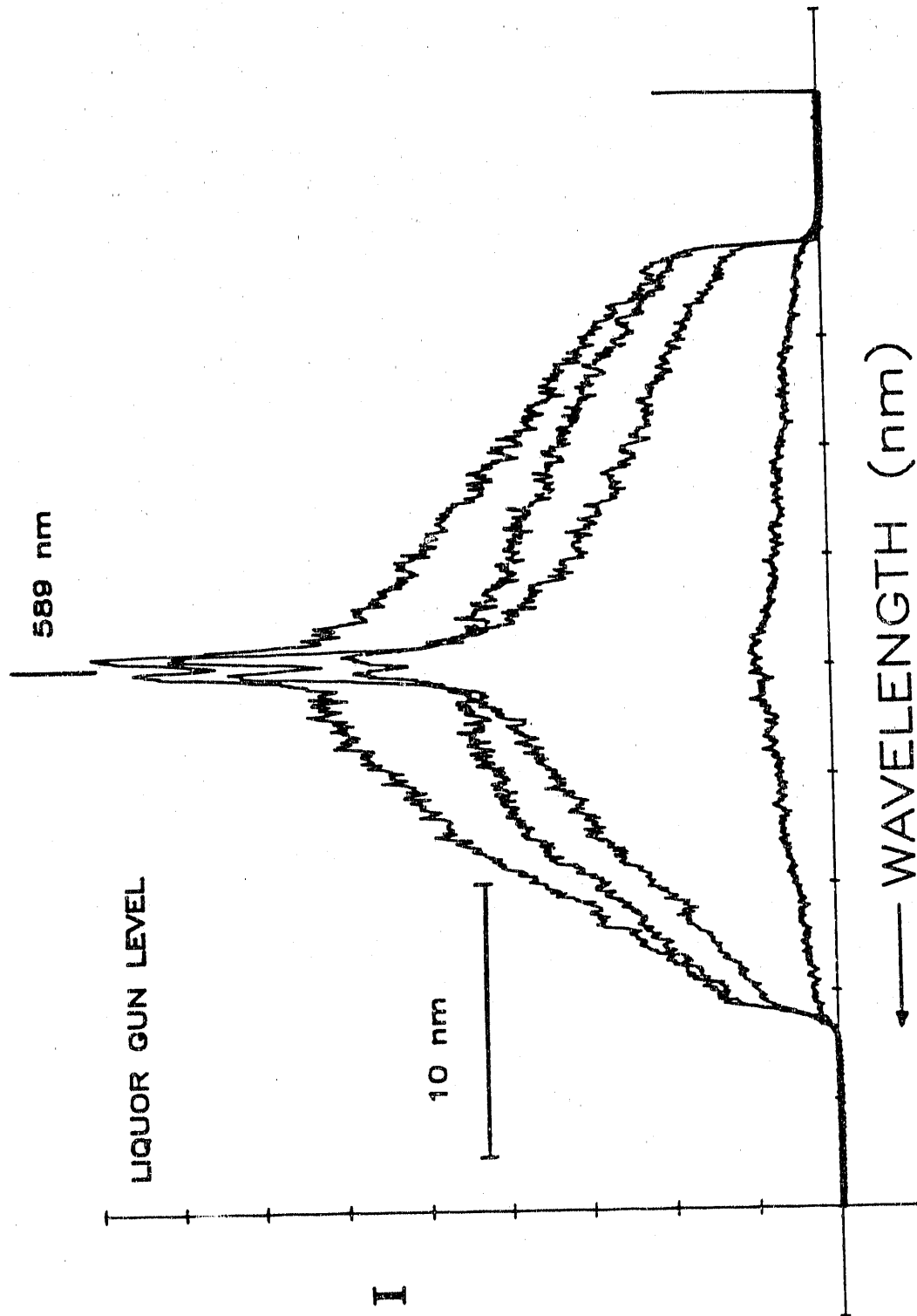


Figure 23. Sodium Emission Lines at 589 nm Observed at Liquor Gun Level (Weyerhaeuser Mills, Plymouth, NC)

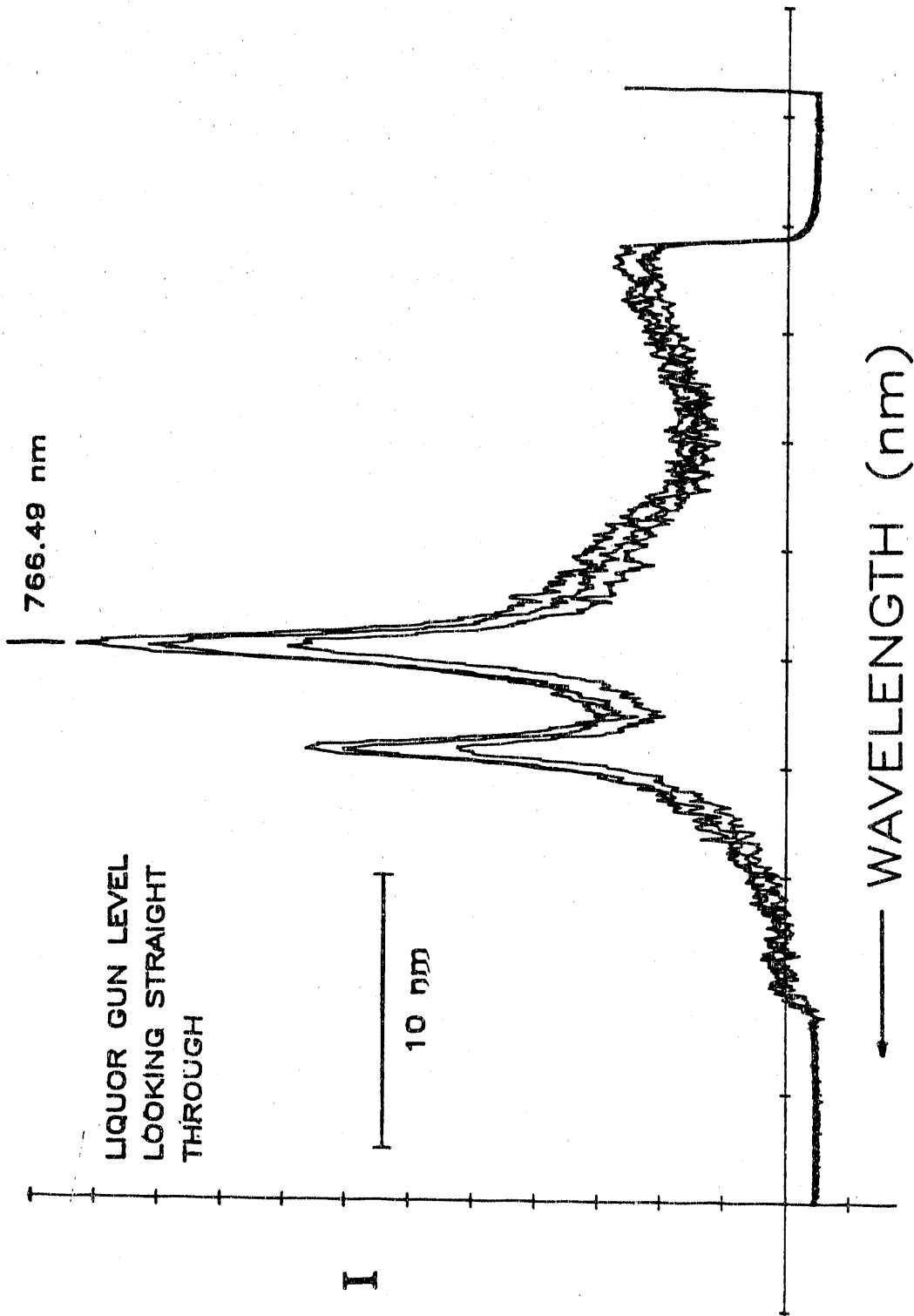


Figure 24. Potassium Emission Lines at 766.49 nm Observed at Liquor Gun Level (Weyerhaeuser Mills, Plymouth, NC)

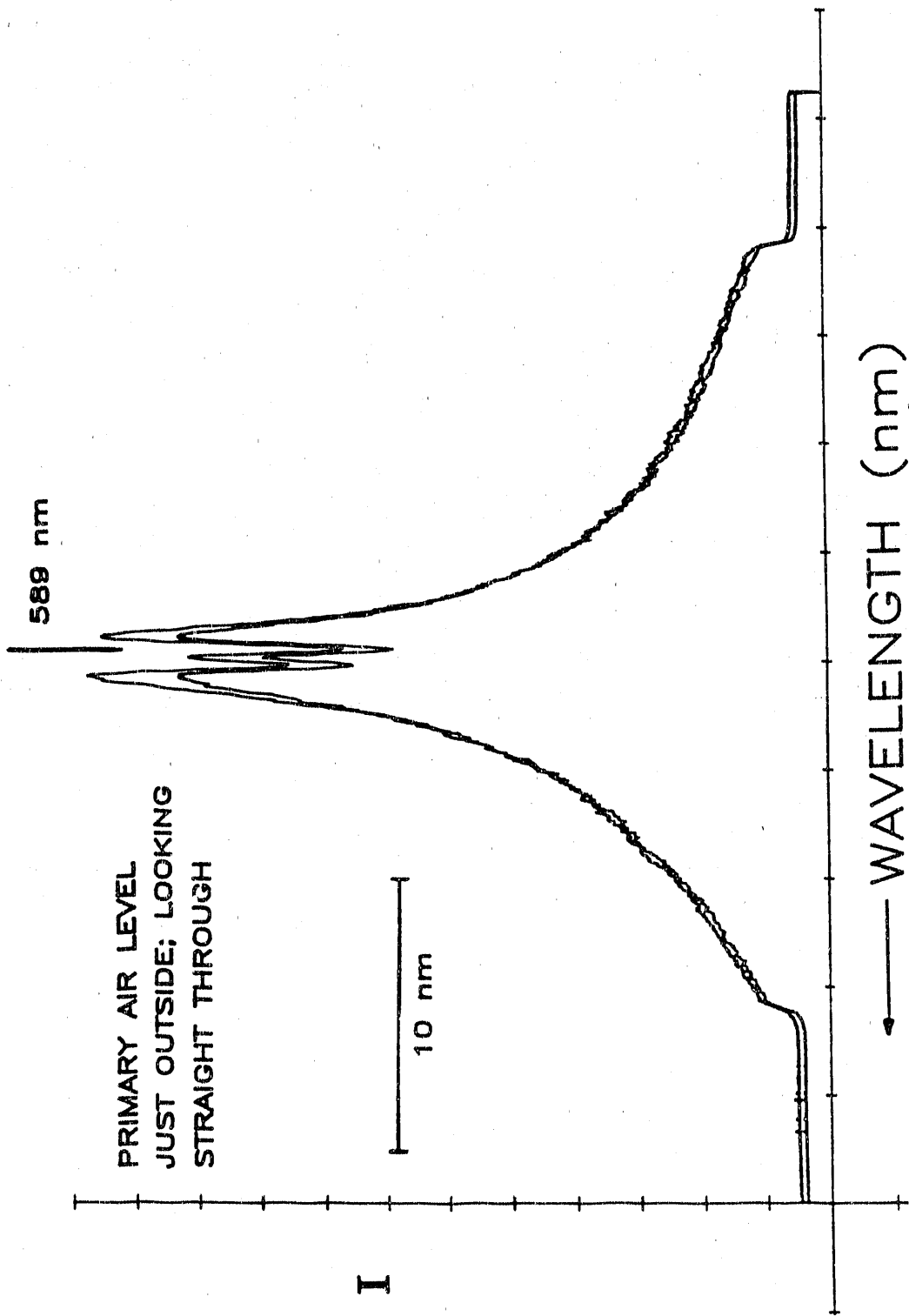


Figure 25. Sodium Emission Lines at 589 nm observed at Primary Air Level (Weyerhaeuser Mills, Plymouth, NC)

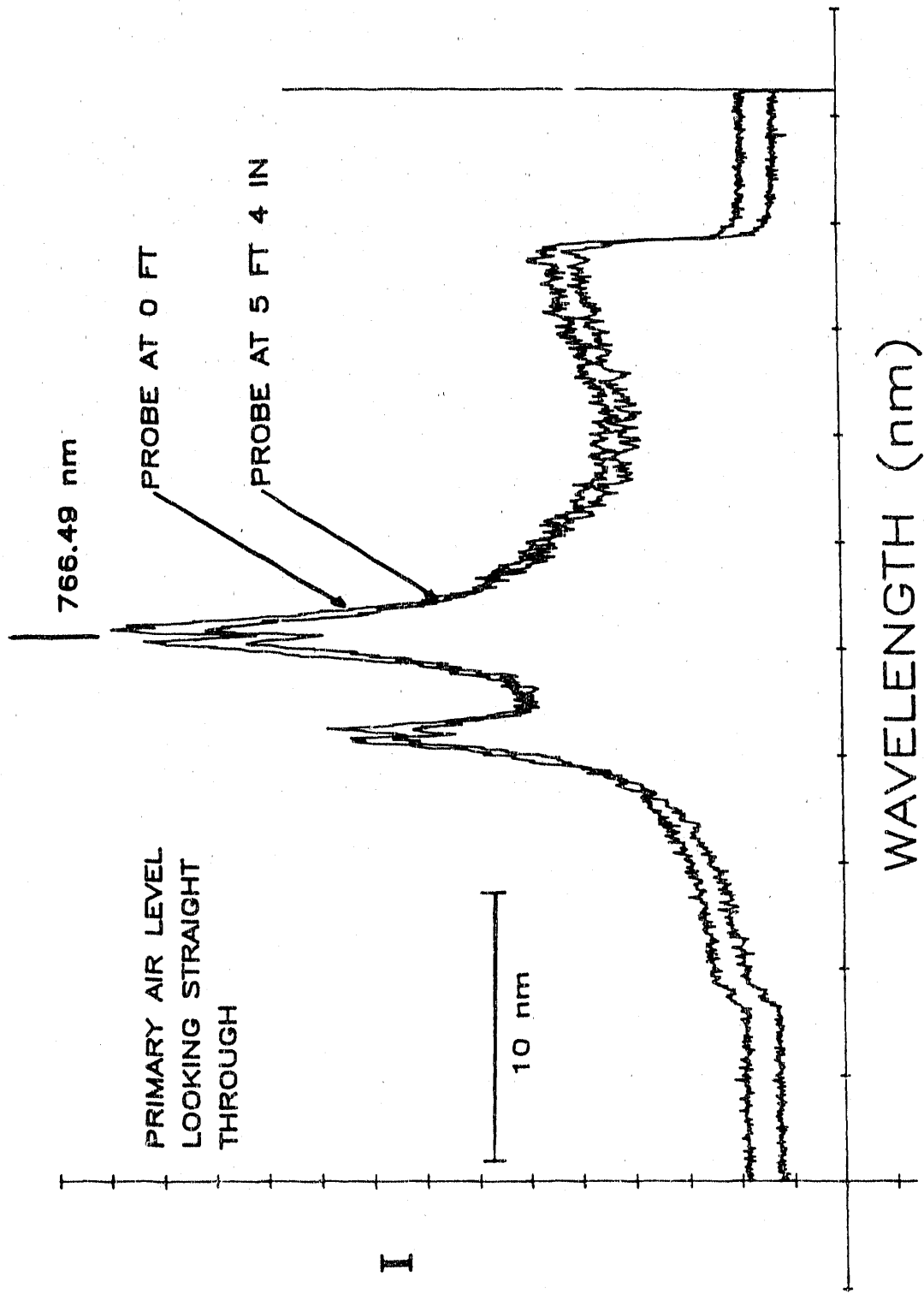


Figure 26. Potassium Emission Lines at 766.49 nm Observed at Primary Air Level (Weyerhaeuser Mills, Plymouth, NC)

positioned to view straight into the boiler before insertion. These profiles demonstrated that the level of intensity varies widely, obviously indicative of the dynamic nature of reaction zone; in addition, there is evidence of self-absorption as indicated by the dip at the line center and the nearly equal amplitudes of each line of the doublet. These records also indicated that the weak emission intensity indicating absence of potassium emission lines. In addition, figures 27 to 30 show the composite profiles of emission spectra obtained with the probe positioned successively at four different penetration depths (24, 48, 64 and 78 inches) for the forward and backward looking fiber optics. These were obtained over an extended period of time during which significant changes in combustion conditions occurred as shown by the variation in profile shapes. Nevertheless, some conclusions can be drawn. For example, the line broadening observed when viewing straight through the boiler remained about the same and did not depend on the probe penetration depth, as can be concluded by comparing the corresponding profiles in figures 27 to 30. However, the extent of self-absorption appeared to vary to some degree, indicating changes in the cool layer near the wall.

The data obtained through the 180 degree fiber optics probe looking backwards can be compared with that of the probe looking straight through in figures 27 to 30. Generally, the emission profiles obtained with the backward looking probe were relatively weak and showed less self-absorption. Obviously, this pattern of spectra suggests the existence of a temperature profile with a relatively high temperature in the recovery boiler interior and low near the walls. This agrees with the previous conclusion made on the basis of the dips noticed at the line centers in a number of emission spectra obtained in previous tests and in the present tests. These conclusions also agree with the data obtained with the heat flux sensors. Although these data are limited in extent and primarily qualitative, the trends appear to be consistent, although they do not yield a quantitative measure of the optical depth.

Figure 31 shows a composite plot of local heat flux measured when the probe was inserted, successively to three different penetration depths (24, 52 and 59 inches), into the reaction zone showing that the heat flux (and therefore the temperature) increases with distance from the furnace wall. As the heat flux sensor locations are discrete, these data do not necessarily yield any information regarding local hot spots or cool layers. However, these data clearly show that the heat flux ranges from a high of about 20 W/cm² (in the interior away from the furnace wall) to a low of about 8 W/cm² near the wall; these data represent the heat flux measured by the sensors covered to some extent with black liquor and char. The heat flux measured by the sensors located on the probe bottom, where the black liquor deposits were minimal, was 30% greater than that measured on the probe top.

HEAT FLUX IN A RECOVERY BOILER

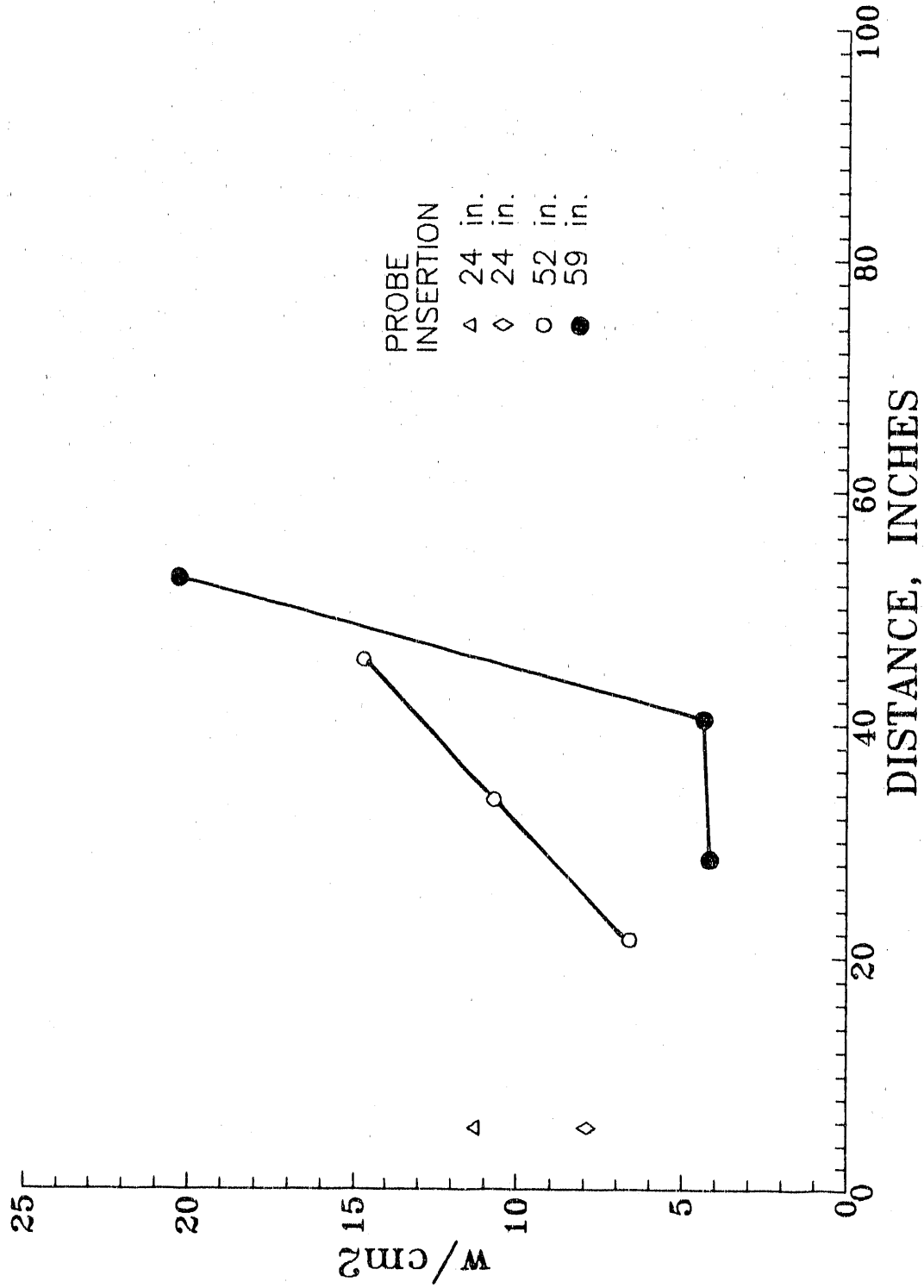


Figure 27. Effect of Probe Penetration on Emission Spectra (Weyerhaeuser Mills, Plymouth, NC)

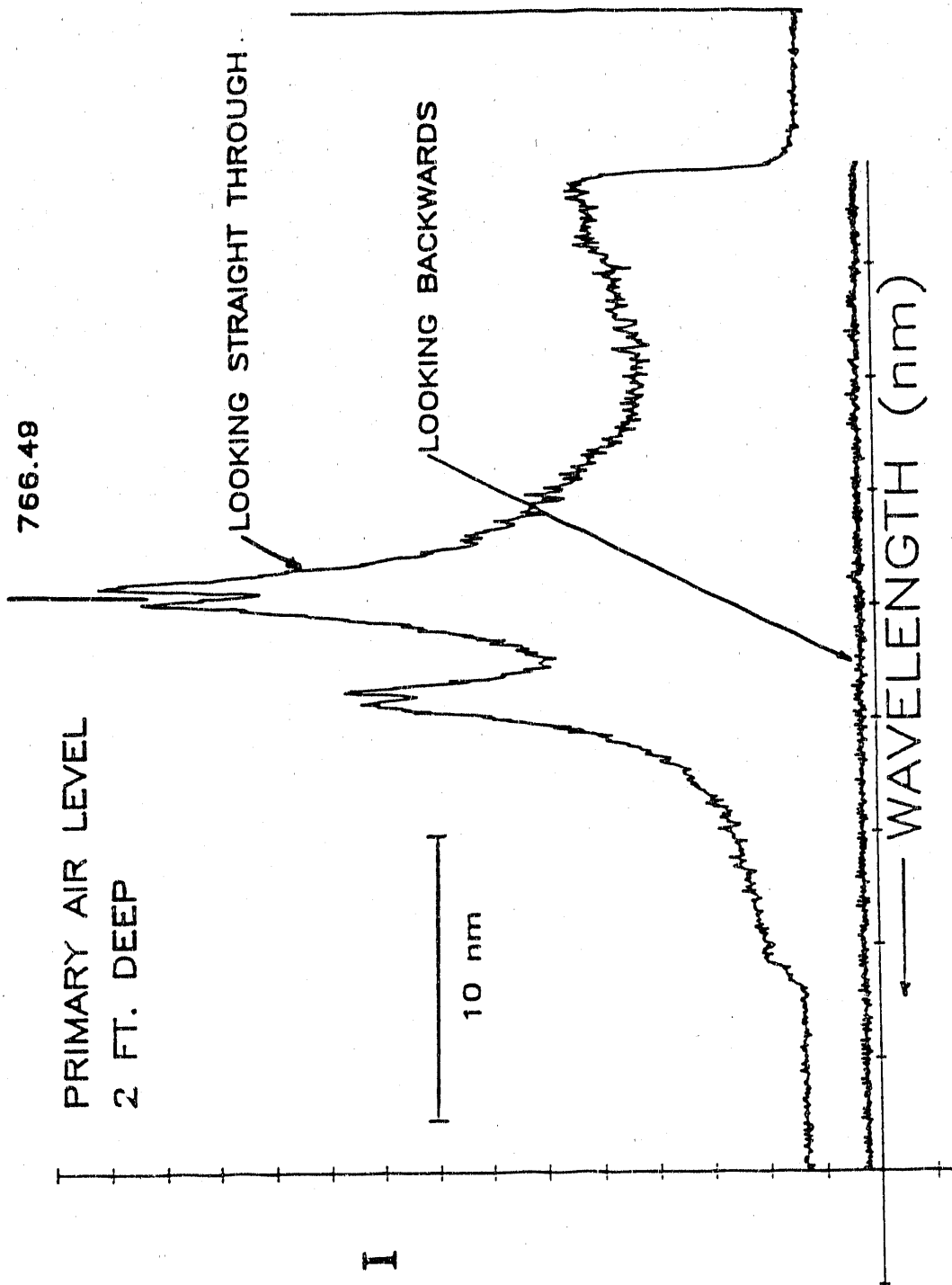


Figure 28. Comparison of Emission Spectra from 0 Degree Probe with 180 Degree Probe, Probe Depth 2 Ft (Weyerhaeuser Mills, Plymouth, NC)

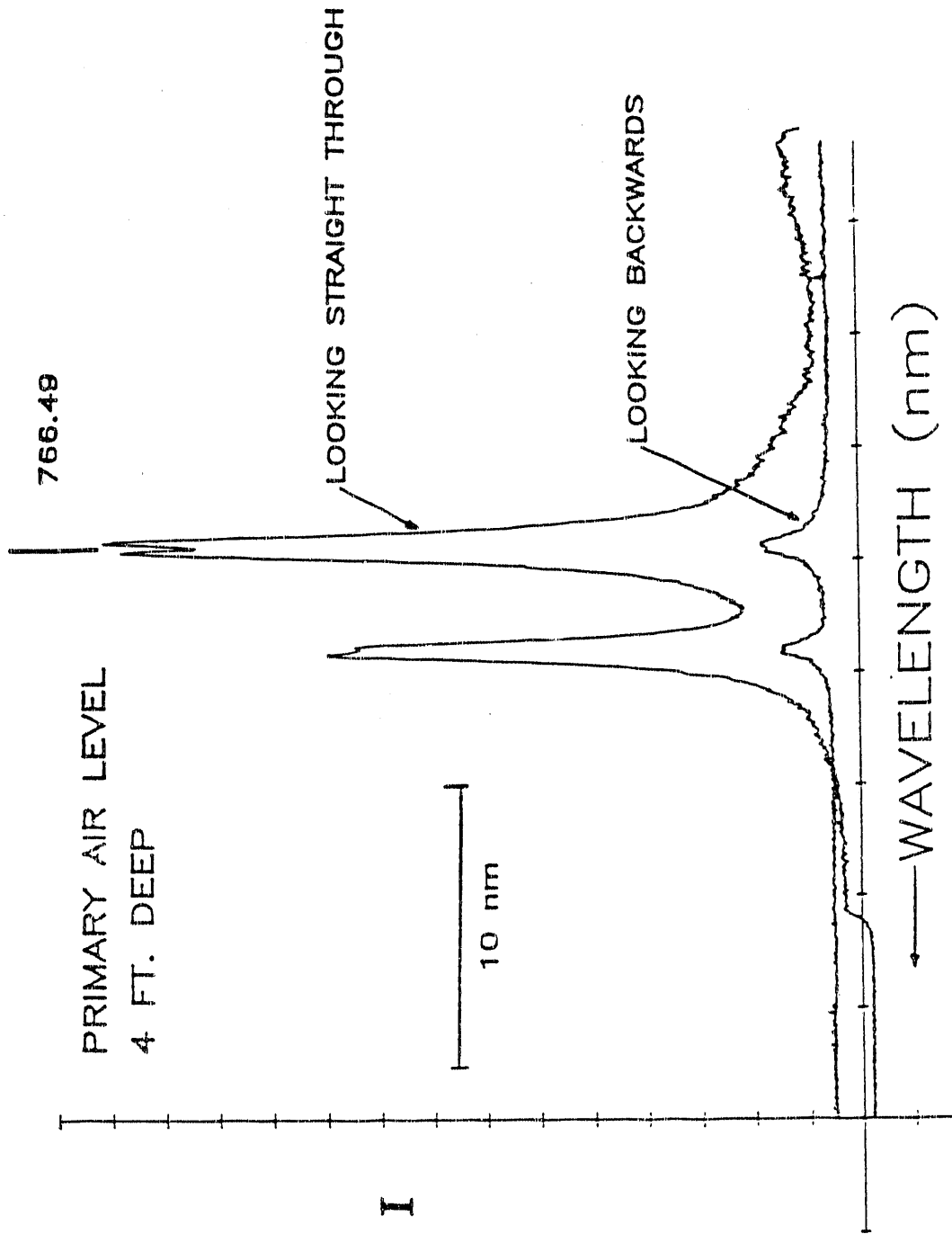


Figure 29. Comparison of Emission Spectra from 0 Degree Probe with 180 Degree Probe, Probe Depth 4 Ft (Weyerhaeuser Mills, Plymouth, NC)

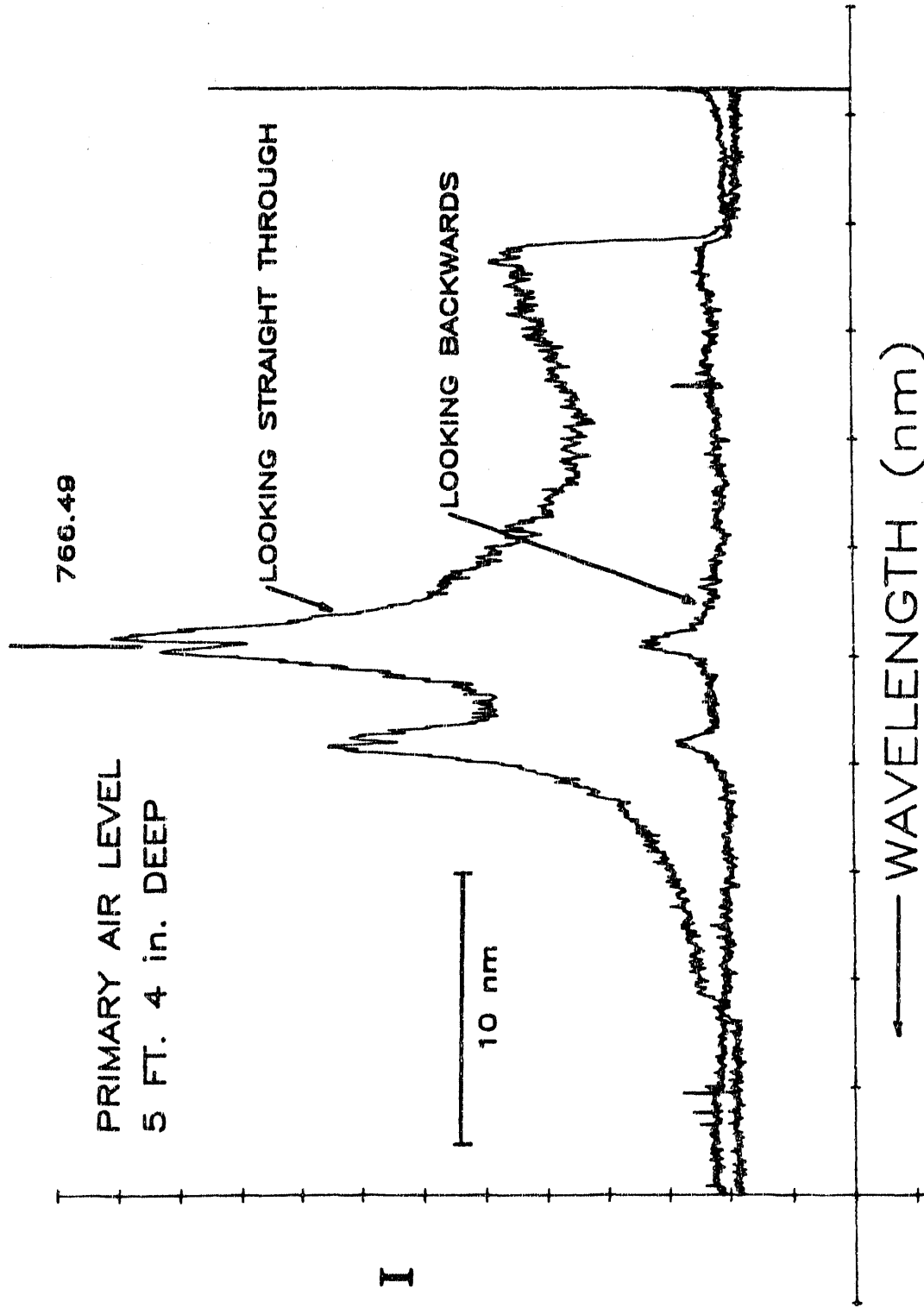


Figure 30. Comparison of Emission Spectra from 0 Degree Probe with 180 Degree Probe, Probe Depth 5 Ft (Weyerhaeuser Mills, Plymouth, NC)

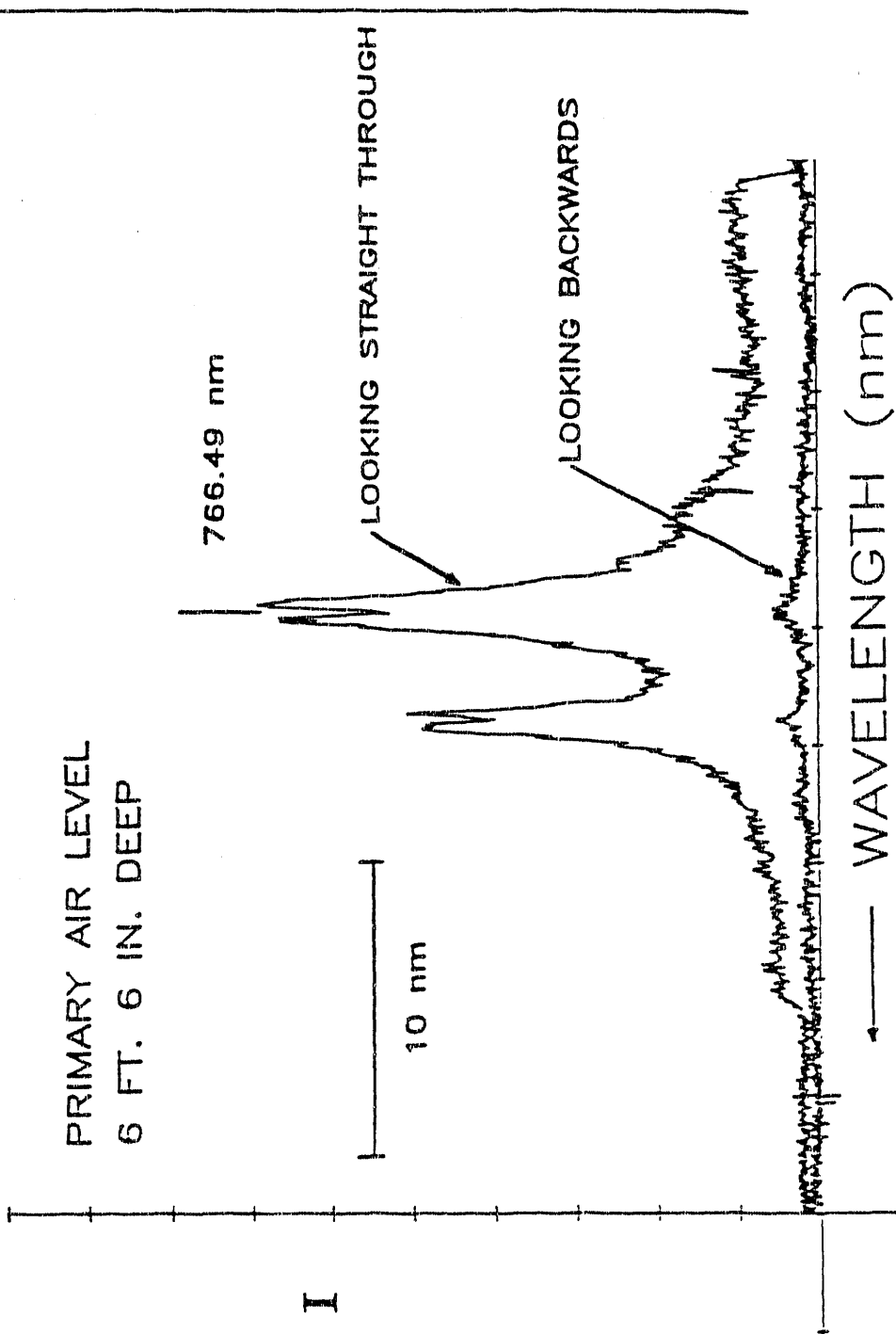


Figure 31. Comparison of Emission Spectra from 0 Degree Probe with 180 Degree Probe, Probe Depth 6 Ft (Weyerhaeuser Mills, Plymouth, NC)

5. Mathematical Modeling and Laboratory Verification

5.1 The Effect of Optical Depth on Observed Emission Intensity Profiles

The basic requirement for utilizing the line intensity ratio technique, i.e., use of amplitude ratio only, is that the environment be optically thin. The data obtained for emission lines of interest (doublets at 404.41 nm and at 766.49 nm) provide an insight into the optical thickness of the environment. For example, the emission line profiles obtained at the Union-Camp Mills in Franklin, Va provided data, although to a limited extent, for emissions of the doublet (404.41/404.7 nm). The ratio of peak emission intensity at 404.41 nm to that at 404.7 nm has been calculated from the OMA records. This ratio, listed in table 4, was consistently found to be substantially less than two, contrary to the theoretical ratio of two for optically thin gas streams. This ratio was found to be equal to two from the records obtained from premixed gas flames seeded with a nebulized mist of dilute KOH solution. Consequently, the gas stream in the recovery boiler is deduced to be "not optically thin". Similar data were not obtained at the 766.49 nm wavelength during these early tests as no spectra were obtained beyond a wavelength of 600 nm.

Table 4. Ratio of peak intensities ($I_{404.41}/I_{404.7}$) Measured in recovery boiler mill tests

Record No.	Measured Ratio ($I_{404.4}/I_{404.7}$)
M48	1.14
M52	1.26
M54	1.04
M60	1.37
M62	1.28
M72	1.15
M74	1.17

Likewise the emission line profile records obtained at the Weyerhaeuser Mills, New Bern, NC provide limited data for emissions at the 766.49/769.9 nm doublet. Again, this ratio was always found to be much less than two, contrary to the theoretical ratio of two for optically thin gas environments. This departure from two, as summarized in table 5, clearly indicates that the gas environment is not thin at this wavelength either. In addition, these OMA records show a dip at the line centers; this dip is due to self-absorption arising from temperature gradients (for example due to a cool layer near the furnace

wall) along the optical path. The OMA records obtained at 404.41 nm indicated that the signal to noise ratio is inadequate for any quantification; however, qualitatively, this ratio was much smaller than two and most probably closer to one.

Table 5. Ratio of peak intensities ($I_{766.49}/I_{769.9}$) measured in Weyerhaeuser recovery boiler at New Bern, NC

Record No.	$I_{766.49}/I_{769.9}$
WT1M44	1.19
WT1M46	1.27
WT1M48	1.21
WT1M50	1.36
WT1M52	1.27
WT1M54	1.28
WT1M56	1.27
WT1M76	1.31
WT1M78	1.29
WT1M80	1.32
WT1M82	1.50
WT2M82	1.11
WT2M84	1.27
WT2M86	1.18
WT2M104	1.34
WT2M106	1.28
WT2M108	1.30
WT3M72	1.55
WT3M76	1.38
WT4M50	1.47
WT4M52	1.44
WT4M54	1.46
WT4M56	1.43
WT4M58	1.57
WT4M106	1.42
WT4M108	1.58
WT4M110	1.10
WT4M112	1.37

Based on these data, it is concluded that the recovery boiler environment is "not optically thin" at the two potassium doublet wavelengths under investigation. In order to confirm this conclusion, at least qualitatively, two mathematical models have been developed. The first mathematical model, described next, is based on an integral approach and does not yield a detailed line shape whereas the second model, discussed subsequently provides some insight in to the line shape.

5.1.1 Emission Line Intensity from a Radiant Gas Column - Integral Absorption Approach

The model consists of a column of gas at a uniform temperature with a uniform concentration of the emitting species. It is assumed that the number density of particulate matter is small and that the presence of particulate matter does not effect emission intensity. An analysis of optical depth due to light extinction from the particulate matter using Mie theory [14] has been performed; the results from this analysis, clearly support this assumption only when the particulate loading is small.

The spectral line radiance is calculated by applying Kirchoff's law for a thermal radiator [8]. According to Kirchoff's law, the emission factor $\epsilon(\lambda)_b$, defined as the ratio of the spectral radiance $B_\lambda(\lambda)$ to that of a black body $B_\lambda(\lambda, T)$ at the same temperature and the same wavelength, is equal to the absorption factor $\alpha(\lambda)$. The black body radiation from the gas column is given by

$$B_\lambda^b(\lambda, T) = 2hc^2 \lambda_o^{-5} / [\exp(-\frac{hc}{\lambda k_B T}) - 1] \quad (3)$$

where

h is Planck's constant,
 c is the speed of light and
 k_B is Boltzmann constant.

For an arbitrary optical thickness and any wavelength, the radiance is given by

$$B_\lambda(\lambda) = A_t B_\lambda^b(T) \quad (4)$$

where the integral absorption, A_t , is defined as

$$A_t(\lambda) = \int \delta(\lambda) d\lambda = \int (1 - \exp[-k_a(\lambda) n_p \ell]) d\lambda \quad (5)$$

The integral covers the entire wavelength interval around the center wavelength, where the absorption factor, k_a , differs significantly from zero. The integral absorption, A_t can be represented as a function of an optical path length parameter, a , as shown in figure 32. This figure clearly shows that the integral absorption coefficient, A_t asymptotically approaches the optically thin approximation for small optical path length parameter values and the optically thick approximation for large optical path length parameter values.

INTEGRAL ABSORPTION VS. PATH LENGTH PARAMETER

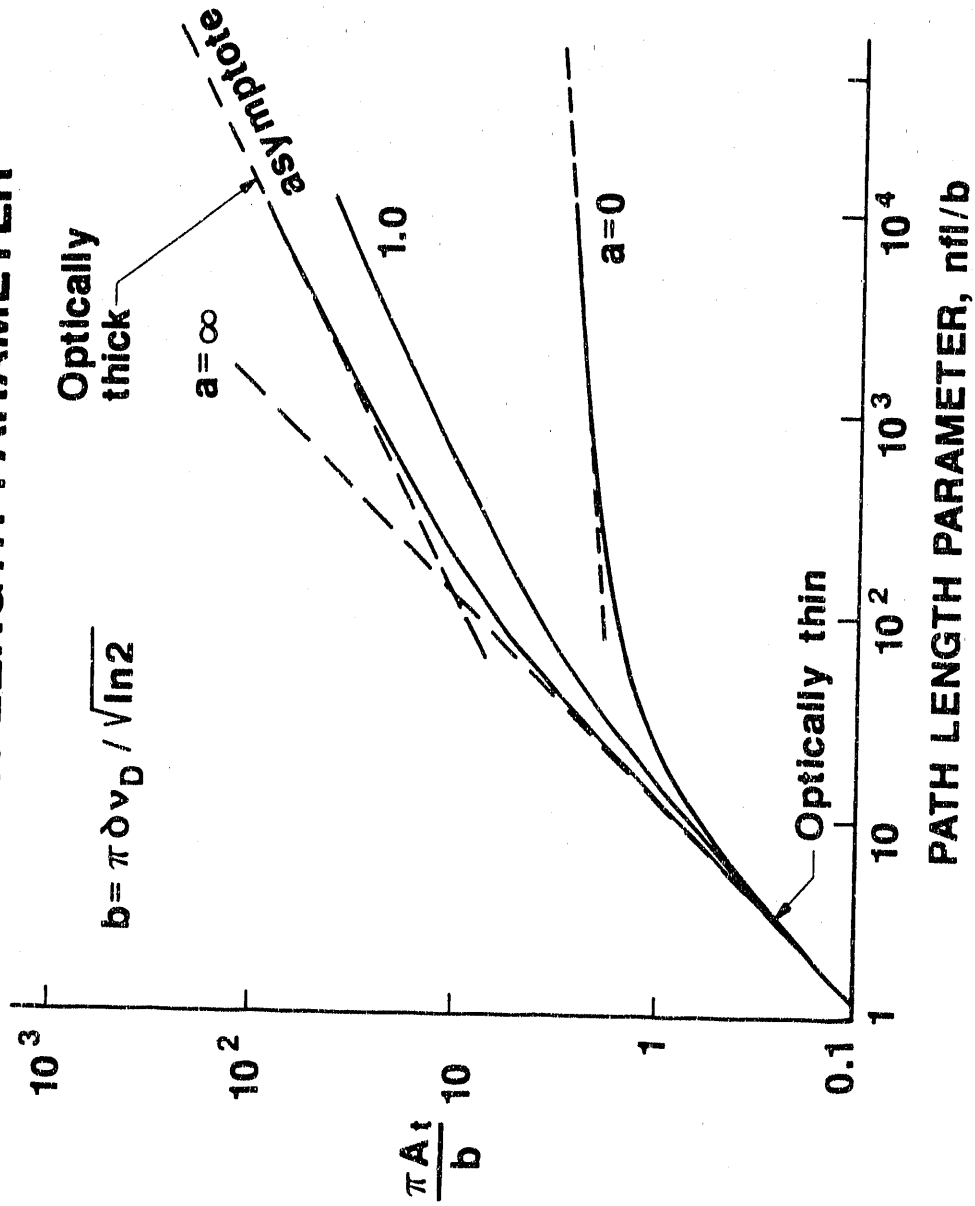


Figure 32. Local Heat Flux, ProbeDepth 52 In. (Weyerhaeuser Mills, Plymouth, NC)

As a consequence, the intensity of thermal emission from a line can be readily determined if the integral absorption, A_t , of the line at the temperature is known. The integral absorption depends on the Einstein coefficients and on the line broadening processes. The Einstein coefficients are known and tabulated [9,10] for potassium and sodium. The line broadening processes are rather complex and require precise calculation from fundamental quantum mechanical models. In this investigation, however, approximations are made following Alkemade [8] to calculate line widths.

5.1.2 Line Shape and Optical Depth

The shape of an individual emission line is modified due to a number of physical processes in the combustion zone. The pertinent mechanisms include:

- 1) Doppler broadening,
- 2) collisional broadening due to foreign gas molecules, and
- 3) self-broadening or collisional broadening due to like gas molecules.

In this model, the self broadening processes due to like gas molecules are not considered.

The Doppler broadening process is well characterized and the Doppler width can be readily calculated by

$$\left| \frac{\delta\nu_D}{\nu_0} \right| = \left| \frac{\delta\omega_D}{\omega_0} \right| = \left| \frac{\delta\lambda_D}{\lambda_0} \right| = 7.16 \times 10^{-7} \sqrt{T/M} \quad (6)$$

where T is the gas temperature and M is the atomic weight of the radiating atom.

The collisional broadening processes, on the other hand, are complex and involve both like atoms (self-broadening or self-absorption) and foreign gas molecules (pressure or Lorentzian broadening); these processes become apparently more complex if polar molecules (such as water) are present. In this analysis, these complexities are neglected.

The collisional processes determine the Lorentzian profile; in the present approximation, the Lorentzian width is related to the Doppler width by

$$\frac{\delta\nu_L}{\delta\nu_D} \approx \frac{a}{(\ln 2)^{1/2}} \quad (7)$$

where the a-parameter is obtained from experiment. The values of a-parameters for a few emitter atoms and some collisional partners were measured and a compilation was made by Alkemade et al [4]. These measured values, obtained from experiments conducted at flame temperatures, have been used in these calculations. To obtain values of a for any temperature, the following relation is used.

$$a = a_r T_r / T, \quad (8)$$

where a_r is known at an experimental temperature of T_r .

The Voigt profile, the spectrum line shape that results from a superposition of the Lorentz and Doppler broadening processes, can be calculated [13] and used to obtain emission line shapes. This detailed calculation will be discussed later in this report. However, as an approximation, the Doppler and effective widths are calculated using further simplifications.

Relating the Doppler and Lorentzian widths through the a parameter of eq (7), the width of the Voigt profile is calculated by

$$\delta\nu_v \approx 1/2 \delta\nu_L + \sqrt{1/4 \delta\nu_L^2 + \delta\nu_D^2} \quad (9)$$

The peak value of the Voigt profile is determined from

$$S_{\nu, v} |_{\nu=\nu_0} = 1/\Delta\nu_{eff} \quad (10)$$

where,

$$\Delta\nu_{eff} \approx \delta\nu_v [1.065 + 0.447 (\delta\nu_L/\delta\nu_v) + 0.058 (\delta\nu_L/\delta\nu_v)^2]. \quad (11)$$

This peak value was shown [8] to be within one percent. As $\Delta\nu_{eff}$ is known, the integrated atomic absorptivity, k_{aMax} can be calculated by

$$k_{aMax} = 8.83 \times 10^{-13} \lambda_0^2 f_{pq} / \Delta\lambda_{eff}. \quad (12)$$

The integrated absorptivity, k_{max} is calculated from

$$k_{max} = k_{aMax} \cdot n_p \quad (13)$$

The optical depth, L is then readily given by

$$L = 1/K_{max} \quad (14)$$

The radiant emissions from a gas column depend on the optical quality of the gas. If the gas is optically thin, the light emitted by the entire column of gas will escape to the outside; if the gas is optically thick, only a fraction of the emitted light at that particular wavelength will leave the gas column.

The criterion used to determine the optical quality of the gas is based on the non-dimensional factor, $k_{max} \ell$. If $k_{max} \ell$ is much less than one, the gas is optically thin. If the factor is much greater than one, the gas column is thick. If this factor is nearly equal to one, the gas column can not be approximated as either thin or thick.

Optically Thin Case

The radiance, B , of the emission line when optically thin is given by

$$B = (hc/4\pi\lambda_o) (g_q/Q) \exp [-E_{qp}/k_B T] A_{qp} n_p \ell \quad (15)$$

The partition function, Q in these calculations is set equal to the statistical weight at the lower energy level.

The integral absorption, A_t , of an optically thin line is approximated as

$$A_t = 8.83 \times 10^{-13} \lambda_o^2 f_{pq} n_p \ell \quad (16)$$

Optically Thick Case

When the emission line is optically thick, the integral absorption is determined by

$$A_t = 1.33 \times 10^{-6} \lambda_o \sqrt{\delta \lambda_L f_{pq} n_p \ell} \quad (17)$$

As a consequence, the radiance of the optically thick line can be readily determined from eq (4) as follows:

$$B = A_t B_\lambda^b(T) \quad (4)$$

For the emission lines which cannot be approximated as either thin or thick, no closed form expressions for the radiance and integral absorption are available. In such a situation, a numerical analysis which accounts for detailed line shapes is needed.

5.2 Calculation of Optical Depth Base on the Integral Absorption Model

A computer program was developed to estimate optical depths and emission line intensities in recovery boiler environments. The basis for the calculations have been discussed in the previous section. The input required for the computer model includes the spectroscopic data for the emission lines of interest as well as specification of relevant parameters describing the boiler.

The spectroscopic constants needed for a few of the atomic lines of potassium and sodium are resident in the program. However, if the user needs to calculate emission intensities of any other lines due to either potassium, sodium or other elements, the relevant spectroscopic data and the corresponding a-parameter values must be provided by the user according to the menu directions.

The other variables and parameters include specification of the emission lines of interest and the concentration of the emitter species, the reaction zone temperature and the optical path length. This computer model does not include an equilibrium model for calculating the emitter species concentrations in the recovery boiler. The program is written in TURBOPASCAL (v 3.02) [12] and requires about 36 KB of RAM on a PC. The model requires the input of a number of variables and parameters including the total optical path length l , the reaction zone temperature T , the wavelengths of interest and the emitter concentrations. The total optical path length or recovery boiler width is treated as a variable because recovery boiler size varies from one mill to another. However, the actual calculations are made for a range of path lengths from 1 cm to 2048 cm, covering the maximum representative path length anticipated from industrial black liquor recovery furnaces. The reaction zone gas temperature depends on the operating conditions as well as the reaction zone location; however, as these temperatures are not known, the

temperature is treated as a parameter. In most of the computations, these temperatures are set to vary from 900K (1161 °F) to 1600K (2421 °F).

The concentration of the emitter species is not well known. Because of the absence of any relevant measurements, these concentrations had to be assumed, and as a first approximation, are set to be equal to those obtained from equilibrium models such as the A. D. Little model [15] and the SOLGASMIX model [16]. The validity of these equilibrium models for the computation of potassium or sodium concentrations in recovery boiler environments is considered to be somewhat uncertain based on recent work [17] by the Institute of Paper Chemistry on fume production.

5.2.1 Calculation Procedure

The calculation procedure is summarized in the flow chart, shown in figure 33. Initially, the spectroscopic data and a-parameter values corresponding to the wavelengths of interest are loaded into the data file. Subsequently, the optical path length of the combustion zone and the reaction zone temperature (boiler temperature) are specified. In addition, the emitter concentration is either specified or is computed from one of the equilibrium models mentioned above.

For a given wavelength, the sequence of calculations is as follows:

Step # 1:

Computation of the frequency, ω and wave number, ν for the emission line using the equations,

$$\text{frequency, } \omega = 1/\lambda \quad (18)$$

and

$$\text{wave number, } \nu = c/\lambda \quad (19)$$

In this step, the computations are also made for the Doppler width using eq (6).

Step # 2:

The widths of Lorentzian and Voigt profiles together with an effective width are calculated using eqs (7) to (11). The equations used are approximations [8] with an accuracy claimed to be within one percent.

In addition, the oscillator strength, f_{pq} is calculated if needed using

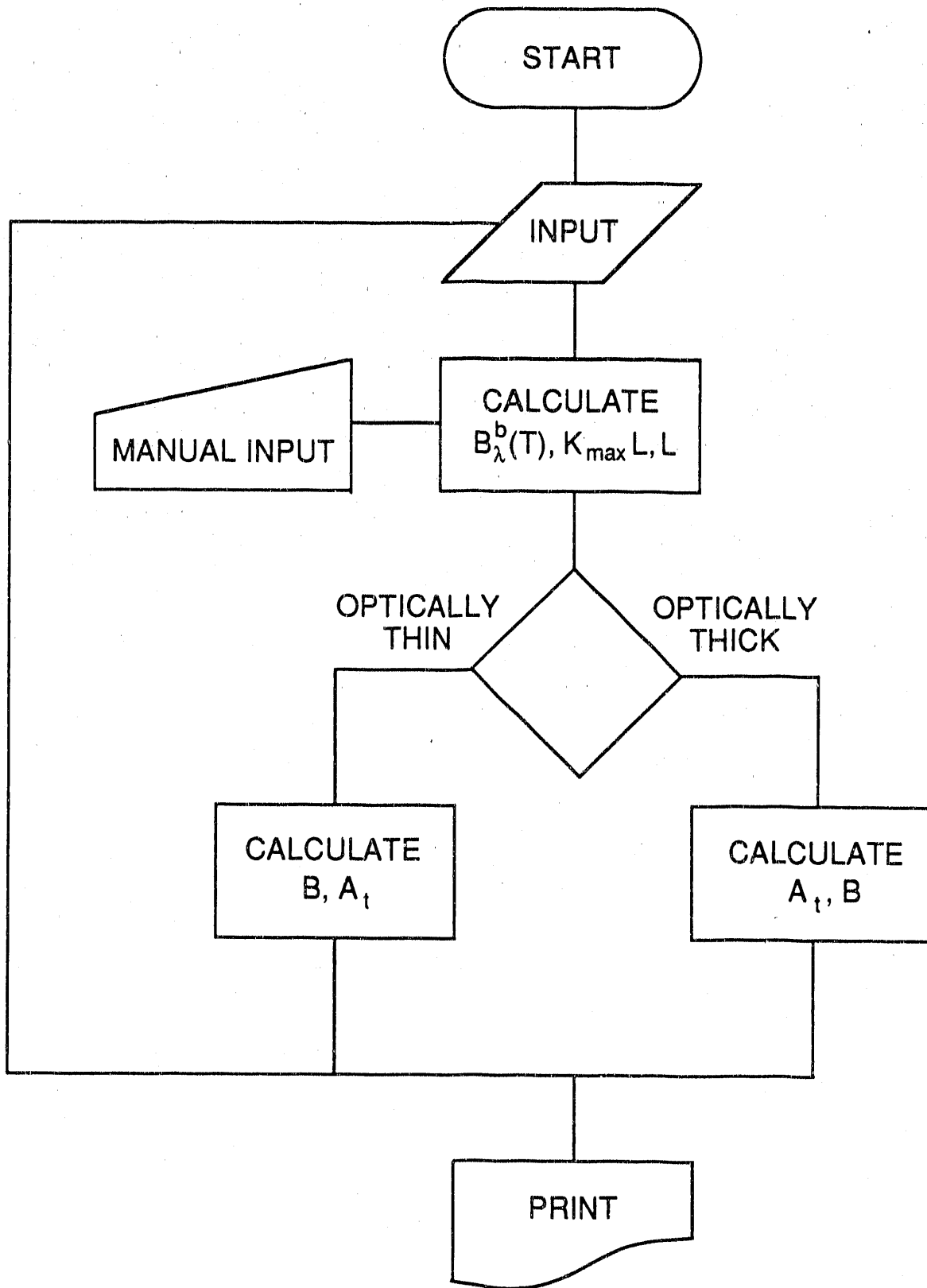


Figure 33. Computation Procedure (Flow Chart)

$$f_{pq} = 1.50 \lambda_o^2 A_{qp} g_q / g_p \quad (20)$$

Step # 3:

The black body radiation is computed using eq (3). In addition, values for the factors necessary to determine the optical quality of the reaction zone are developed. These factors are then used to determine whether the gas column is optically thin, thick, or somewhere in between. In any event, the optical thickness is computed using eqs (12) to (14).

Step # 4:

Calculations are made to determine the radiance, B, of the emission line and the integral absorption, A_t , in the following manner:

For an optically thin gas environment, the radiance B and integral absorption, A_t are computed from eqs (15) and (16).

If the gas column is found to be optically thick, the computations of B and A_t are made according to eqs (4) and (17), respectively.

If it is determined that the gas column is neither thick nor thin then the computations are somewhat involved and simplified approximations are not available.

5.2.2 Sample Calculations

Three different sets of calculations are made and the results from these calculations are summarized below for various emitter concentrations.

5.2.3 A. D. Little Model

The results from the A. D. Little model do not provide potassium atom concentrations. In order to perform these calculations, it is assumed that the ratio of potassium atom concentrations to the sodium concentrations in the recovery boiler combustion zone is equal to the ratio of these atoms in the black liquor feed. These computations further assume that the a-parameters available in the published literature as compiled by Alkemade [8] are valid.

The input for these calculations are:

Temperature	=	1400K
Mole fraction of Na (A. D. Little model)	=	1.4×10^{-4}
Moles of K / Moles of Na in the black liquor	=	0.0342
Range of Optical Path Length	=	1 - 2048cm

The results are plotted in figures 34 and 35 to show the integral absorptivity, A_λ as a function of optical path length. These results indicate that the potassium doublet at 766.49 nm is thick for the entire path length while the line at 404.41 nm is thin only for short optical path lengths and thick for long optical paths.

5.2.4 Measured Line Widths

These computations were made to compare and check the results from the present model with Ariessohn's computations. Ariessohn [18] has measured the line widths of potassium and these measured line widths are clearly much larger than the calculated widths.

The input for these calculations is as follows:

Temperature	= 1400	K
Potassium atom number density	= 2.8×10^{13}	cm ⁻³
g_2/g_1	= 1.5	
Delta Omega for 404.41 line	= 73	cm ⁻¹
Delta Omega for 766.49 line	= 285	cm ⁻¹

These results are summarized in table 6.

Table 6. Comparison of calculated optical depths with Ariessohn's calculations

Wavelength (nm)	Calculated Optical Depth, L (cm)	
	Ariessohn	Present
404.41	650.0	647.08
766.49	23.4	22.53

5.2.5 SOLGASMIX Model

The SOLGASMIX program was developed and used extensively for black liquor recovery boiler applications. This model gives equilibrium compositions for both the gas phase and the condensed phase (smelt bed). For example, the model [16] gives the equilibrium concentration of potassium atoms in the gas phase as a function of temperature for a number of black liquor feeds with different sulfidity, chlorine and potassium content. These computations were made with air throughput corresponding to 70% theoretical air.

A. D. Little Equilibrium Model

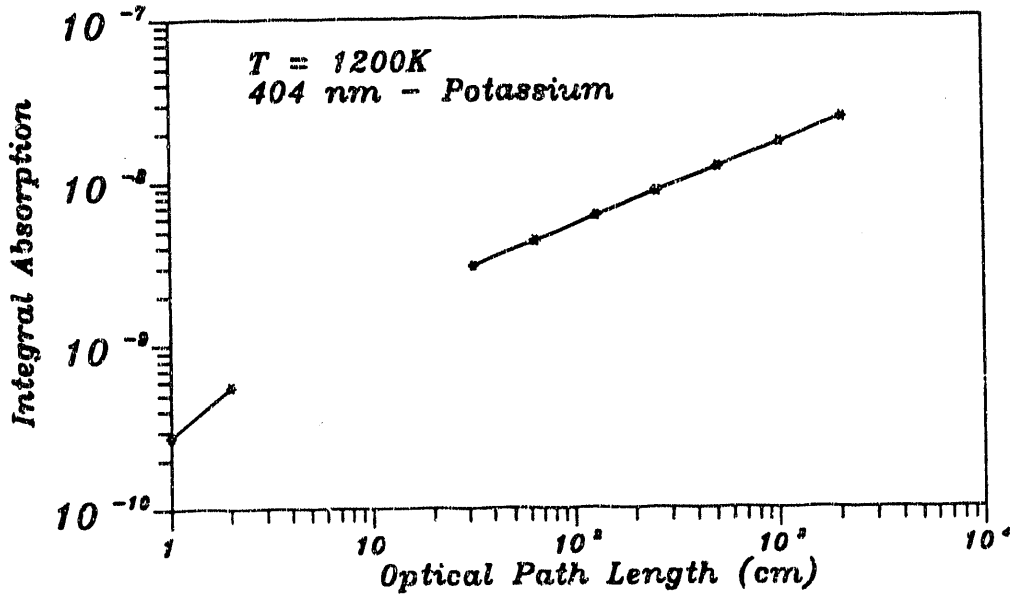
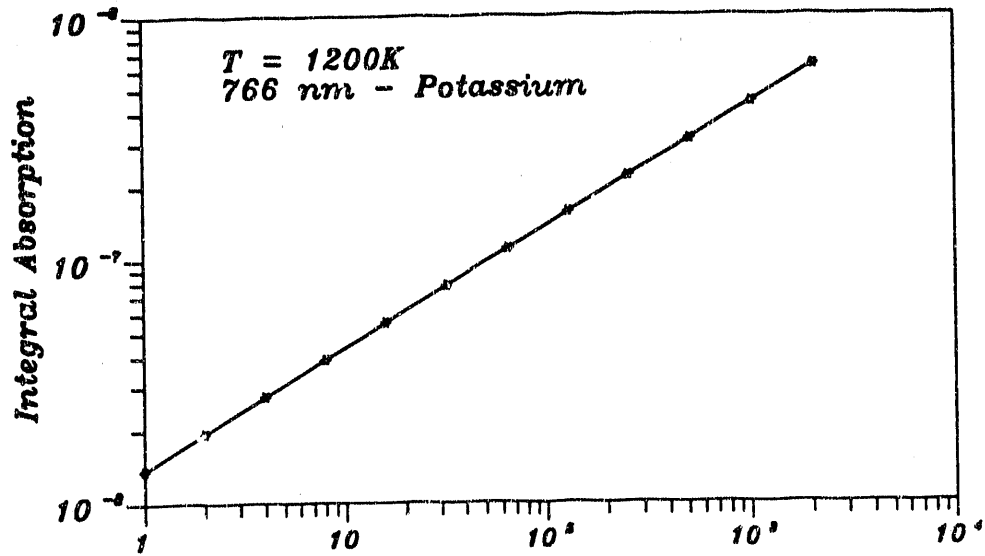


Figure 34. Integral Absorption for Various Path Lengths at 1200K (Based on K atom Concentrations from A. D. Little Equilibrium Model)

A. D. Little Equilibrium Model

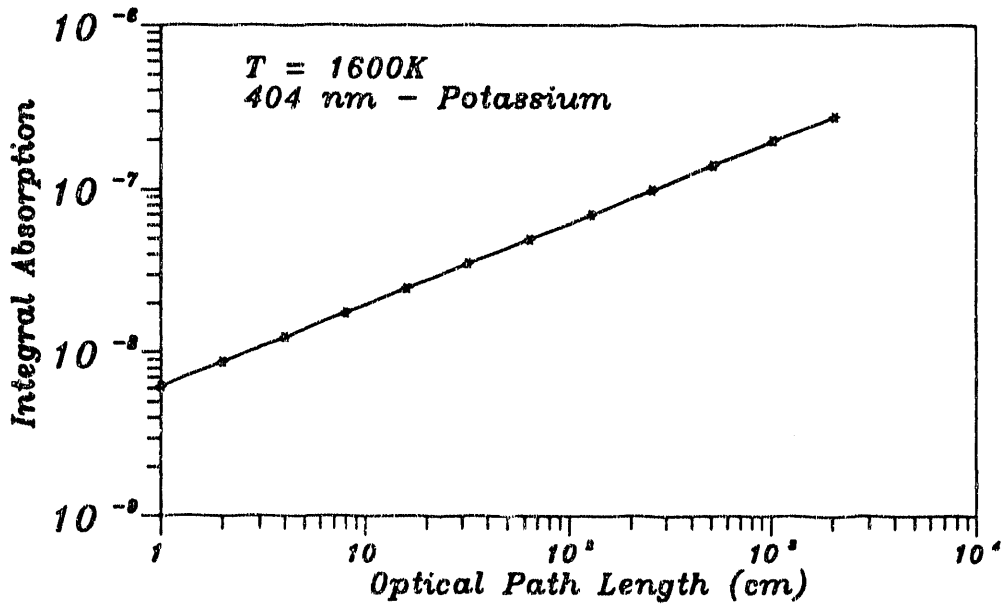
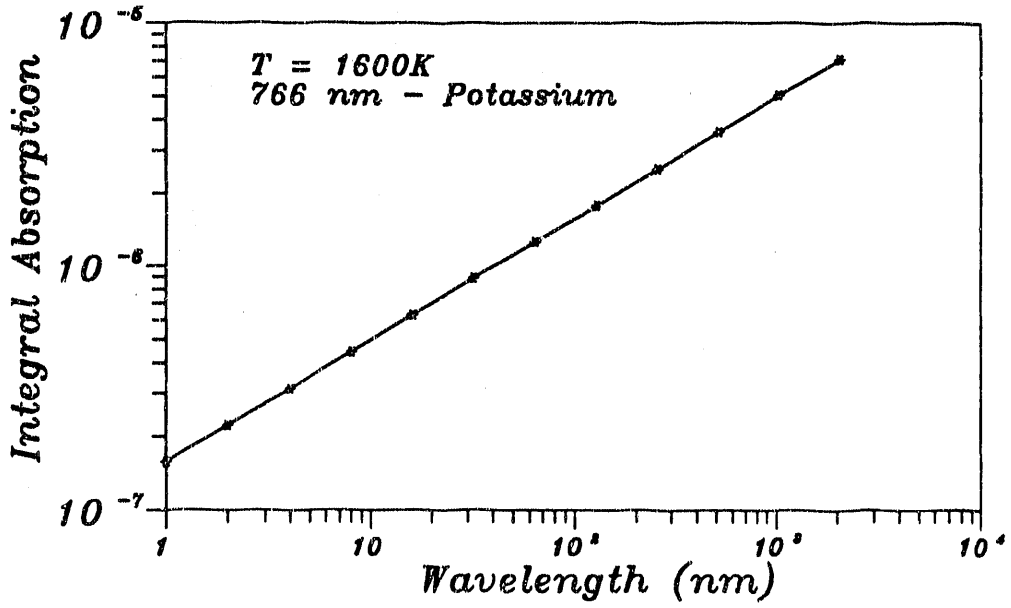


Figure 35. Integral Absorption for Various Path Lengths at 1600K (Based on K atom Concentrations from A. D. Little Equilibrium Model)

One set of results from the equilibrium calculations, made for one of the black liquors with composition shown in table 7, has been used in the present calculations.

Table 7. Black liquor composition

Atoms	C	H	O	S	Na	K	Cl
mols	10	12.5	7	0.36	2.4	0.36	0.36

The potassium concentrations, obtained in the equilibrium computations, are plotted as a function of temperature as shown in figure 36. For the purpose of the present calculations, a curve fit for these data has been generated and used.

As the equilibrium concentrations of potassium are much greater than those obtained from the A. D. Little model, the potassium lines are optically thick for almost all of the path lengths. The computed optical depths are summarized in table 8.

Table 8. Computed optical depths

T (K)	[K] (cm ⁻³)	Optical Depth, L (cm)	
		404.41 nm	766.49 nm
1200	4.2×10^{13}	2.33	9.5×10^{-3}
1400	1.6×10^{15}	5.82×10^{-2}	2.4×10^{-4}
1600	6.4×10^{15}	1.37×10^{-2}	5.6×10^{-5}

5.2.6 Model Results

The computer model, which is based on semi-empirical approximations for line widths, has yielded estimates for the intensity of emission lines and optical depths. This model has been used to compute the emission intensities and optical depths of potassium emission lines for a few sample conditions. These sample computations have been made using the equilibrium potassium concentrations at three selected recovery boiler temperatures: 1200, 1400, and 1600 K. The results indicate that the potassium emission lines at the wavelengths of 404.41 nm and 766.49 nm are optically thick. As the model is based on assumed potassium concentration levels in the recovery boiler combustion zone, the results

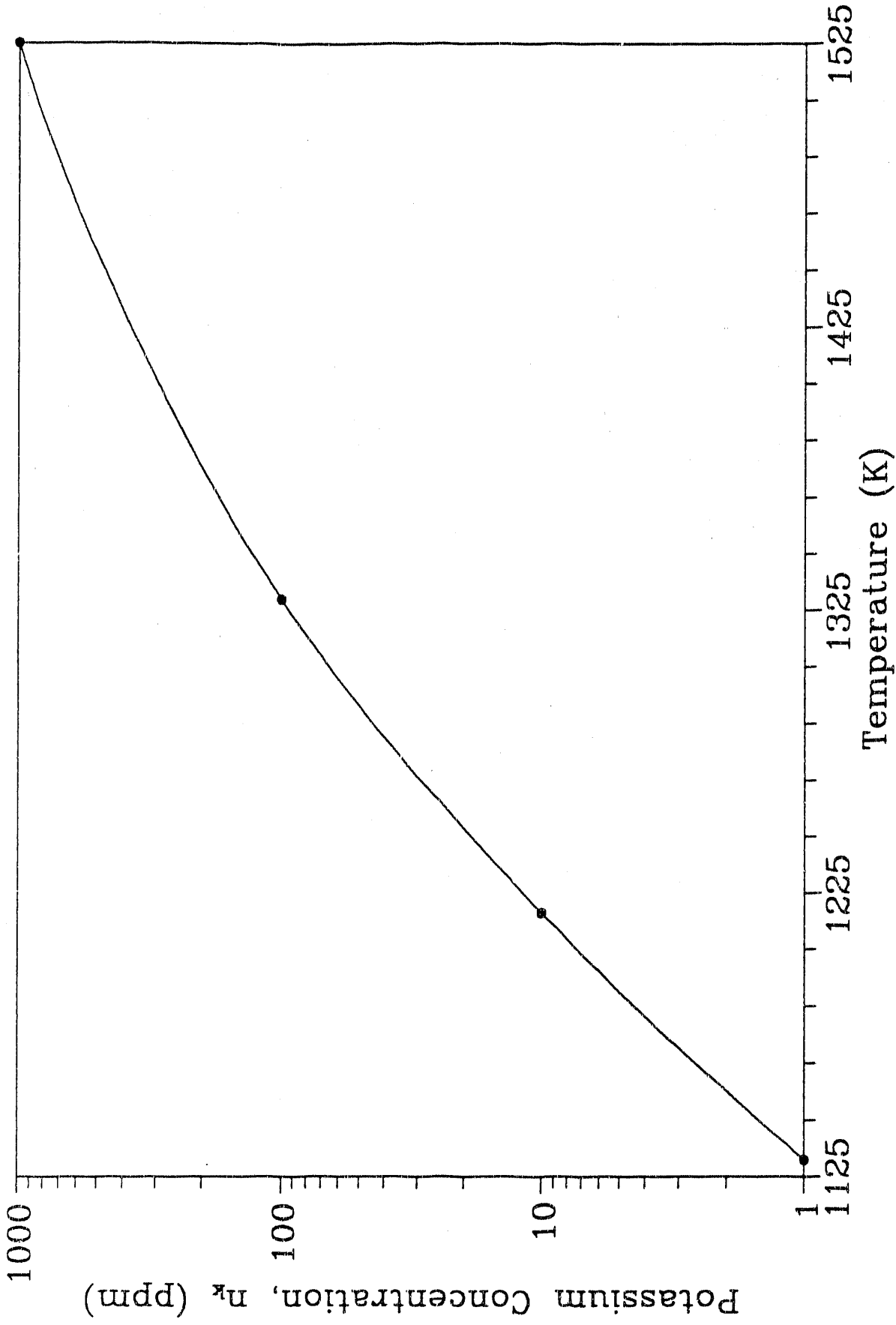


Figure 36. Integral Absorption at 404.4 nm for Various Path Lengths (Based on K atom Concentrations from SOLGAS MIX MODEL, T=1200K)

will be as accurate as the assumed concentration levels. Consequently, a dependable model for estimating these atom concentrations is needed. The SOLGASMIX model is anticipated to provide the needed atom concentration levels at least as a first approximation for various recovery boiler conditions. Since the results obtained from the model suggest that the potassium emission lines are thick, it is essential to verify both the approach used in the model and the input provided to the model. As a consequence, an effort to calculate in detail the shape of emission lines was undertaken.

6. Emission Profile and Optical Depth Models

A model was developed to characterize emission line profiles of thermometric species as viewed from the side of a combustion zone, having temperature profiles and species concentrations similar to those of recovery boilers. The primary assumptions of this model are

- 1) the combustion zone is in a state of local thermodynamic equilibrium, and
- 2) the concentration of emitting/absorbing species is explicitly dependent on temperature.

Effects due to scattering by particulates are not considered, although this is possible with the addition of algorithms based on the appropriate scattering theory. Also, the effects of collisional broadening due to polar molecules, i.e., water molecules, which may be significant are not explicitly considered due to lack of data and models describing these interactions.

The profile of a single spectral line is obtained from a calculation procedure for the Voigt profile given by Armstrong [14]. Since doublet states of potassium are the spectral lines of interest, a superposition of the Voigt profile was used to develop a wavelength grid, with associated amplitudes. This is used to cover the wavelength regions of interest near 766 and 404 nm. Appropriate selection of Voigt profile calculation parameters provides a means to include varying degrees of collisional and Doppler broadening effects on the line shape.

6.1 Emission/Absorption Model

The expression for the intensity emitted, B_{gen} , at wavelength, λ , from an elemental volume of width L containing n_p emitters is

$$B_{gen} = S_{\lambda} [hc/4\pi\lambda] (g_1/g_2) \exp[(E_2 - E_1)/kT] A_{12} n_p L \quad (21)$$

where	h - Planck's constant	g_i - statistical weights of the upper and lower energy levels of transition
	c - speed of light	E_i - the upper or lower level energy
	k - Boltzmann constant	A_{12} - the transition's Einstein Coefficient
	T - Temperature	
	S_λ - Voigt amplitude at λ .	

This expression does not account for absorption effects. (In the terminology used in discussing the integral absorption model, the emission zone is considered to be optically thin.)

This model is a solution of the radiative heat transfer equation which involves integration along a path traversing the combustion zone to obtain the intensity observed or detected at the edge of the boiler. To obtain predicted profiles from the model the integration was performed at each wavelength grid point covering the doublet region under consideration. Non-uniformity in the optical path along which the integration proceeds results from temperature variations along it. To account for absorption effects along a non-uniform optical path, each integration element's width was tested for the level of absorption of incident radiation. The element's width was adjusted to minimize absorption effects which are neglected in the intensity source term of the integral.

Attenuation of the intensity at every wavelength occurs as the numerical integration of the emission intensity proceeds across the combustion zone. The radiation intensity transmitted through each integration element, B_{trans} , is dependent upon the absorption coefficient, K_a , the species number density, n_p , and the optical path length.

$$B_{trans} = B_{in} \exp(-K_a n_p L).$$

The total intensity leaving a spatial integration element, B_{out} , is the sum of the generation and transmission terms,

$$B_{out} = B_{gen} + B_{trans} = B_0 \exp(-K_a n_p L) + B_{gen} \quad (22)$$

where B_0 is the intensity entering the elemental volume. The value of the absorption coefficient, K_a , was computed from the Voigt profile calculated for each line of the doublet considered. To obtain the effective absorption coefficient, contributions from each line of the doublet were included. The method used was to determine the position of the integration wavelength in terms of the Doppler width as measured from each line center of the doublet. The absorption coefficient ratio for each line was obtained using the Voigt profile calculation, and multiplied by the absorption coefficient at the line center of the

corresponding line to obtain each line's contribution to the total absorption coefficient. The sum of these two is the effective absorption coefficient value, K_a , used in both the generation and attenuation terms.

Integration of the radiative heat transfer equation begins at one side of the combustion zone and proceeds to the opposite side using discrete elements of variable length. The length of the integration element used in each step was adjusted so that the absorbed intensity in the element was maintained below a fixed level (5% absorption), i.e., the optically thin assumption for each integration element was maintained. This provided a means to minimize errors in the integration caused by neglecting absorption of intensity generated within the element resulting in a width limit of each integration element. Width limits are maintained below 5 percent absorption in the current element. Investigation of integration element width selection indicated that the 5 percent absorption limit was conservative. A larger value could have been used, however, the use of 5 percent was sufficient to maintain acceptable computation times for all profiles.

Non-Isothermal Temperature Profiles

Selection of the integration element width allows non-isothermal temperature profiles in the combustion zone to be investigated. Four temperature profiles were investigated: isothermal, trapezoidal, a three region isothermal profile, similar to the trapezoidal but having step boundaries rather than sloped ones, and a trapezoidal profile with a lower temperature region in the center of the combustion zone. The isothermal results were used to test the calculation against results computed from the analytical solution of the radiative heat transfer equation and good agreement was obtained.

For the isothermal temperature profile, easily quantifiable optical depths for each grid wavelength could be obtained. The results of the isothermal profile calculations showed that near the center of each line of the doublets optical depths could decrease to the order of several centimeters. The magnitude of the optical depth was strongly dependent on temperature and potassium concentration, n_p . At wavelengths somewhat removed from the line centers, the optical depth increased to the boiler dimension at all wavelengths. At wavelengths near the line centers optical depth was also concentration and temperature dependent.

The trapezoidal profile combines zones of linearly increasing and decreasing temperature bounding an isothermal core region. (Calculations for all temperature profiles used total combustion zone dimensions of 1000 cm to approximate the dimensions of recovery boilers.) The non-isothermal bounding regions were 30-50 cm wide with temperatures lower than the central isothermal region. The trapezoidal profile and the three region isothermal profile were used primarily. Both cases allowed investigation of the effects of cool layers bounding the hotter inner core of the boiler. Initially species concentrations, i.e., potassium number density, n_p , were computed using polynomial fits to the results of the thermal equilibrium model of Pejyrd and Hupa [17] as a function of temperature. This was later modified to either include

a multiplier to reduce n_p , while maintaining the shape of the temperature dependence, or to use a fixed value of n_p for each region of the temperature profile. Pejyrd and Hupa's n_p values caused the model to produce line intensity profiles that approached the black body radiation limits for all grid wavelengths and at temperatures thought to be considerably lower than expected for recovery boilers, i.e., 1125 - 1200 K (1565 - 1700 °F).

6.2 Model Calculation Results

The results of the calculations are spectral line shapes for the two potassium doublets. To test the capability of the model to reproduce known optically thin profiles, calculations were made for very low potassium concentrations which resulted in line shapes closely approximating those expected and observed for optically thin conditions in laboratory flames. The calculated profiles are shown in figure 37 for both potassium doublets and an isothermal temperature profile. The ratio of the longer wavelength line to its doublet partner is 2 as predicted by the ratio of statistical weights for each doublet. Use of potassium concentration, n_p , values as given by Pejyrd and Hupa cause the line shapes of both doublets to change radically due to re-absorption effects, i.e., attenuation of previously emitted photons by potassium atoms located closer to the observer. The effect of such re-absorption is to limit the distance over which photons from the interior of the boiler may be observed from its edge, i.e., a decrease in optical depth.

This occurs because emission, which is greatest at the doublet line centers, reaches the blackbody limit there first. Once this happens, further increase in intensity only occurs at wavelengths away from the line centers resulting in a change in the emission profile. For these doublets, having statistical weight ratios of 2, the ratio of amplitudes of the doublet's transitions begin to decrease toward unity as the lower amplitude transition increases intensity while the other remains at the blackbody limit. In the case of isothermal temperature profiles and higher temperature and/or concentration values, both transitions become blackbody limited and continued intensity increases occur in the line's wing regions, further distorting emission profiles.

Emission profiles observed through the cooler bounding layers of non-isothermal temperature profiles (three region profile with step boundaries) are additionally modified by strong re-absorption around the line centers. These effects, illustrated in figure 38, are most pronounced near the line center. These results, calculated using the Pejyrd and Hupa equilibrium concentration values computed for the three temperatures, illustrate the evolution of line shape distortion caused by re-absorption as temperature and concentration increase. The ratio of amplitudes for the 404 nm doublet decreases as the temperature increases from 1125 to 1175 K. At 1175 K the shorter wavelength line has begun to show reduced intensity near the line center due to re-absorption in the 50 cm. cool layer. Both lines are at the black body emission limit for that temperature. Similar effects are seen for the 766 nm doublet. However, the blackbody limit is reached at the lowest temperature with dips formed at both line centers. As the temperature increases, the

Potassium Emission Line Intensity

Optically Thin Line Shapes

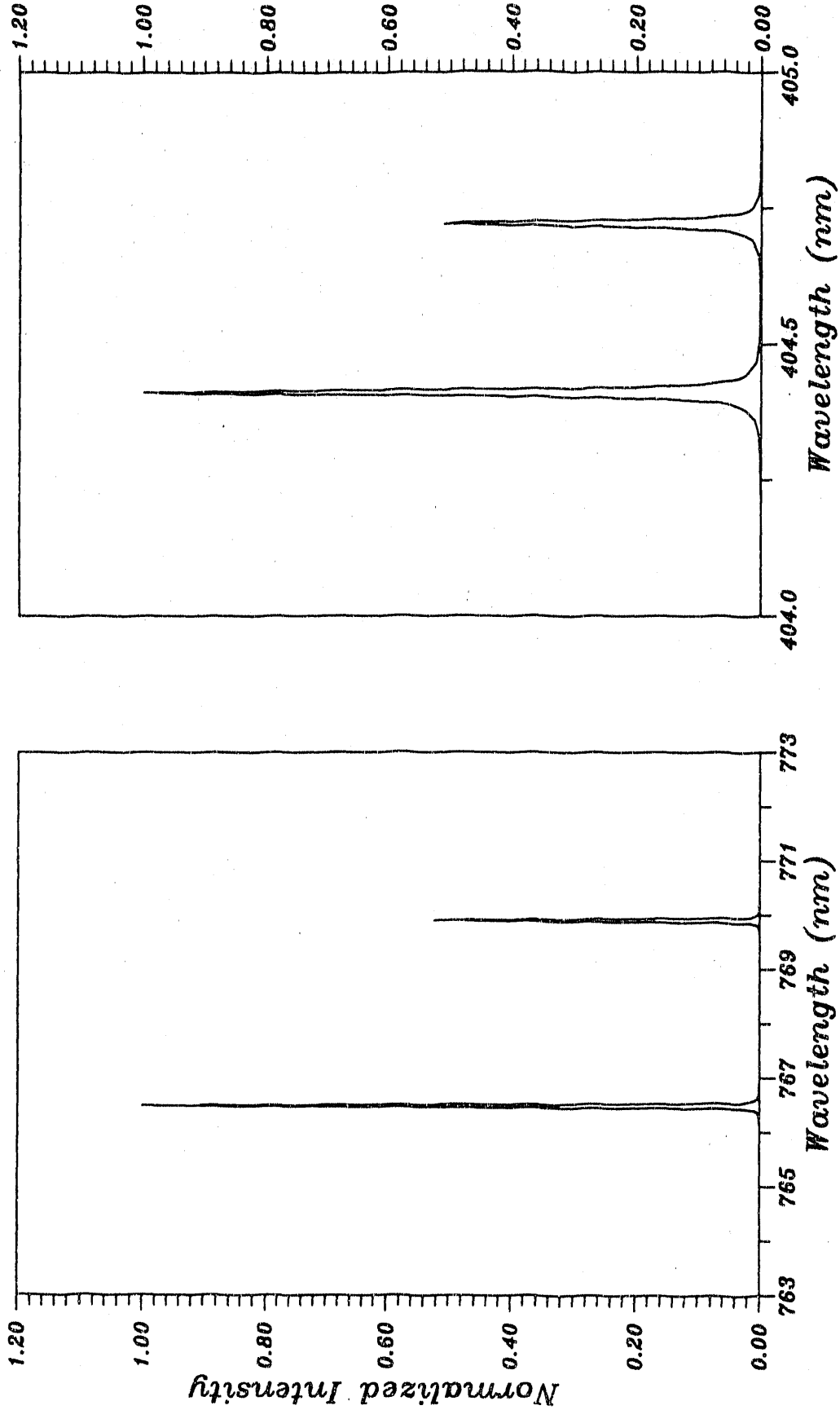


Figure 37. Optically Thin Line Shapes of Potassium Emission Intensity

Potassium Emission Line Intensity

Tcore 1125, 1150 & 1175K Tcool 1110K 50 cm. Cool Zone

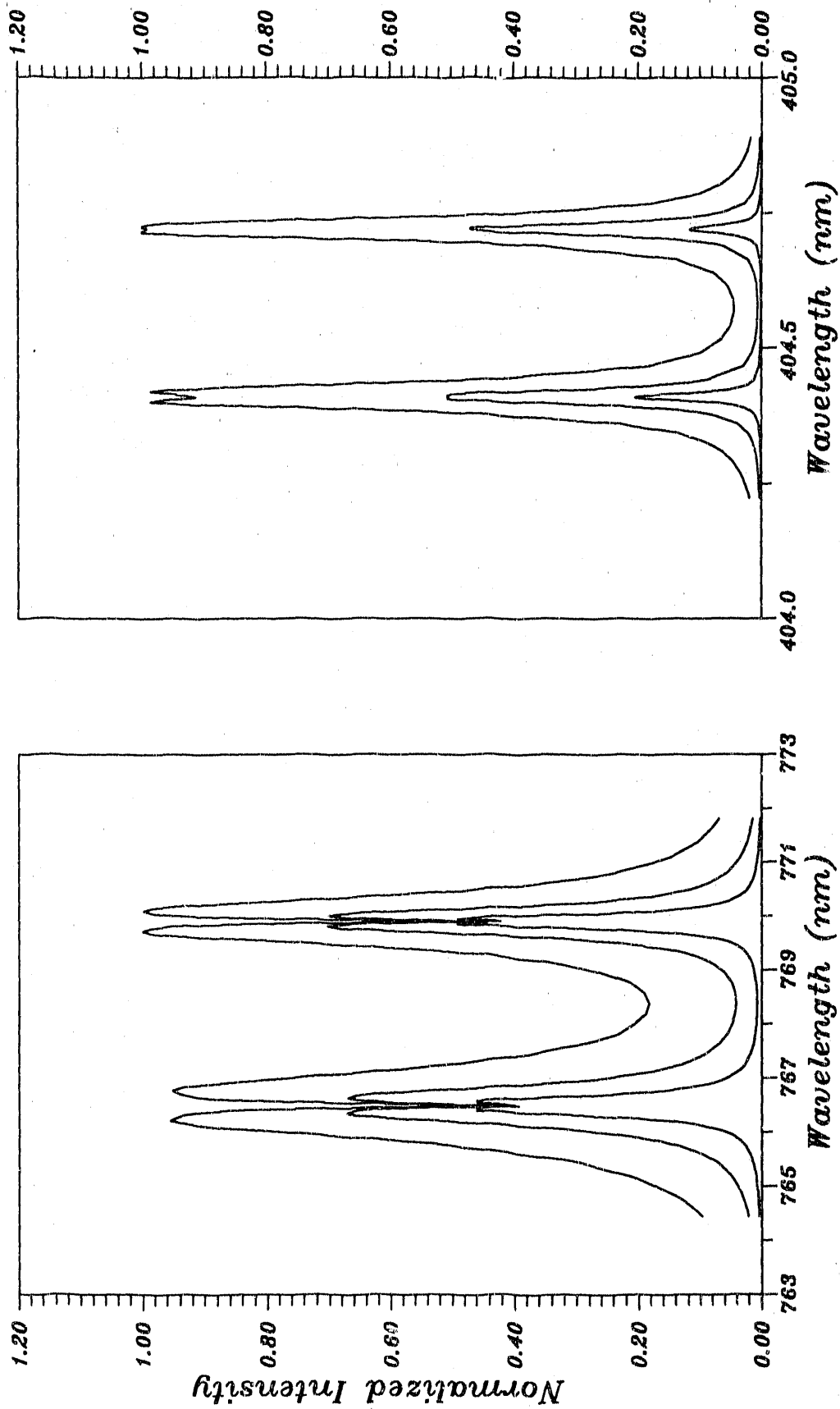


Figure 38. Emission Line Intensity Shapes - Effect of a Cool Layer

magnitude of the dip around the line center is increased due to intensity increase in the wings of each line.

Similar emission profiles result from calculations in which the temperature values for the core and cool layer regions are held constant while n_p values are varied, or for fixed n_p values with variation in temperature, illustrating the interdependence of temperature and concentration. Figures 39 and 40 illustrate such a situation. Emission intensities are less for the lower core region concentration levels used in computing the profiles in figure 39. Each line of the 766 doublets are narrower, and the amplitude ratio of the 404 nm doublet are closer to 2 than in the higher concentration case of figure 40. Figure 41 also illustrates the similarity in profile characteristics obtained for fixed temperatures of the core and cooler bounding layers.

Models such as the one discussed here are dependent upon correct estimates of n_p to realistically predict emission line shapes in a strongly absorbing medium. Comparison between recovery boiler emissions and the results of this model show that the calculated line shape of the potassium doublets can be made to closely resemble those observed. This is accomplished by decreasing the n_p values, relative to Pejyrd and Hupa, and temperatures as free parameters until the calculated line shapes resemble those of the observations. For temperatures ranging from 1125 to 1300 K, use of n_p values in the range of one to two orders of magnitude below those predicted by Pejyrd and Hupa resulted in emission profiles of similar shape to those observed in recovery boilers. Further decrease in n_p values would produce similar profiles for the temperatures normally thought to occur in the recovery boiler.

6.3 Optically Thick Gas - Analytical Expressions

A similar approach, which is valid for both optically thin and thick environments depends on the relationship of Einstein coefficients for emission and absorption. The Einstein coefficient, A_{qp} for emission at energy level, q , is related to the Einstein coefficient for absorption, B_{qp} by the following relation:

$$A_{qp}/B_{qp} = 8\pi h\nu_o^3/c^3 \quad (23)$$

The absorption coefficients B_{qp} and B_{pq} are related by the statistical weights of the two levels.

$$B_{qp}/B_{pq} = g_p/g_q \quad (24)$$

The oscillator strength is given by

$$f_{pq} = (hm_p\nu_o/\pi e^2)B_{pq} \quad (25)$$

Potassium Emission Line Intensity

T_{core} 1366, 1316, & 1266K T_{cool} 900K 30 cm. Cool Zone, Np 2.4 E11 atoms/cc

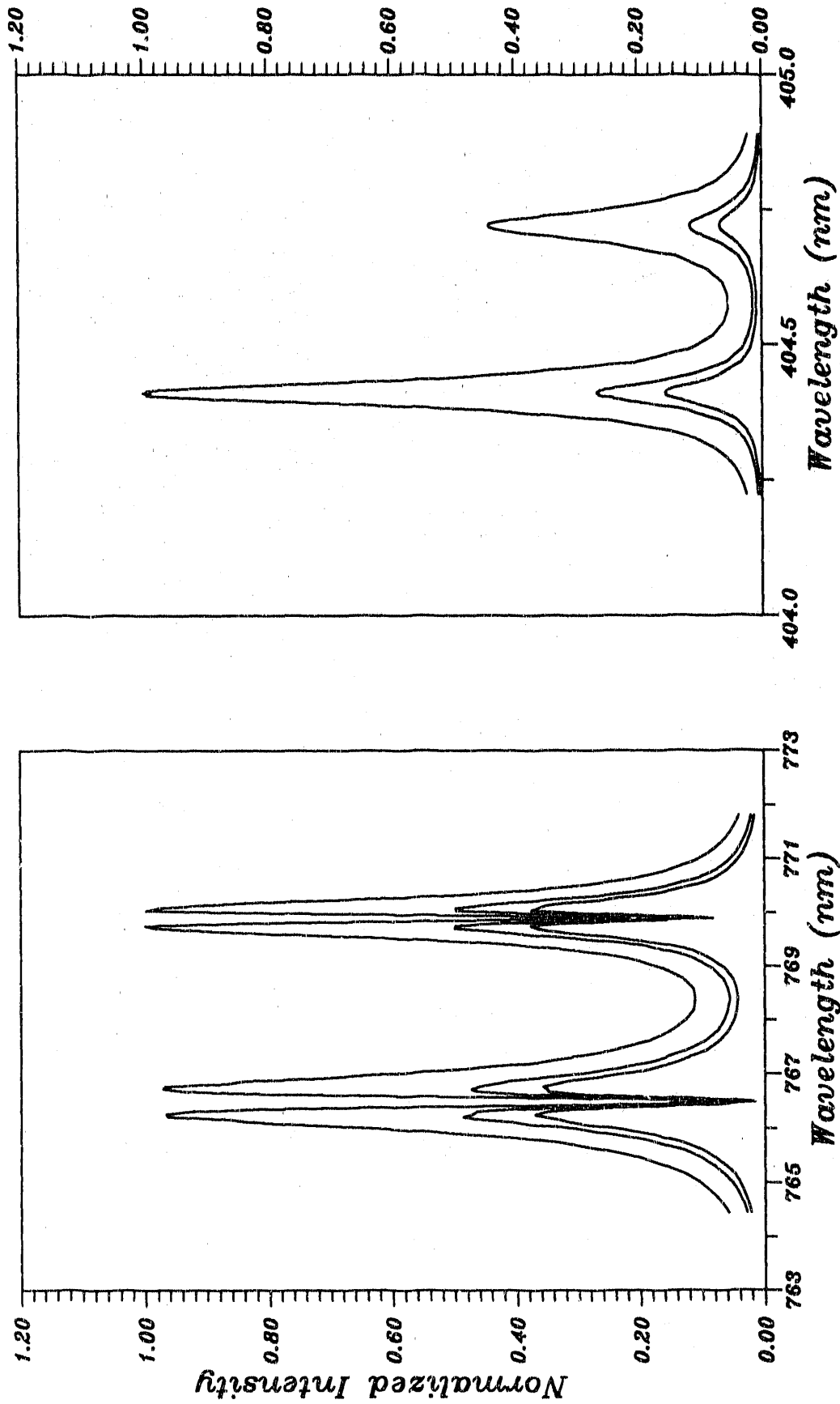


Figure 39. Emission Line Intensity Shapes - Effect of a Cool Layer
NP = 2.4×10^{11} Atoms/cm³

Potassium Emission Line Intensity

Core 1366, 1316, & 1266K Tcool 900K, 30 cm. Cool Layer
Np - 2.42E11 (Cool Layer) 1.29E12 Atoms/cc (Core)

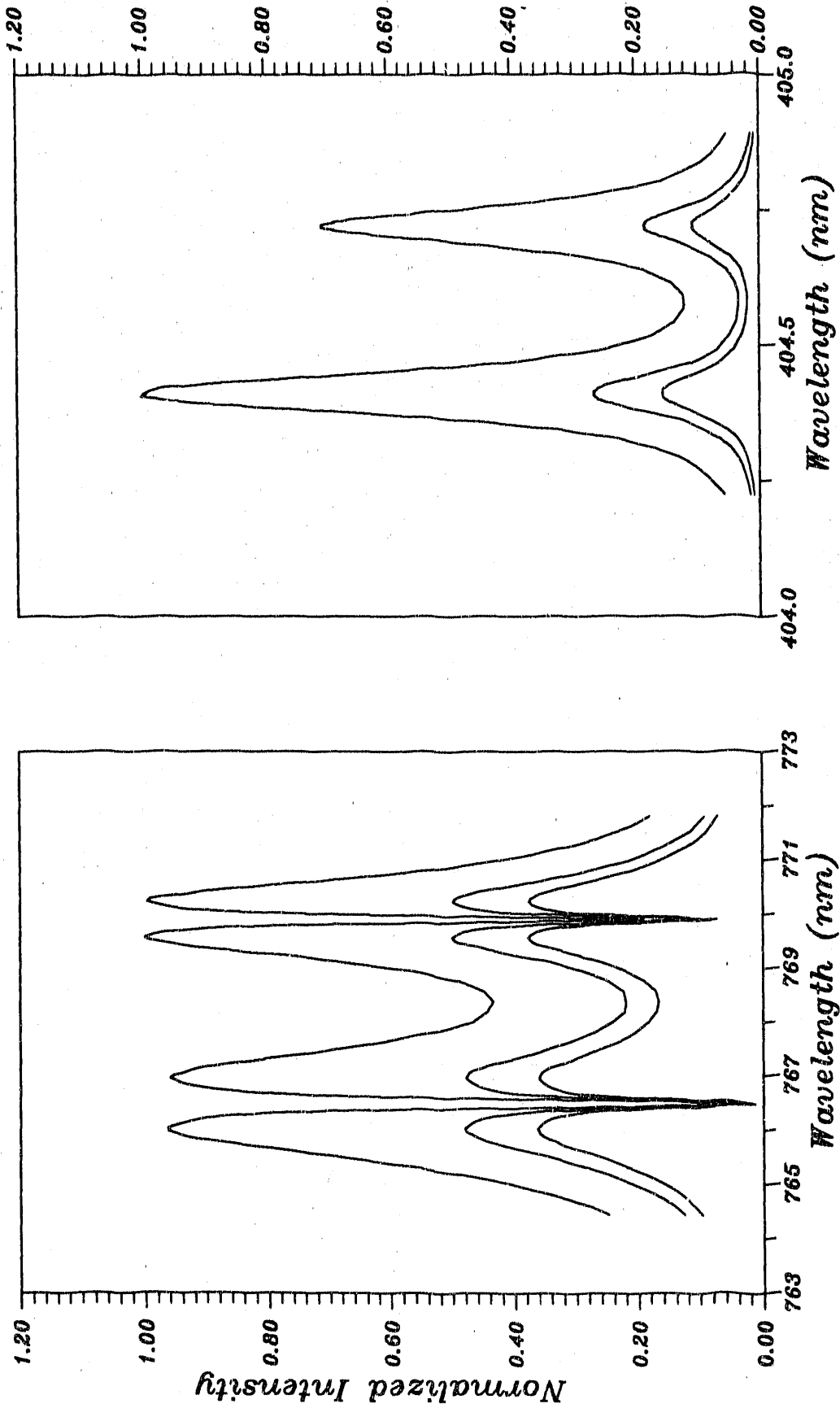


Figure 40. Emission Line Intensity Shapes - Effect of a Cool Layer Np = 1.29×10^{12} Atoms/cm³

Potassium Emission Line Intensity

T_{core} 1366K T_{cool} 900K 30 cm. Cool Layer: Np 0.2, 1.3, and 8.7E12 atoms/cc

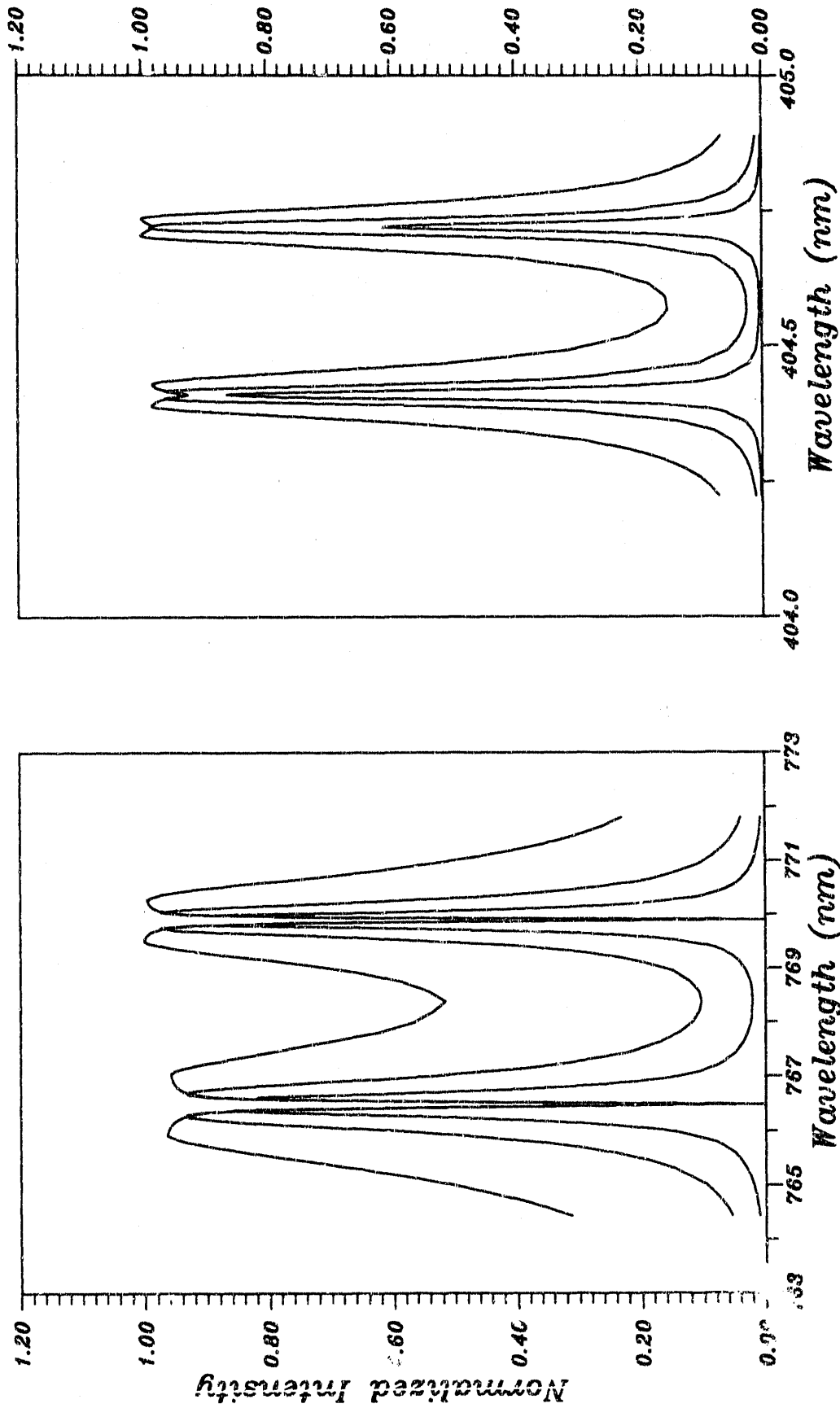


Figure 41. Emission Line Intensity Shapes - Effect of a Cool Layer and Various K atom Concentration Levels

The absorption coefficient, $K(\nu)$ is determined from

$$K(\nu) = B_{pq} S_\nu h \nu_o n_p / c = \left(\frac{c^2}{8\pi \nu_o^2} \right) (g_g / g_p) n_p S_\nu A_{qp} \quad (26)$$

where S_ν is the function that describes the line shape, i.e., the Voigt profile function for this calculation.

The line shape as a function of wavelength is obtained from

$$S_\nu = S_\lambda (\lambda_o^2 / c). \quad (27)$$

The absorption coefficient, $K(\nu)$ is then given by

$$K(\nu) = \left(\frac{c \lambda_o^2}{8\pi \nu_o^2} \right) (g_q / g_p) S_\lambda n_p A_{qp}. \quad (28)$$

The atomic absorption coefficient, k_a for a resonance line is given by

$$k_a(\nu) = \left[\frac{c}{8\pi} \frac{\lambda_o^2}{\nu_o^2} \right] (g_1 / g_o) S_\lambda A_{10}. \quad (29)$$

The intensity of emission of a resonance line, with line center at λ_o , at a wavelength of λ is given by

$$\begin{aligned} B_\lambda &= \int dB_\lambda = \left(\frac{A_{10} hc}{4\pi \lambda_o} \right) S_\lambda \int_0^l n_1(x) dx \exp \left[- \int_0^x k_a(\lambda) n_o(x') dx' \right] \\ &= \left(\frac{A_{10} hc}{4\pi \lambda_o} \right) \frac{S_\lambda}{k(\lambda)} \int_0^x \frac{n_1(x)}{n_o(x)} \exp[-u] \frac{du}{dx'} dx' \end{aligned} \quad (30)$$

where

$$u = \exp \left[- \int_0^x k_a(\lambda) n_o(x') dx' \right]; \quad \frac{du}{dx} = k_a(\lambda) n_o(x) \quad (31)$$

Substitution of eq (29) into eq (30) yields

$$\begin{aligned} B_\lambda &= \left(\frac{A_{10} hc}{4\pi \lambda_o} \right) \left(\frac{S_\lambda}{k_a(\lambda)} \right) \left(\frac{g_1}{g_o} \right) \exp \left[\frac{hc}{\kappa_o KT} \right] \int_0^{u(l)} \exp[-u] du \quad (32) \\ &= \alpha(\lambda) \frac{2h c^2}{\lambda_o^5} \exp \left[- \frac{hc}{\lambda_o k_B T} \right] \end{aligned}$$

where

$$\alpha(\lambda) = 1 - \exp \left[- \int_0^l k_a(\lambda) n_o(x') dx' \right] \quad (33)$$

6.4 Laboratory Tests

Laboratory tests were performed to confirm the model results, especially to show that the ratio of the two peak intensities of a potassium (or sodium) doublet is equal to 2 the ratio of statistical weight, g_1/g_0 i.e., when optically thin, less than 2 when one of the lines is optically thick, and nearly equal to one when the gas is optically thick. When both lines are optically thick, the peak emission intensity ratio corresponds to that of a black body at the temperature of the gas stream.

The apparatus used in these tests consisted of a 3 inch diameter premixed methane/air burner equipped with a nebulized mist injector; the experimental arrangement used was essentially the same as the one used in the earlier laboratory tests (fig. 2).

Initially, several KOH solutions of different concentrations were prepared by diluting a saturated KOH solution with varying amounts of distilled water. In the first series of experiments, the potassium emission spectra at 404.41 nm and 766.49 nm were obtained from a fuel-rich flame injected with only dilute KOH solutions. The peak intensity ratios (I_1/I_2) of either of the potassium doublets were found to be equal to 2 as expected for emissions from optically thin gases. The peak intensity ratio of each of the potassium doublets remained equal to two even when the flame was injected with saturated solutions of KOH, provided the effective path length was kept to a minimum. Figure 42 shows the emission spectra of potassium doublet at 766.49/769.9 nm, obtained in both fuel-rich, and fuel-lean flames at about the same adiabatic flame temperatures; as can be seen the peak intensity ratios are nearly equal (1.9 and 1.96 respectively); at these conditions, the peak value at the wavelength of 766.49 appears to be saturated, especially in the fuel-rich flame. However, when the KOH spray was increased to increase the effective path length, the ratio was found to decrease as shown in figure 43. This decrease varied depending on the quantity of potassium in the flame and approached values as low as 1.2.

In addition to these tests with KOH solutions, a sequence of tests with sodium hydroxide solution were conducted. Dilute NaOH solutions injected into premixed flames yielded the peak intensity ratio of two (fig. 50) for the sodium doublet at 589 nm. However, when a saturated NaOH solution was injected at an increased flow rate, this peak

K-LINE EMISSIONS FROM LABORATORY FLAMES INJECTED WITH KOH SPRAY

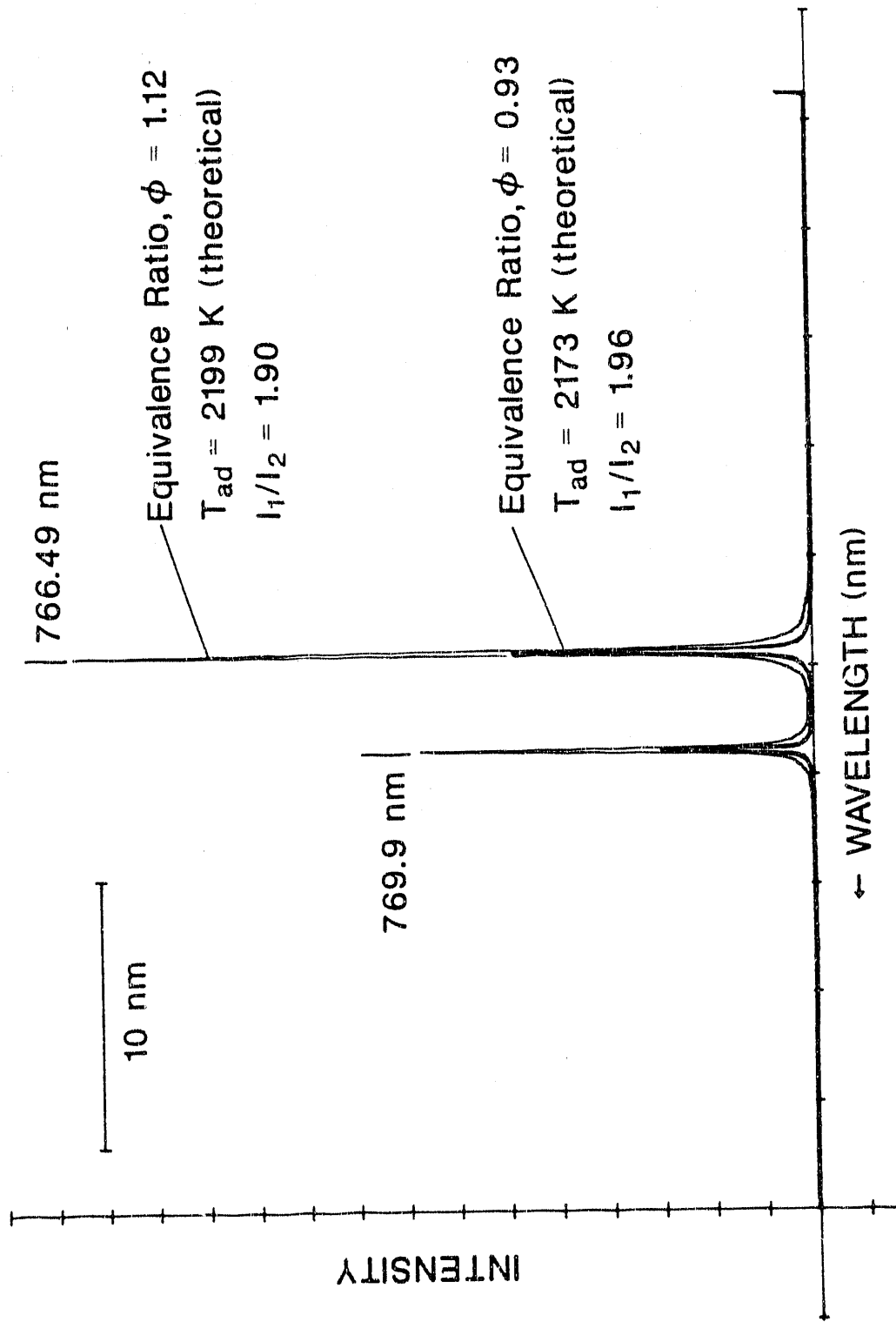


Figure 42. Measured Line Profiles from Laboratory Flames Injected with KOH - Optically Thin Emission

K-LINE EMISSIONS FROM LABORATORY FLAMES INJECTED WITH KOH SPRAY

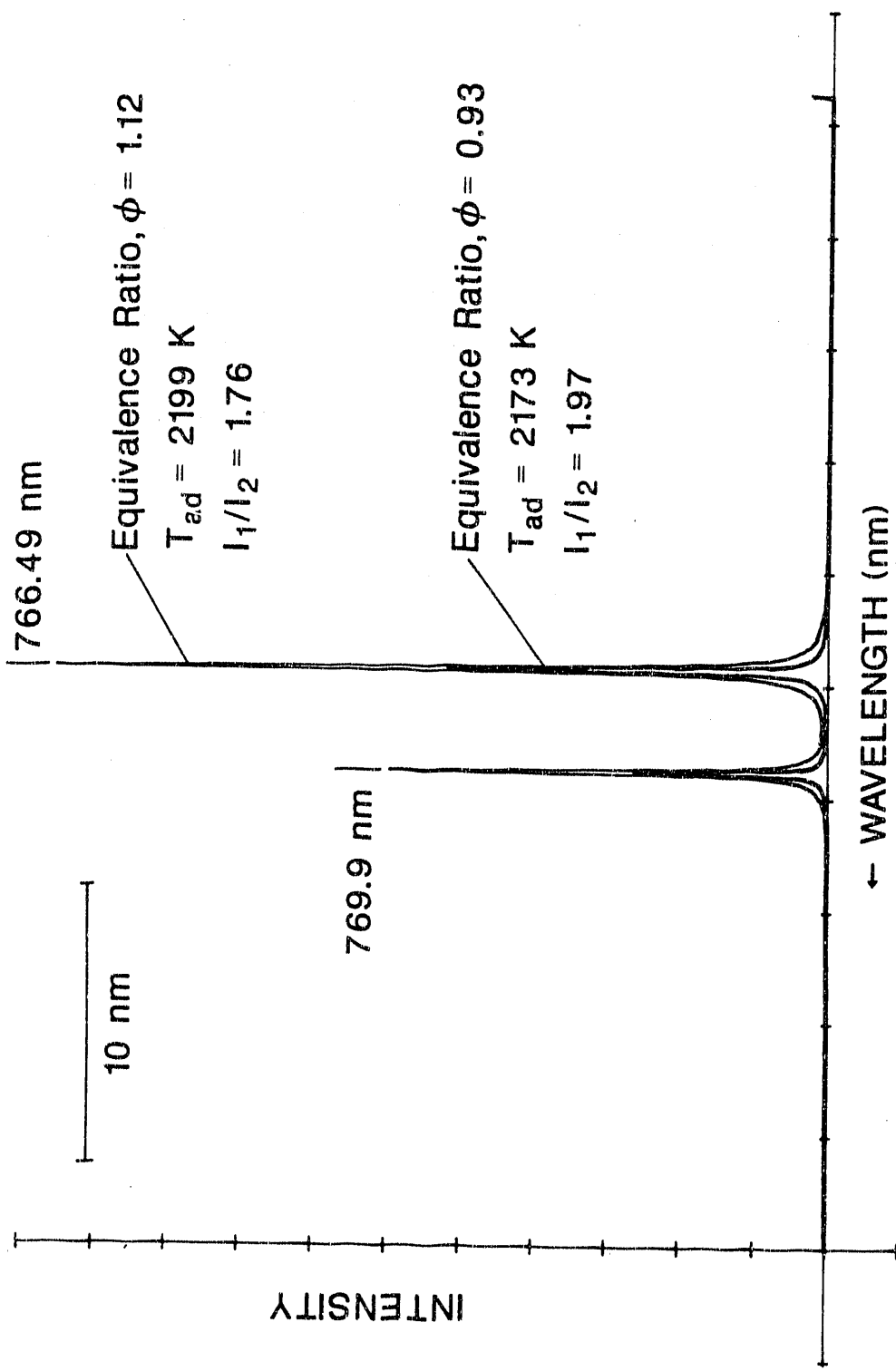


Figure 43. Measured Emission Line Profiles - KOH Injection for Optically Thin and Thick Cases

intensity ratio was found to decrease to a value much lower than two but still greater than one, as expected.

Based on these limited data it was concluded that it is feasible to demonstrate that the emission intensity of an optically thick line is equal to the emission intensity from a black body at the gas temperature. Such an effort, which would require further modifications to the burner and nebulizer, was not undertaken because of limitations in time.

Theoretical considerations suggest that an appropriate increase in optical path length causes an optically thin gas stream to become an optically thick one. To illustrate this, a simple approach was developed and tested. A ceramic rod, about 3 mm (1/8 inch) diameter was dipped into a saturated KOH solution so as to cover the rod up to a length of 6 inches. The rod was then removed to dry and obtain a KOH coating. This rod was inserted horizontally, just 1/8th inch above the burner plate, into a fuel rich flame. Once the rod was inserted into the flame, it generates a vertical sheath of yellow flame. The light emitted by this sheath was observed through collection optics located about an inch above the ceramic rod. The light gathered was transmitted into the spectrometer to obtain emission spectra. These spectra were obtained when looking normal to the flame sheath, which is about 0.5 cm thick, the peak intensity ratio was found to be very closely equal to two. On the other hand, when looking along the 6.5 cm long sheath, the peak ratio decreased to 1.14. These results clearly demonstrate that if the peak ratio were measured to be less than two, the combustion zone is optically thick. Similar results were obtained when the sodium doublet at 589.0 nm was investigated.

These results clearly demonstrate that the emission lines observed in the recovery boilers investigated thus far -- Na doublet at 589 nm and potassium doublets at 404.41/404.7 nm and 766.49/769.9 nm -- are optically thick.

7. Summary and Conclusions

The investigations reported here from the mill tests have yielded the following results:

1. Molecular flame spectra (OH, CH, C₂) have not been observed in recovery boilers.
2. In addition to the sodium spectral line at 589 nm, observed largely in self-absorption, strong emission from the potassium at 766/769 nm was observed in all boiler tests. In addition, a much weaker potassium doublet at 404 nm was observed at sufficiently high temperatures.

3. The observed line shapes show that the 766/769 nm doublet was always optically thick, i.e., re-absorption or self-absorption effects distort the line shape. The limited data on the 404 nm doublet is also indicate probable self-absorption effects.

Since the simplest form of line intensity ratio technique is primarily useful for measuring temperatures from observation of optically thin lines, i.e., negligible re-absorption, this approach doe not appear promising for combustion temperature measurement in recovery boilers.

A computer-based model was written allowing correlation of spectral line profiles and intensities with boiler gas temperatures and concentrations of thermometric species (n_p). This model was applied to the potassium lines. The results of the model calculations demonstrate a high degree of sensitivity to thermometric species concentration, n_p , values. The integrated absorption and intensity models discussed here are dependent upon correct estimates of n_p to realistically predict emission line shapes and optical depths in the strongly absorbing medium found in recovery boilers. Comparison between recovery boiler emissions and the results of the intensity model show that with reliable concentration data, the calculated line shape of the potassium doublets can be made to closely resemble those observed in the boiler. This can be accomplished by adjusting the n_p values and temperatures as free parameters until the calculated line shapes resemble those observed.

For temperatures ranging from 1125 to 1300 K, values of n_p in the range of one to two orders of magnitude below the values predicted by Pejyrd and Hupa were necessary to obtain generally expected line shops. Higher temperatures require a corresponding decrease in n_p to obtain similar line shapes. It would appear from the results of the intensity model studies that concentrations published by Pejyrd and Hupa do not correspond well with conditions in the recovery boilers in which observations were made. This may be the result of large disparities between the black liquor compositions actually used and that on which the equilibrium model is based.

Generally the results of the intensity model for isothermal cases indicate that optical depths near the line centers of both potassium doublets are a small fraction of the size of the boiler. This is in agreement with the integral absorption model results and the results from laboratory-burner experiments performed after boiler experiments. Inference of temperature from observations of the potassium doublets at 404 and 766 nm appears to be quite complex, requiring detailed information of the shape of each doublet. Essential to such an approach is realistic prediction of potassium concentration in the boiler which would require a realistic equilibrium model and, perhaps, on-line sampling of the black liquor feed stream for potassium concentration in boiler fuel. This suggests, that with correct values for the potassium concentration, that combustion temperature measurements are possible when combined with this type of intensity model and could be the basis for a valid gas temperature measurement for the recovery boiler.

8. Acknowledgements

The authors would like to acknowledge the help received from various mills -- the Westvaco Mills, the Union-Camp mills and the Weyerhaeuser Mills -- and to extend special thanks to Dr. Peter Ariessoehn of the Weyerhaeuser Technical Center for providing a pump and heat exchanger system necessary to conduct the probe tests. The authors also deeply appreciate the cooperation and helpful suggestions provided by Dr. Ariessoehn. The assistance given by Mr. Michael J. Carrier in performing the calculations and generating the plots is appreciated. The first author (SRC) acknowledges and appreciates the assistance in programming received from Mr. Sridhar Charagundla, a student at Thomas Jefferson High School for Science and Technology, Alexandria, VA. This project is a part of a program that is funded by the U. S. Department of Energy (DOE IA No.: DE-AI01-76PRO6010). Mr. Stanley Sobczynski of the Department of Energy is the program manager.

9. References

- [1] Advanced Sensor Development Program for the Pulp and Paper Industry, Annual Report No. 2, DOE/PR/O6010-T33 (DE84008548).
- [2] S. R. Charagundla and H. G. Semerjian; A Remote Sensing Technique for Combustion Gas Temperature Measurement In Black Liquor Recovery Boilers, SPIE Vol. 665, Optical Techniques for Industrial Inspection (1985).
- [3] D. W. Emerson and B. Whitworth; Proceedings of the DOE/Industry Research and Development Sensor Working Group Meeting, Chicago, Ill, CONF-8611136-(DE87006159); Nov 14, 1986.
- [4] Andrej Macek and Charles Bulik; Direct Measurement of Char particle Temperatures in Fluidized-Bed Combustors, Twentieth Symposium (International) on Combustion, The Combustion Institute, pp. 1223-1230, 1984.
- [5] A. Macek, S. R. Charagundla, J. Allen, and H. G. Semerjian; Gasifier Report submitted for publication.
- [6] D. B. Vaidya, J. J. Horvath, and A. E. S. Green; Remote Temperature Measurements in gas and gas coal flames using the OH(0,0) Middle-UV Band, Applied Optics, Vol.21, p. 3357, September 15, 1982.
- [7] P. W. J. M. Boumans; Theory of Spectrochemical Excitation, Plenum Press, New York, 1966.
- [8] C. T. J. Alkemade, T. Hollander, W. Snelleman, and P. J. T. Zeegers; Metal Vapors in Flames, Pergamon Press, New York, 1982.
- [9] J. Reader, C. H. Corliss, W. L. Wiese, and G. A. Martin; Wavelengths and Transition Probabilities for Atoms and Atomic Ions, NSRDS-NBS 68, U. S. Government Printing Office, Dec. 1980.
- [10] W. L. Wiese, M. W. Smith, and B. M. Miles; Atomic Transition Probabilities, vol II, Sodium through Calcium, NSRDS-NBS 22, U. S. Government Printing Office, Oct 1969.
- [11] J. R. Whetstone, et al.; Advanced Sensor Development Program for the Pulp and Paper Industry, Annual Report No.1,
- [12] Certain commercial equipment and instruments are identified in this paper in order to describe the experimental procedures and results adequately. In no case does such identification imply recommendation or endorsement by the National Bureau of Standards nor does it imply the material or equipment is necessarily the best available for the purpose.

- [13] J. R. Whetstone, et al.; Operating and Maintenance Manual for Furnace Heat Flux Probe System for the National Bureau of Standards, Medtherm Corporation, Huntsville, Alabama, July 1986.
- [14] W. J. Wiscombe; Mie Scattering Calculations: Advances in Technique and Fast, Vector-Speed Computer Codes, NCAR Technical Note, NCAR/TN -140+STR, June 1989.
- [15] B. H. Armstrong; Spectrum Line Profiles: The Voigt Function, J. Quant. Spectrosc. Radiat. Transfer, Vol. 7, pp. 61-88, Pergamon Press Ltd., 1967.
- [16] R. L. Merriam; Kraft, Version 2.0 Computer Model of a Kraft Recovery Furnace, A. D. Little Inc., Dec 1980.
- [17] L. Pjryd and M. Hupa; Bed and Furnace Gas Composition in Recovery Boilers - Advanced Equilibrium Calculations, TAPPI Proceedings, 1984 Pulping Conference.
- [18] J. H. Cameron; Vaporization from Alkali Carbonate Melts, The Institute of Paper Chemistry, IPC Technical Paper Series, No.: 237, Apr 1987.
- [19] Personal Communication with Peter Ariessohn of Weyerhaeuser Company.

END

DATE FILMED

04 / 30 / 91

